AN ABSTRACT OF THE DISSERTATION OF

Rhonda Sue Kaetzel for the degree of Doctor of Philosophy in Toxicology
presented on March 4, 2003.
Title: A Proteomic Approach to 1,2-Dichloroethane Bioactivation and
Reaction with Redox-Active Protein Disulfide Isomerase.

Abstract approved: Redacted for privacy

Donald J. Reed

Protein disulfide isomerase (PDI), a member of the thioredoxin superfamily,
contains two domains with significant sequence homology to the active sites
in thioredoxin. PDI facilitates the folding of nascent proteins in the
endoplasmic reticulum (ER), binds hormones and Ca^{2+}, catalyzes the
glutathione dependent reduction of dehydroascorbate, serves as a major
chaperone molecule in the ER and serves as a subunit for prolyl-4-
hydroxylase and microsomal triglyceride transferase. Because of its
abundance in the ER and association with disease and chemically induced
toxicity, the goal of this research was to investigate the relative susceptibility
of PDI thiols to alkylation. The sensitivity of PDI to 1-chloro-2,4-
dinitrobenzene (CDNB), iodoacetamide (IAM) and biotinoylated
iodoacetamide (BIAM) was explored. The relative susceptibility of the thiolate
anions present in the two active sites of PDI each containing the –CGHC–
sequence was investigated with mass spectrometric techniques. PDI was
inactivated by CDNB but was not found as sensitive as thioredoxin reductase
as shown by Arner and coworkers (1995). IAM and BIAM were used as
model alkylating agents to explore the two active sites of PDI and determine

the residues most susceptible to alkylation. Alkylation by IAM and BIAM was first detected at the N-terminal cysteine in each active site (–C*GHC–) followed by alkylation at the second cysteine residue (–C*GHC*–) as shown by tandem mass spectrometry. Mass spectroscopy showed that the episulfonium ion derived from the glutathione conjugate of 1,2-dichloroethane, S-(2-chloroethyl)glutathione (CEG), decreased activity and protein thiols of PDI. CEG produced two protein adducts at very low excesses of CEG over PDI; however, higher concentrations resulted in several protein adducts. Only one modification in each active site at the N-terminal cysteine residue can be identified, indicating that while these thiolate anions of PDI are susceptible, it would appear that the episulfonium ion may present itself to other sites as well. This may have important toxicologic significance regarding the mechanism of 1,2-dichloroethane toxicity and the role of PDI in the redox status of the cell.

A Proteomic Approach to 1,2-Dichloroethane Bioactivation and Reaction
with Redox-Active Protein Disulfide Isomerase

by
Rhonda Sue Kaetzel

A DISSERTATION

Submitted to

Oregon State University

in partial fulfillment of
the requirements for the
degree of

Doctor of Philosophy

Presented March 4, 2003
Commencement June 2003

Doctor of Philosophy dissertation of Rhonda Sue Kaetzel
presented on March 4, 2003.

APPROVED:

Redacted for privacy

_____

Major Professor, representing Toxicology

Redacted for privacy

_____

Chair of Department of Environmental and Molecular Toxicology

Redacted for privacy

_____

Dean of the Graduate School

I understand that my dissertation will become part of the permanent
collection of Oregon State University libraries. My signature authorizes my
dissertation to any reader upon request.

Redacted for privacy

_____

Rhonda S. Kaetzel, Author

ACKNOWLEDGEMENTS

I express sincere appreciation to Dr. Donald J. Reed for his guidance, support, and friendship, and for the opportunity to pursue my studies in toxicology. I thank my committee members, Drs. Donald Buhler, Balz Frei, Jean Hall, and David Williams, for their willingness and critical evaluation of my dissertation. In addition, I would like to thank Dr. Michael Schimerlik for his useful discussions on enzyme kinetics and Drs. Max Deinzer and Douglas Barofsky for their education and advice on mass spectrometry applications.

I thank Marda Brown and Tamara Fraley for their unending technical assistance, advice, guidance, and positive attitude. I thank Dr. Yvonne Will for her time and patience in teaching me many skills that I have used throughout my research. I also thank Corwin Willard for his expertise in chromatography and mechanical maintenance of the instruments available in the laboratory. I would also like to thank Brian Arbogast, Lilo Barofsky, Jeff Morré, and Don Griffin for their excellent technical support and patience in mass spectrometry and low-flow chromatography. I also appreciate the many discussions and ideas shared with me by my labmate Marcus Calkins as well as Dr. Heidi Zhang, Dr. Xuguang Yan, Martha Staples and April Mixon of the EHSC mass spectrometry laboratory. I also appreciate the support given to me by the administrative staff in the Department of Environmental and Molecular Toxicology and the Environmental Health Sciences Center of OSU. I thank Monica Perri for her technical review and editing of my dissertation.

I owe very special thanks to my parents and sister for loving and believing in me. I thank my husband, Théo, for his love and faith in me, and my abilities. Finally, I thank my sons, Tyler and Charles, and my nephew Joseph for teaching me how deep love and happiness can be.

CONTRIBUTION OF AUTHORS

TABLE OF CONTENTS

TABLE OF CONTENTS (continued)

TABLE OF CONTENTS (continued)

LIST OF FIGURES

LIST OF FIGURES (continued)

LIST OF FIGURES (continued)

LIST OF FIGURES (continued)

LIST OF FIGURES (continued)

LIST OF ABBREVIATIONS

ATSDR	Agency for Toxic Substances and Disease Registry
CID	Collision induced dissociation
BAM	Biotin-amidomethylated
CAM	Carbamidomethylated
cCMP	Cyclic cytodine monophosphate
CDDP	Cisplatin or *cis*-diamminedichloroplatinum (II)
CDNB	1-Chloro-2,4-dinitrobenzene
CEG	S-(2-chloroethyl)glutathione
CGHC	PDI active site amino acid sequence
Cys	Cysteine
Da	Dalton
DCE	1,2-Dichloroethane
Dsb	Disulfide bridge protein family in *E. coli*
EHSC	Environmental Health Sciences Center
ER	Endoplasmic reticulum
ESI	Electrospray ionization
Grx	Glutaredoxin
GSH	Reduced glutathione
GSNO	S-Nitrosated glutathione
GSSG	Oxidized glutathione
GST	Glutathione-S-transferase
HPLC	High performance liquid chromatography
IAM	Iododacetamide
KDEL	ER amino acid retention sequence
LC	Liquid chromatography
MA	Methamphetamine
MALDI	Matrix-Assisted Laser Desorption Ionization
MASCOT	Matrix Science mass spectra search engine
$[M+H]^+$	Singly charged ion
$[M+2H]^{2+}$	Doubly charged ion
MS	Mass spectrometry
MS/MS or MS2	Tandem mass spectrometry or spectra
MS1	Full spectrum or
NMR	Nuclear magnetic resonance
NO	Nitric oxide
OONO	Peroxynitrite
OSU	Oregon State University

LIST OF ABBREVIATIONS (continued)

PDI	Protein disulfide isomerase (55 kDa)
weePDI	Truncated protein disulfide isomerase (21 kDa)
PPARg	Peroxisome proliferator activated receptor
ProSSG	Protein-glutathione mixed disulfide
PSOH	Protein sulfenic acid
RNase	Ribonuclease
RSNO	S-Nitrosothiol group
RSOH	S-Sulfenic acid group
SALSA	Scoring ALgorithm for Spectral Analysis
SeC	Selenocysteine
SEQUEST	ThermoFinnigan mass spectra search engine
TOF	Time of Flight mass analyzer
TR	Thioredoxin reductase
Trx	Thioredoxin
YAPWCGHCKALAPEY	Peptic PDI peptide containing active site in domain **a**
YAPWCGHCKQLAPIW	Peptic PDI peptide containing active site in domain **a'**

I dedicate this dissertation to the memory of my friend
Matthew Anthony Thomson (1981-1996)

He won so many battles against his cancer, but he lost the war.
His courageous life was a testament to his love of life,
the love for his parents, and his purpose.

A PROTEOMIC APPROACH TO 1,2-DICHLOROETHANE BIOACTIVATION AND REACTION WITH REDOX-ACTIVE PROTEIN DISULFIDE ISOMERASE

1.0   INTRODUCTION

Toxicology is the study of the adverse effects of chemicals on living organisms. The mechanism of toxicity of a chemical is directly related to its delivery to a target cell or tissue, followed by the interaction between the chemical or its metabolite(s) with a specific molecules(s) resulting in dysfunction. The specific molecule at the target site can be a protein, lipid, nucleic acid or other macromolecular complex. In a toxic response, this dysfunction results in cellular injury that can manifest itself in many different ways, ranging from temporary loss of protein function to permanent DNA damage leading to cancer. In this thesis, an attempt is made to address the effects of electrophilic compounds on the redox-active protein disulfide isomerase (EC 5.3.4.1), a member of the thioredoxin superfamily. Protein disulfide isomerase (PDI) has many roles *in vivo* including the isomerization of disulfide bonds in nascent proteins, oxidoreduction, chaperone/ antichaperone function and as a subunit to two larger protein complexes.

Background on the thiol status of the cell, redox-active proteins including PDI, modification of thiols as well as proteomics and mass spectrometry is presented in chapter 2. An investigation of the sensitivity of PDI to alkylation by the common glutathione-S-transferase substrate, 1-

chloro-2,4-dinitrobenzene, is presented in chapter 3. Titration of active site thiols of PDI by iodoacetamide and its derivative, biotin-conjugated iodoacetamide, and identification of residues modified by liquid chromatography and electrospray tandem mass spectrometry are also described in chapter 3. In chapter 4, the susceptibility of PDI to alkylation by the episulfonium ion of S-(2-chloroethyl)glutathione, a reactive metabolite of 1,2-dichloroethane, is presented. Finally, a summary and conclusion of these studies are delineated in chapter 5 and a discussion of the future of proteomics in mechanistic studies is presented.

2.0   BACKGROUND

2.1   THIOL STATUS OF THE CELL

The thiol redox status of intracellular and extracellular compartments is critical in the determination of protein structure, regulation of enzyme activity, cell signaling, and control of transcription factor activity. The composition and redox status of the available thiols in a given compartment are variable and play a part in determining the metabolic activity of each compartment. Thiol antioxidants act through a variety of mechanisms, including as components of the general thiol/disulfide redox buffer, as metal chelators, as radical quenchers, as substrates for specific redox reactions, and as specific reductants of individual protein disulfide bonds (Deneke, 2000). The intracellular redox environment is a tightly regulated parameter that provides the cell with an optimal ability to counteract the oxidizing extracellular environment. Intracellular redox homeostasis is regulated by thiol-containing molecules, such as glutathione (a low molecular weight thiol)

and thioredoxin (thiol-containing protein). Cells have devised a number of mechanisms to promote increased intracellular levels of thiols such as glutathione and thioredoxin in response to a wide variety of stresses.

2.1.1   Low Molecular Weight Thiols

Among the low molecular weight thiols, the unique tripeptide glutathione (GSH) is the most abundant and prominent in mediating the cellular thiol redox environment. GSH can protect cells from both endogenous and exogenous electrophiles that react with cellular constituents and cause cell damage (Reed, 1985). GSH plays an important role in the detoxification of xenobiotic compounds and as an antioxidant against reactive oxygen species and free radicals. Increasing evidence of S-glutathionylation of protein cysteinyl thiols implicates GSH and/or glutathione disulfide (GSSG) in redox signaling and regulation of protein function.

The synthesis of GSH involves formation of the unique amide bond between cysteine and glutamic acid, followed by peptide bond formation with glycine. The first reaction is catalyzed by γ-glutamyl cysteine synthetase; the second by glutathione synthetase. At each step, ATP is utilized and hydrolyzed to ADP and inorganic phosphate. The first reaction is inhibited by buthionine-S-sulfoximine, which can be used *in vivo* to decrease GSH levels in experimental animals.

The conjugation of xenobiotics with GSH is catalyzed by a family of glutathione-S-transferases (GSTs). GSTs are present in most tissues with high concentrations in the liver, intestine, kidney, testis, adrenal and lung where they are localized in the cytoplasm (>95%) and the endoplasmic

reticulum (5%). The high concentration of GSH in the liver (8-10 mM) parallels the abundant GST concentration (near 10% of the total cellular protein). Substrates for GSH conjugation include an enormous array of endogenous and exogenous electrophilic compounds. GSH conjugates are thioethers, which form by nucleophilic attack of the GSH thiolate anion with an electrophilic carbon atom in the target molecule. The GST-catalyzed conjugation of GSH with electrophilic substrates is the first step in the mercapturic acid pathway that is associated with the detoxification, excretion or bioactivation of xenobiotics.

Increased levels of GSH and other thiols have been associated with increased tolerance to oxidant stresses in all of these systems and in some cases, with disease prevention or treatment in humans. A wide variety of thiol-related compounds has been used to increase cell and tissue thiol levels in cell cultures, animal models, and humans. These include thiols such as GSH and its derivatives, cysteine and N-acetyl cysteine, lipoic acid, which is reduced to the dithiol form intracellularly, and "prothiol" compounds such as L-2-oxothiazolidine-4-carboxylate (OTC), which are enzymatically converted to free thiols within the cell. Endogenously produced sulfhydryl-containing cofactors such as coenzyme A and lipoic acid are vital to many metabolically important enzyme reactions.

These compounds must be considered carefully as therapeutic agents as large increases in free thiols in the circulation are associated with toxic effects. These effects may be the result of radical-mediated reactions but could also be due to destabilizing effects of increases in thiol/disulfide ratios in the plasma, which normally is in a more oxidized state than intracellular compartments. Changes in the thiol redox gradient across cells could also adversely affect any transport or cell signaling processes, which are

dependent on formation and rupture of disulfide linkages in membrane proteins and in the active site of enzymes.

2.1.2 Protein Thiols

Of the 20 common amino acids which constitute the building blocks of proteins, the polar amino acid cysteine is the only one that contains a free – SH (sulfhydryl or thiol group) on the side chain. The thiols of cysteine residues present in proteins play a remarkably broad and essential role in cell biology. The redox status of cysteine thiol groups dictates the native structure and activity of many enzymes, receptors, protein transcription factors, and transport proteins. Equally important is the role of thiol reduction as a mechanism against oxidative stress. In the human lung carcinoma cell line A545, total protein thiol concentration of the cell is estimated to be ~100 nmol/10^6 cells (Brodie and Reed, 1987). Protein thiol groups are also expressed as GSH equivalents/mg (e.g., hepatocytes have ~275 GSH equivalents/mg) (Moridani et al., 2002) though it is a dynamic measurement and dependent upon the redox status of the cell.

Much research has been focused on characterizing the physical and catalytic properties of a class of enzymes called thiol-disulfide oxidoreductases that are involved in cellular thiol homeostasis through their catalysis of thiol-disulfide interchange reactions. This class of enzymes includes but is not limited to thioredoxin, glutaredoxin, Dsb proteins and protein disulfide isomerase (see Table I for a list of thioredoxin superfamily proteins). These redox-active proteins are referred to as the thioredoxin superfamily of proteins because of their similarity to the structure of thioredoxin. The thioredoxin system, in concert with GSH and glutaredoxin

system, constitutes a reducing cellular environment. A description of the substrate specificity, redox potential., pKa, and redox state of the cellular compartment in which each protein resides sets the stage for the differing roles for these catalytically similar proteins.

Table I: The Thioredoxin Superfamily of Proteins.

Protein[a]	Synonyms	Mass (kDa)	Domain structure[b]	Sequence	Locations
DsbA		21		CPHC	Periplasm
DsbC		23		CGYC	Periplasm
DsbD	CutA	59		CVAC	Inner membrane
DsbG		25		CPYC	Periplasm
Thioredoxin		12		CGPC	Periplasm Nucleus, Cytosol, Mitochondria
Glutaredoxin	thioltransferase	12		CPYC	Periplasm, Cytosol, Mitochondria
PDI		55	a-b-b'-a'-c	CGHC	ER, secreted on cell surface, nucleus, Cytosol Mitochondria,
P5	CaBP1	46	a°-a-b-c	CGHC	ER
ERp72	CaBP2	71	c-a°-a-b-b'-a'	CGHC	ER
ERp57	GRp58, ER-58, ERp58, ERp60, Calreticulin, ERp61, Q2	54	a-b-b'-a'	CGHC	ER, secreted on cell surface, Nucleus, Plasma membrane rafts, Cytosol
PDIp		~55	a-b-b'-a'	CGHC CTHC	ER
PDIR		57	b-a°-a-a'	CSMC CGHC CPHC	ER
ERp44		44		CRFS	ER
ERp29	ERp31, ERp28	26	b-D	none	ER

[a] Information on these proteins can be found in the following reviews: prokaryotic Dsb family (Collet and Bardwell, 2002), thioredoxin and glutaredoxin (Holmgren, 1989) and the eukaryotic PDIs (Ferrari and Soling, 1999 and Turano et al., 2002).

[b] Domain structure denotes PDI family proteins. Domains a°, a, and a' are redox-active thioredoxin domains, whereas domains b and b' are redox-inactive domains.

2.2   THIOL-DISULFIDE REDOX-ACTIVE PROTEINS

2.2.1   Thioredoxin

2.2.1.1   Localization and Function

Thioredoxin (Trx) is a small (12 kDa) ubiquitous protein with the active site –CGPC– being conserved between prokaryotic and eukaryotic species (Holmgren, 1989). Human and other mammalian thioredoxins contain two catalytic site cysteine residues, Cys^{32} and Cys^{35} (numbering is for human Trx1), and three other cysteine residues (Cys^{62}, Cys^{69}, and Cys^{73}) not found in bacterial thioredoxins (Gasdaska et al., 1994). In *E. coli*, Trx was identified as an electron donor for ribonucleotide reductase (Laurent et al., 1964) and 3'-phosphoadenosine-5'-phosphosulfate reductase (Tsang and Schiff, 1976; Ejiri et al., 1979). Trx was found essential for the life cycle of some bacteriophages such as T7, M13, and f1 (Modrich and Richardson, 1975; Russel and Model, 1985; Lim et al., 1985).

Trx activity has been found outside the eukaryotic cell (cell growth stimulation and chemotaxis) in the cytoplasm (as an antioxidant and a reductant cofactor), in the nucleus (regulation of transcription factor activity), and in the mitochondria (for review see Powis and Montfort, 2001). Trx is required to regenerate an active site dithiol after each catalytic cycle in synthesis of deoxyribonucleotides by ribonucleotide reductase (Holmgren and Bjornstedt 1995; Holmgren, 1976; 1989). Disulfide reduction by Trx is also involved in the redox regulation of transcription factors (e.g., NFκB or AP-1) (Schenk et al., 1994) and may exert separate activities in the nucleus compared to the cytosol (Hirota et al., 1999). Secreted mammalian Trx has co-cytokine-like activity on certain mammalian cells by an unknown

mechanism but probably involving disulfide exchange (Powis et al., 1995, Holmgren and Bjornstedt, 1995; Yodoi and Tursz, 1991). Trx dependent peroxidases (peroxiredoxins) are also important cellular defense systems protecting from apoptosis as a result of oxidative stress (Zhang et al., 1997).

2.2.1.2   Structure and Characteristics

Trx is a compact globular protein with five beta sheets forming a hydrophobic core surrounded by four alpha helices on the external surface (Figure 2.1). The conserved active site amino acids, –CGPC–, link the second beta strand to the second alpha helix and form the first turn of the second helix in a protrusion of the protein. This stable tertiary structure is called the thioredoxin fold (Martin, 1995).

This conserved site of Trx undergoes a reversible oxidation to the cystine disulfide (Trx-S$_2$) through the transfer of reducing equivalents from the catalytic site cysteine residues to a disulfide substrate. The first step in the reaction mechanism proposed by Kallis and Holmgren (1980) is a nucleophilic attack of one of the cysteines in its thiolate form on a disulfide bond of the protein substrate, forming a mixed disulfide intermediate. In *E. coli* Trx, the thiolate form of Cys^{32} is stabilized by an interaction with the thiol hydrogen of Cys^{35}. The preference for deprotonating Cys^{32} before Cys^{35} arises because of the greater solvent exposure of Cys^{32} and the greater influence of the negative charge on Asp^{26} on Cys^{35} than on Cys^{32} (Dillet et al., 1998). Protein dipoles, especially the SH dipole of Cys^{35} can provide sufficient stabilization of the Cys^{32} thiolate to account for its experimentally low pKa near 7.4 relative to the pKa of free cysteine (8.5 ±0.5). The second step in the reaction mechanism is the attack of the deprotonated Cys^{35} on the Cys^{32}SS–protein disulfide bond releasing the reduced protein substrate

and forming Trx-S$_2$, which is then reduced by thioredoxin reductase (Holmgren, 1995).
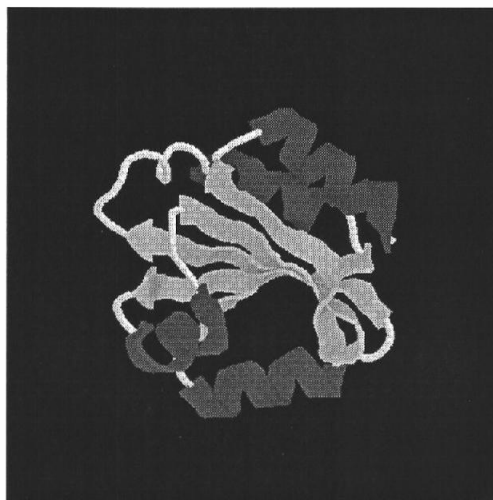
Figure 2.1   NMR structure of human thioredoxin. Thioredoxin is a compact globular protein with five beta sheets forming a hydrophobic core surrounded by four alpha helices on the external surface. The active site contains a – CGPC– conserved sequence.

Thioredoxin reductase (TR) is a member of the pyridine nucleotide-disulfide oxidoreductase family (Williams, 1995). Enzymes in this family such as glutathione reductase, lipoamide dehydrogenase, and trypanothione reductase form homodimers, and each subunit contains a redox-active disulfide bond and a tightly bound flavin adenine dinucleotide. Whereas Trx has been relatively conserved during evolution, mammalian TRs are very different in structure from bacteria, fungi and plants (Luthman and Holmgren, 1982; Holmgren, 1989). Mammalian TRs are larger (55 kDa vs. 35 kDa) with broad substrate specificity. In addition to the conserved redox catalytic site – C^{59}VNVGC^{64}– mammalian TR contains a C-terminal extension of 16 residues carrying a penultimate selenocysteine (SeC) residue in the conserved sequence motif –GC^{497}SeC^{498}G– (Zhong et al., 1998; Gladyshev

et al., 1996). A primary reduction of the $-C^{59}-C^{64}-$ disulfide bridge in the catalytic redox-active site by NADPH via FAD is followed by a transfer of electrons to the $-C^{497}SeC^{498}-$ redox center (Zhong et al., 2000; Williams et al., 2000). After reduction, the C-terminal tail moves away from the catalytic site to a position at the surface of the enzyme where the selenolate anion can attack the disulfide of the Trx (Sandalova et al., 2001).

Using small thiol-containing molecules (Shaked et al., 1980), a relationship between the redox potential of the enzyme and the pKa of the N-terminal active site residue has been established for the thioredoxin superfamily of proteins (Grauschopf et al., 1995) as predicted by the Brønsted relationship. With the Nernst equation, the standard state redox potential $E^{o'}$ for a protein can be calculated from the equilibrium constant of the redox reaction involving a reference with known redox potential. The commonly used references are defined GSH/GSSG buffers or NADPH/NADP+ coupled via an appropriate reductase (Gilbert, 1990). Determination of redox potentials by direct protein-protein equilibrium has also been developed (Aslund et al., 1997). Standard state redox potentials within the thioredoxin family of thiol-disulfide oxidoreductases range from $E^{o'}$ = -124 to -270 mV (Aslund et al., 1997). *E. coli* thioredoxin with a pKa of ~7.4 at Cys^{32} has a redox potential of -270 mV (Krause and Holmgren, 1991) lying between the extremely reductive NAPDH at $E^{o'}$ = -315 mV and GSH at $E^{o'} \approx$ -205 to -260 (for review see Aslund et al., 1997) (Figure 2.2). The chemistry surrounding the active site cysteine residues of thioredoxin creates an enzyme that is posed to donate its electrons.
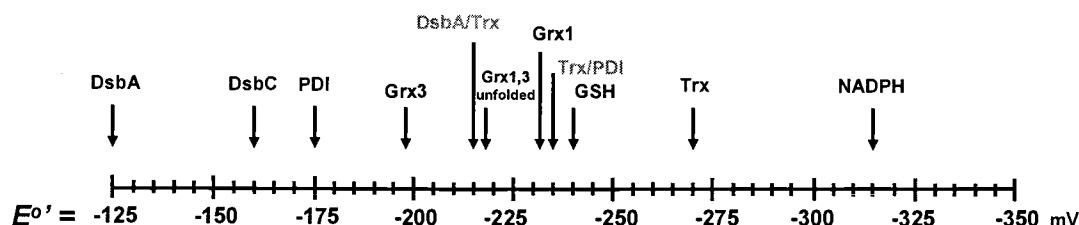
Figure 2.2   Overall scheme of standard state redox potentials of the thioredoxin family of thiol-disufide oxidoreductases. DsbA/Trx has the active site of DsbA mutated from –CPHC– to the Trx –CGPC– and Trx/PDI has the active site of Trx mutated from –CGPC– to the PDI –CGHC– (Adapted from Aslund et al., 1997).

Disulfide bonds in the active sites of protein disulfide oxidoreductases function in various redox reactions. The thioredoxin superfamily of enzymes, including the families of Trx, glutaredoxin, PDI, DsbA and their homologs share a sequence motif of $-CX_1X_2C-$ at their active sites (see Table I). The two cysteine residues can undergo reversible oxidation-reduction by shuttling between a dithiol and a disulfide form in the catalytic process as described above. The following is a description of these enzymes.

2.2   Glutaredoxin

2.2.2.1   Localization and Function

Glutaredoxin (formerly called thioltransferase) was discovered as a GSH-dependent hydrogen donor for ribonucleotide reductase in *E. coli* mutants lacking the first identified electron donor, thioredoxin (Holmgren, 1976) in the cytosol. Glutaredoxins exist in all prokaryotic and eukaryotic cells containing GSH. *E. coli* contains at least three different glutaredoxins: Grx1, Grx2 and Grx3 (Aslund et al., 1994). Glutaredoxins have been

identified in yeast (Rodriguez-Manzaneque et al., 2002), as well as mammalian species (Padilla et al., 1995; Katti et al., 1995).

The glutaredoxin system includes glutaredoxin, GSH, NADPH, and glutathione reductase. The glutaredoxin system complements the Trx system as an alternative electron donor system (Holmgren, 1989). Glutaredoxin is distinguished from thioredoxin by the ability to be reduced by GSH. Glutaredoxin selectively deglutathionylates protein-glutathione mixed disulfides (ProSSG) (Bushweller et al., 1992; Gravina and Mieyal., 1993; Yang et al., 1998). Because ProSSG are a prevalent form of cysteine modification in cells during oxidative stress (Chai et al., 1994; Rokutan et al., 1994; Rahman et al., 1995), glutaredoxin plays a key catalytic role in redox-regulation of various cellular processes that involve glutathionylated proteins. This dependence on GSH may serve important redox regulatory functions in several different processes including redox control of transcription factors (Bandyopadhyay et al., 1998), protection from oxidative stress after cadmium exposure (Chrestensen et al., 2000) or regulation of enzyme function, such as in the case with HIV-1 protease (Davis et al., 1997).

2.2.2.2   *Structure and Characteristics*

Glutaredoxins belong to the thioredoxin superfamily of structurally similar thiol-disulfide oxidoreductases. All glutaredoxins contain (1) a conserved highly specific binding site for GSH and (2) the characteristic structural feature of these enzymes, the active site sequence –CPYC– (Hoog et al., 1983) in the thioredoxin fold motif (Qin et al., 2000) (Figure 2.3). The solvent accessible surface area at the active site of reduced *E. coli*

glutaredoxin is increased compared to the oxidized form, which may be important for its function (Xia et al., 1992).
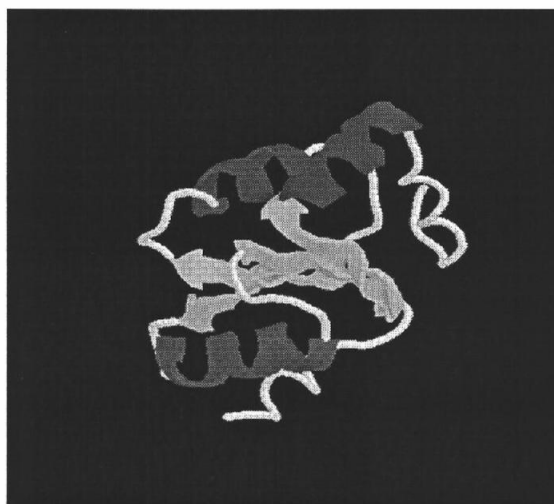
Figure 2.3   NMR Structure of Human Glutaredoxin. Glutaredoxin is a globular protein with four beta sheets forming a hydrophobic core surrounded by three alpha helices maintaining a thioredoxin fold-like structure. In addition to the active site sequence –CPYC–, glutaredoxin contains a highly specific binding site for GSH.

The redox potentials of *E. coli* Grx1 (-233 mV) and Grx3 (-198 mV) are both higher than GSH (-240 mV), and are both higher than Trx (-270mV) (Aslund et al., 1997). One consequence of the difference in redox potential is that Grx1 is a 15-times better disulfide reductant than Grx3, which explains why Grx3 has 5-8% the activity of Grx1 as a hydrogen donor for ribonucleotide reductase (Aslund et al., 1996). The pKa value of the sulfhydryl group of the N-terminal cysteine residue (Cys^{22}, pKa = 3.8) in the –CPYC– sequence is much lower than that of normal cysteine (pKa = 8.5 ±0.5) (Papayannopolos et al., 1989; Sun et al., 1998). It is this cysteine residue that is essential for catalytic activity. The role of Arg^{26} is to facilitate the low pKa of Cys^{22} by enhancing its S-nucleophilicity necessary for the

catalytic reaction (Yang and Wells, 1991). GSH binding is primarily via electrostatic interactions (Bushweller et al., 1994; Yang et al., 1998).

2.2.3   Dsb and Protein Disulfide Isomerase

2.2.3.1   *Prokaryotic Protein Disulfide Isomerase (Dsb Family)*

The disulfide-bond forming enzymes in prokaryotes, known as the Dsb (disulfide bond) proteins have a single thioredoxin active site and are localized to the periplasmic space (Rietsch and Beckwith, 1998). The *E. coli* Dsb family of proteins contains the active site sequence –CPHC– and the general thioredoxin fold motif. The best characterized protein is DsbA, a soluble monomeric 21 kDa molecule that functions as an oxidant, donating its unstable active site disulfide bond to substrate protein thiols (Zapun et al., 1998). DsbA is reoxidized in the periplasm by the inner membrane protein DsbB, which is in turn oxidized by components of the electron transport pathway (Bader et al., 1999). DsbC is a soluble 23 kDa homodimer that, like DsbA, contains an unstable active site disulfide bond (Zapun et al., 1995). DsbC is maintained in the reduced state by the inner membrane protein DsbD, which is in turn reduced by cytoplasmic thioredoxin (Rietsch et al., 1997). DsbG, also a homodimer, has been identified as a homolog of DsbC that is also reduced by DsbD (Bessette et al., 1999).

DsbA is the strongest protein oxidant for the formation of disulfides yet known and is involved in catalyzing protein folding in the periplasm. The oxidative force of DsbA is supported by experimental quantification of the extremely low pKa of 3.5 of the N-terminal nucleophilic thiol Cys^{30} and the redox potential of -122 mV (Nelson and Creighton, 1994; Kortemme and

Creighton, 1995). It has been suggested that the stabilization of the thiolate anion of Cys^{30} is due to its favorable electrostatic interaction with the helix dipole of the active site α-helix (Schirra et al., 1998).

In both prokaryotic and eukaryotic cells, the formation of disulfide bonds is sequestered within a specialized compartment and catalyzed by enzymes from the thioredoxin superfamily. The eukaryotic equivalent to Dsb, PDI, was first isolated from the endoplasmic reticulum. Due to the high similarity between the active-site domains of PDI and thioredoxin, it is commonly assumed that eukaryotic PDI and thioredoxin share a common ancestry (Sahrawy et al., 1996; Kanai et al., 1998). Phylogenetic analyses support common ancestry of all eukaryotic PDIs from a thioredoxin ancestor and independent duplications of thioredoxin-like domains within PDIs throughout eukaryotic evolution (McArthur et al., 2001). Other than the single domain Dsb family found in prokaryotes, eukaryotic PDIs can be classified into four groups: PDI1, PDI2, PDI3 and PDI4. PDIs 1 and 2 have two Trx-like active site domains and PDIs 3 and 4 have three. PDI1 includes mammalian and yeast PDI and ERp57, PDI2 includes P5, PDI3 includes ERp72, and PDI4 includes PDIR (Kanai et al., 1998). A comparison of the prokaryotic and eukaryotic families is presented in Table I, the thioredoxin superfamily proteins.

2.2.3.2   *Eukaryotic Protein Disulfide Isomerase*

2.2.3.2.1   LOCATION

Eukaryotic PDI is primarily localized in the lumen of the endoplasmic reticulum (ER), where it participates in the folding of newly synthesized

proteins (Gilbert, 1997; Noiva, 1994; Freedman et al., 1989) and serves as a chaperone (Wang, 2002; Delom et al., 2001; Lumb and Bulleid, 2002). It is highly abundant in the ER lumen constituting approximately 0.8% of total cellular protein (Freedman et al., 1994) and reaching near-millimolar concentrations in the ER in some tissues (Zapun et al., 1992). The family of PDIs (shown in Table I) is composed of several well characterized proteins formed by multiple domains, each representing the typical fold of thioredoxin (Ferrari and Soling, 1999; Turano et al., 2002). All of the proteins of the family are present in the ER and while some exert the activities exclusively here, some of the family members have a different subcellular distribution and have activities that differ from those displayed in the lumen of the ER.

Proteins of the PDI-family have been found outside the cell either as secreted proteins or proteins located on the cell surfaces. PDI has been found secreted from a variety of cell types including hepatocytes (Terada et al., 1995; Akagi et al., 1988), pancreatic cells (Yoshimori et al., 1990), endothelial cells (Hotchkiss et al., 1998) and platelets (Essex et al., 1995). PDI has also been detected at the surface of plasma membrane of several cell types such as B-lymphocytes (Kroning et al., 1991) and thyroid cells (Couët et al., 1996) where it is involved in a variety of functions related to the thiol groups of surface proteins.

PDI activity has been detected at the outer membrane level of rat liver mitochondria (Rigobello et al., 2000; 2001). In addition to the thioredoxin peroxidase/thioredoxin reductase (localized in the matrix) and glutathione peroxidase/glutathione reductase, the presence of PDI can play a role in the redox control of mitochondrial membrane thiols and hence membrane permeability.

It has been suggested that PDI is present in the nucleus. PDI has been detected among the proteins from the nuclear matrix of human lymphocytes and monocytes (Gerner et al., 1999), although contamination from the cytosolic or ER compartments is possible. Recently, VanderWaal et al. (2002) showed that PDI could be cross-linked to DNA after exposure to cisplatin in nuclei isolated from HeLa cells. PDI lacks a known nuclear localization signal, so its mechanism of import is not clear.

2.2.3.2.2 STRUCTURE AND CHARACTERISTICS

The three dimensional structure of intact PDI is not yet available, but its primary structure and tertiary domain structures reveal a modular protein consisting of multiple domains (Figure 2.4). PDI1 (hereafter referred to as PDI) is a modular protein consisting of four domains, **a**, **b**, **b'**, and **a'**, plus an acidic C-terminal extension, **c** (Kemmink et al., 1997).
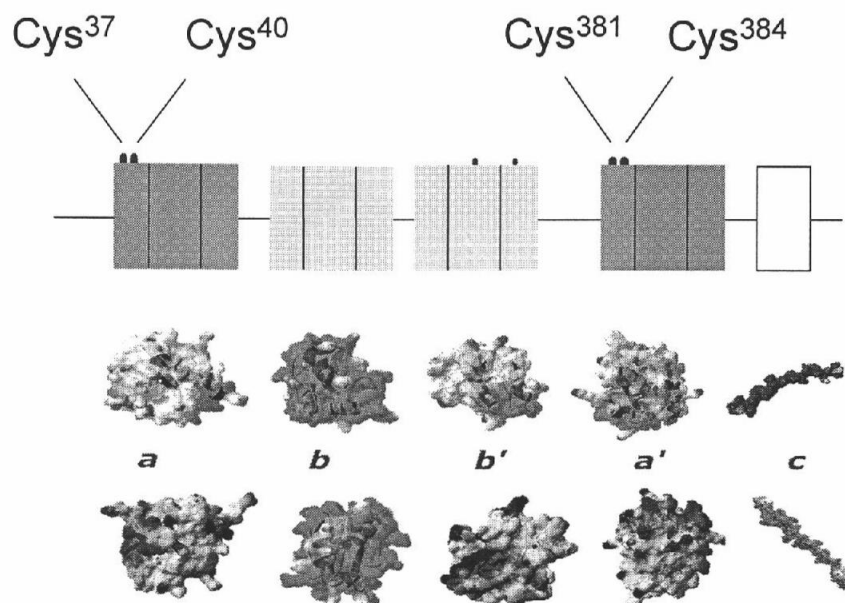
Figure 2.4   The Modular Domains of PDI. Electrostatic surface of the individual domains of protein disulfide isomerase. The NMR structures of the **a** (Kemmink et al., 1996) and **b** (Kemmink et al., 1999) domains are shown. The hypothetical structures for **b'** and **a'** were constructed by homology modeling. The acidic c-terminal tail (c) is likely unstructured (modeled structures are courtesy of HF Gilbert's website).

The NMR structure of the **a** domain (and **a'** domain by sequence homology) shows sequence similarity to thioredoxin, contains the catalytic site motif –CGHC–, and has the thioredoxin fold (Kemmink et al., 1996; 1997) (Figure 2.5a) The **b** and **b'** domains show no amino acid sequence similarity to thioredoxin and have no catalytic site sequence, but NMR studies have indicated that the **b** domain (and by homology the **b'** domain) also has the thioredoxin fold (Freedman, 1999; Kemmink et al., 1999) (Figure 2.5b).

A   **B**
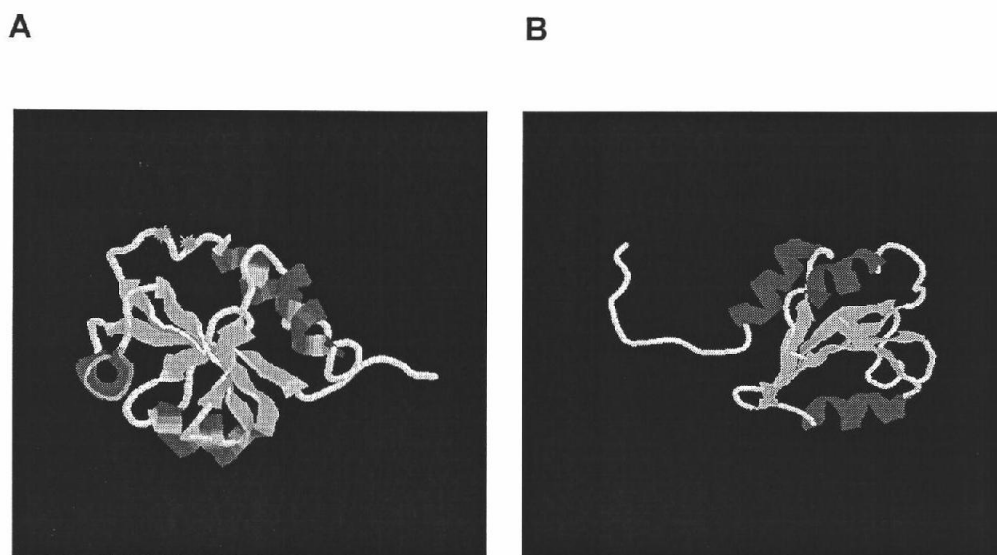
Figure 2.5   NMR structures of domains **a** and **b** of human PDI. Panel **A** shows the **a** domain contains a five-stranded beta sheet hydrophobic core surrounded by four alpha helices in the typical thioredoxin fold motif. The green dots indicate the cysteine residues in the –CGHC– active site sequence. Panel **B** shows the **b** domain containing five-stranded beta sheet hydrophobic core surrounded by three alpha helices. The **b** domain does not contain a catalytic sequence.

PDI is also capable of binding proteins and peptides. For binding small peptides, the **b'** domain is essential and sufficient. For larger peptides, nonnative proteins such as scrambled RNase, and the interaction as a subunit of prolyl-4-hydroxylase, the **a'** domain contributes significantly to the binding performed by the **b'** domain and the **b** and **a** domains enhance binding (Pirneskoski et al., 2001).

The acidic **c** domain contains the –KDEL sequence, which is commonly found in proteins retained in the ER. The **c** domain has a putative low-affinity, high capacity Ca^{2+} binding site. PDI has been noted to be sensitive to Ca^{2+} levels in the ER and has been shown to interact with Ca^{2+} dependent proteins such as calreticulin and Ero1 (Frand and Kaiser, 1999).

These interactions may play a role in the chaperone/antichaperone activities of PDI.

The N-terminal cysteine residue in each active site of PDI (Cys^{37} and Cys^{381} by recombinant rat PDI numbering) has a pKa of 4.5, and is stabilized partly by the nearby histidine imidazole group within the –CGHC– sequence and partly by partial positive charges at the N-terminus of the α-helix occurring just after this cysteine (Kortemme et al.; 1996, Ferrari and Soling, 1999). The second cysteine residue (Cys^{40} and Cys^{384}) has a higher pKa of 8.5, more representative of free cysteine. The second cysteine in each active site domain is required for net oxidation of substrate proteins *in vitro*, but its role *in vivo* may be to facilitate disruption of intermolecular disulfides, allowing efficient scanning of several disulfide isomers and preventing trapping of PDI in disulfide linked complexes (Walker and Gilbert, 1997; Schwaller et al., 2002). The disulfide form of PDI is much less stable than the corresponding disulfide of thioredoxin (Dyson et al., 1997). This is reflected in the oxidative function of PDI in contrast to the reductive role of thioredoxin. When PDI is reduced to the dithiol state, the more N-terminal cysteine residue of each pair is predominantly in the thiolate anion form at physiological pH (Hawkins and Freedman, 1991).

The standard redox potential of PDI is approximately -180 mV, much more oxidizing than that of thioredoxin (-270 mV) yet less oxidizing than DsbA (-122 mV) (Figure 2.2) (Lundstrom and Holmgren, 1993; Aslund et al., 1997). The difference is due to the nature of the two intervening residues of the –CGHC– sequence (Lundstrom and Holmgren, 1993).

There is evidence that the two sites, **a** and **a'**, do not contribute equally to catalysis. The **a** domain contributes more to isomerase activity whereas the **a'** domain affects substrate recognition and steady-state binding of the substrate (Lyles and Gilbert, 1994). This unequal contribution to folding by these domains (equal in redox character) indicates that tertiary/quaternary structures bestow unique characteristics to chemically equal domains.

2.2.3.2.3   FUNCTION

The mammalian PDI family encompasses several highly divergent proteins some of which are listed in Table I. PDI is a multifunctional protein catalyzing the reduction, formation and isomerization of disulfide bonds. PDI acts as a molecular chaperone/antichaperone and serves as a component of the enzymes prolyl-4-hydroxylase and of microsomal triglyceride transfer protein.

PDI constitutes one of several classes of well characterized accessory proteins that catalyze the folding of nascent membrane and secreted polypeptides synthesized in the ER (Bulleid and Freedman, 1988; 1990; Boston et al., 1996). PDI catalyzes disulfide formation (oxidative folding activity) as well as the rearrangement of incorrect disulfide pairings (isomerase activity) (Gilbert 1998), accelerating both processes without drastically altering the refolding pathway. The oxidative folding activity of PDI or chaperone is dependent upon the oxidizing environment of the ER and upon the molar ratio of PDI to disulfide bond-containing proteins (Gilbert 1997; Wang and Tsou, 1998). For PDI to isomerize a disulfide, the active site of reduced PDI must first attack a substrate disulfide (Lambert and Freedman, 1983), then two mechanisms can accomplish disulfide

isomerization (Figure 2.6): (1) an intramolecular rearrangement of the substrate while bound to PDI as a disulfide and/or (2) multiple cycles of disulfide reduction and reoxidation in a different orientation (Schwaller et al., 2002). GSH inhibits the reduction/reoxidation pathway by depleting oxidized PDI that is required to reoxidize the reduced substrate in the second mechanism. The redox potential of ER is reflected in the ratio of reduced to oxidized glutathione (GSH/GSSG ranging from 1:1 to 3:1) (Hwang et al., 1992). Under reducing conditions and in the presence of an abundance of disulfide bond-containing proteins, PDI facilitates protein aggregation, an activity proposed to be a protective mechanism for unfolded proteins in stressed cells (Gilbert 1997). The contribution of intramolecular isomerization of the substrate compared to cycles of reduction or reoxidation will be governed by how fast the intramolecular rearrangement of the substrate occurs compared to the clock that is set by PDI's second active site cysteine (Schwaller et al., 2002).

PDI associates with peptides or proteins functioning as a chaperone (Noiva et al., 1993; Holst et al., 1997; Klappa et al., 1998; 2000). A chaperone is a protein that can assist unfolded or incorrectly folded proteins in attaining their native state by providing a microenvironment, which prevents losses due to competing aggregation reactions. PDI may also perform as an antichaperone by facilitating aggregation of non-native proteins (Puig and Gilbert, 1994; Puig et al., 1994). There is evidence that PDI acts as a redox-dependent chaperone to unfold the cholera toxin A1 fragment, thereby facilitating retrograde transport of the protein from the ER into the cytosol (Tsai et al., 2001). When PDI is reduced, it binds to the substrate and when oxidized it is released. On the contrary, other lines of evidence show that the chaperone activity of PDI is independent from its thioredoxin-like active site. Adding reducing agents (Cai et al., 1994),

alkylating agents (Quan et al., 1995; Yao et al., 1997), or mutating active site cysteine residues (Vuori et al., 1992) does not prevent either chaperone activity or protein binding. Further studies by Lumb and Bulleid (2002) have been able to disrupt the interaction between PDI and P4H by the addition of GSSG and suggest that the GSSG-dependent dissociation of PDI from cholera toxin can be explained by peptide competition rather than an effect on the redox state of PDI. The sensitivity of PDI to the redox state of its environment does implicate PDI as a redox-controlled protein.
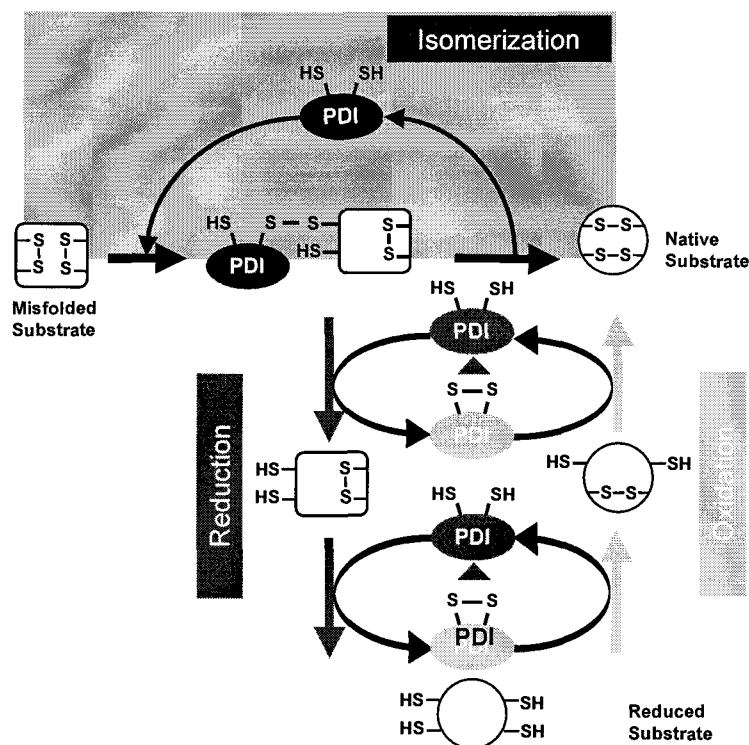
Figure 2.6 Mechanism of PDI-catalyzed disulfide isomerization. Two alternative pathways can accomplish disulfide isomerization. The top (blue) pathway represents an intramolecular rearrangement of the substrate while bound to PDI as a disulfide. The lower pathway (yellow) represents cycles of disulfide reduction and reoxidation in a different orientation. GSH (red) inhibits the reduction/reoxidation pathway by depleting oxidized PDI required to reoxidize the reduced substrate. (Schwaller et al., 2002)

Prolyl 4-hydroxylase (P4H) catalyzes the formation of 4-hydroxyproline in collagens and other proteins with collagen-like sequences. P4H is an enzyme present in the lumen of the ER and exists as a heterotetrameric ($\alpha 2\beta 2$) protein containing two PDI molecules as β subunits (Pihlajaniemi et al., 1987). The function of PDI may be the retention or stabilization of the complex in the ER (Myllyla et al., 1989; Vuori et al., 1992) by keeping the highly insoluble α subunits in a catalytically non-aggregated conformation. Although the active site cysteines are inaccessible in the complex and PDI isomerase activity is reduced by 50%, the interaction between the α and β subunits is independent of the active-site cysteines (Vuori et al., 1992). PDI is also the β subunit of the heterodimeric microsomal triglycerol transfer protein, which facilitates the incorporation of triglycerols into lipoproteins (Wetterau et al., 1990). PDI is necessary to keep the complex in solution as irreversible inactivation and aggregation ensues upon removal of the β subunit (Wetterau et al., 1991).

Other functions of PDI include the ability to reduce dehydroascorbate (Wells et al., 1990); high capacity, low affinity binding to the hormones estradiol and 3,3',5-triiodo-l-thyronine (T3) (Primm and Gilbert 2001; Guthapfel et al., 1996); and rearrangement of disulfides that may initialize the cascade of platelet aggregation via the fibrinogen receptor (Essex et al., 2001). The role of PDI on the cell surface ranges from reducing surface thiols to interacting with other surface-located proteins and regulation of adhesion (for review see Turano et al., 2002). The role of PDI in the nucleus and in DNA interactions is just beginning to be understood. PDI is upregulated during stress and its role in transcription may be related to the redox state of transcription factors such as Fos and Jun (Ueno et al., 1999; Hu et al., 2002) required to bind DNA.

Proteomic studies are beginning to show alterations of PDI levels *in vivo*. In the correlation of clinical data with proteomic profiles of patients with B-cell chronic leukemia, patients with shorter survival times exhibit increased levels of redox enzymes including PDI (Voss et al., 2001). Changed levels of redox enzymes including PDI may or may not correlate with drug resistance. The protein expression profiles in ductal carcinoma versus normal breast tissue showed increased expression of PDI as well (Bini et al., 1997).

2.3 Modification of Thiols

The concept of redox regulation has emerged to accommodate a rapidly growing body of evidence that cellular redox status regulates individual aspects of cellular function (Nakamura et al., 1997). A range of cysteine modifications exists that induce biological signals on one hand and underlie toxicity on the other (Stamler and Hausladen, 1998).

2.3.1 Reversible Modification

Cysteine (and methionine) residues of proteins are by far the most sensitive to oxidation by reactive oxygen species (ROS) (for review see Stadtman, 2001). Unlike other amino acid oxidation reactions, however, the primary oxidation products of cysteine residues to form protein disulfides can be repaired by disulfide exchange reactions carried out by the glutaredoxin system or thioredoxin system to regenerate the protein sulfhydryl groups. Redox regulation through modifications of proteins has emerged as one of the major cellular responses to oxidative and nitrosative stresses. A wide range of reversible modifications to protein thiols is identified as S-

glutathionylation, S-nitrosation, S-nitration, sulfenic acid, and inter- and intramolecular disulfide.

2.3.1.1 S-Glutathionylation

Formation of mixed disulfides between glutathione and the cysteines of some proteins (glutathionylation) has been suggested as a mechanism through which protein functions can be regulated by the redox status. One example was presented by Fratelli and coworkers (2002) where they used proteomic profiling to identify glutathionylated proteins in oxidatively stressed human T lymphocytes. Glutathione thiosulfinite (GS(O)SG) is formed from many reactive oxygen and nitrogen species and may also play a role in integrating both the oxidative and nitrosative cellular responses through thionylation of thiols (Huang and Huang, 2002). There are many reports in the literature showing a correlation between increased oxidative stress and the formation of protein mixed disulfides at the expense of GSH both in the cytosol and in mitochondria (for review see Reed, 1985).

2.3.1.2 S-Nitrosation

Nitric oxide (NO) can exert its effects by covalently modifying or oxidizing critical protein thiols (S-nitrosation) or transition metals (S-nitrosylation) associated with proteins (Stamler 1995; Stamler et al. 1997). Additionally, nitrative stress results from covalent modification by peroxynitrite (OONO-, the product of NO and superoxide). Excessive or uncontrolled nitrosation can lead to the loss of cellular function, inducing nitrosative stress. Thiols in proteins can recognize both nitrosative and oxidative events and moreover, can distinguish between them. Either

monothiols or dithiols serve different sensory and regulatory functions, or particular chemical modifications of thiols (nitrosation versus oxidation) elicit distinct functional changes, or both (Xu et al., 1998). The presence of polynitrosated proteins *in vivo* (Simon et al., 1996) strengthens this hypothesis and parallels a similar modulation of protein function by phosphorylation. The important players in nitrosative stress (NO and S-nitrosated glutathione, GSNO) and nitrative stress (OONO-) deserve attention as oxidants of cysteine thiols. These compounds react with reduced cysteine residues to give the S-nitrosothiol (RSNO) and/or sulfenic acid products, or in the presence of additional thiols, mixed disulfide bonds (Stamler and Hausladen, 1998). In biological systems GSNO is formed primarily by nitrosation of GSH with NO generated by NO synthase in the presence of oxygen which produces N_2O_3 as an electrophilic nitrosating agent (Huang and Huang, 2002). GSNO undergoes transnitrosation with another thiol to form GSH and another RSNO.

2.3.1.3   Protein Sulfenic Acids

Sulfenic acid (RSOH) is the most simple organosulfur oxyacid and is generally very unstable and highly reactive in contrast to sulfinic (RSO_2H) and sulfonic acids (RSO_3H), which are quite often stable compounds (Claiborne et al., 1993). Protein sulfenic acids (PSOH) are generated as reversibly oxidized cysteinyl residues formed on reactions of thiols with peroxides, nitric oxide, peroxynitrite and other reactive or nitrogen species (Stamler and Hausladen, 1998). Hydrolysis of nitrosothiol groups also generates the PSOH and HNO (Percival et al., 1999).

Sulfenic acid formation in enzymes and transcriptional regulators is well documented and clearly an important component of redox sensitive catalysis and regulation in many systems (Poole, 2002). While PSOH can be a stabilized redox form in these proteins, it can also readily react with proximal thiol groups of other cysteines or external agents to form disulfide residues. PSOHs are readily reducible by cellular thiols; however, cysteine sulfenic acids can be further oxidized to the irreversible form of cysteine sulfinic and sulfonic acid forms (Claiborne et al., 1999). The use of selected enzyme digestion and mass spectrometry has demonstrated that peroxiredoxins can be irreversibly oxidized at the active-site cysteine into cysteine sulfinic or sulfonic acid. This kind of analysis provides a useful marker of oxidative damage to the cells (Wagner et al., 2002).

2.3.2   Irreversible Modification

In addition to the oxidation of sulfenic acid into irreversible modifications of thiols due to oxidative stress, other chemicals have been implicated as irreversible thiol modifiers in the active sites of proteins. Several studies have demonstrated a correlation between cellular toxicity of *cis*-diamminedichloroplatinum (II) (cisplatin or CDDP) and inhibited intracellular activity of the thioredoxin system (Arner et al., 2001). Resistance to CDDP, an effective antitumor agent widely used in chemotherapy, confers an increased cellular activity of the Trx system. CDDP or the metabolite GS-Pt (a glutathione conjugate of CDDP) is assumed to alkylate the penultimate selenocysteine residue of thioredoxin reductase as demonstrated with other electrophilic compounds including 1-chloro-2,4-dinitrobenzene (Nordberg et al., 1998), bromoacetate (Gorlatov and Stadtman, 1998), and biotin conjugated iodoacetamide (Kim et al., 2000). GS-Pt was also found to inhibit glutaredoxin (Arner et al., 2001) similar to inhibition by other compounds

such as cadmium (Chrestenson et al., 2000); however, the mechanism of inactivation at the active site cysteine has yet to be identified.

Covalent modification of a cysteine residue present in the ATP binding pocket of epidermal growth factor receptor (EGFR) tyrosine kinase and erbB2 tyrosine kinase is the mechanism employed to arrest these enzymes implicated in the development and progression of certain human cancers (Fry et al., 1998). The 5-tryptamine-4,5-dione (T45D) is formed as a result of oxidation of 5-hydroxytryptamine by superoxide, NO, and peroxynitrite due to methamphetamine (MA) induced serotonergic energy impairment. Conjugation of T45D with GSH inhibits TPH by covalent modification of one or more active site cysteine residues (Wrona and Dryhurst, 2001). While evidence of T45D in MA treated brains has not been reported, T45D also inhibits mitochondrial NADH-coenzyme Q1 reductase (complex I) and cytochrome oxidase (complex IV) probably by covalent modification of active site cysteine residues of these enzyme complexes (Jiang et al., 1999).

Modifications of cysteine residues of phosphatidylinositol transfer protein showed that a buried cysteine that constituted part of the binding site could undergo covalent modification only upon association of the protein with a membrane and that such modification resulted in the loss of lipid transfer activity (Tremblay et al., 2001). Chemical modification of a reactive cysteine residue at the subunit interface of *Plasmodium falciparum* triose-phosphate isomerase can lead to a large structural perturbations and concomitant loss of enzymatic activity that can lead to development of parasite-specific therapeutic agents (Maithal et al., 2002).

In a search for antagonist ligands of the peroxisome proliferator activated receptor-γ (PPARγ), Leesnitzer and coworkers (2002) identified a conserved cysteine residue in the ligand binding site as the site of covalent modification. Acrolein, a reactive α,β-unsaturated aldehyde, is a common environmental pollutant, a metabolite of the anticancer drug cyclophosphamide, and a by-product of lipid peroxidation. Acrolein is a potent inhibitor of cell proliferation and may act through effects on redox-regulated transcription factors including NF-kB activation (Horton et al., 1999) and AP-1 activity (Biswal et al., 2002). The mechanism of AP-1 inhibition correlates with changes in the cellular redox state as well as covalent modification of Jun (a subunit of AP-1) by acrolein.

There is a general trend of cysteine modification within the thioredoxin superfamily that is subject to the $-CX_1X_2C-$ sequence within in the thioredoxin fold active site motif. Studies with Trx (Holmgren, 1985; Meyer et al., 1994), Grx (Gan and Wells, 1987; Gladyshev et al., 2001) and PDI (Hawkins and Freedman; 1991) all show a decrease or inhibition of activity after incubation with the thiol alkylating agents iodoacetamide or iodoacetic acid with a concomitant decrease in protein thiol levels. Erve et al. (1995a) determined that the N-terminal cysteine in the active site of *E. coli* thioredoxin is alkylated by the episulfonium derived from the GSH conjugate of 1,2-dichloroethane. The N-terminal cysteine residue of these proteins is a candidate for modification due to its lowered pKa and thiolate formation whereas the C-terminal cysteine is buried within the protein.

PDI has also been identified as a protein target for adduct formation in toxicological studies. PDI and ERp60 were identified as a target of pyrrolizidine alkaloid monocrotaline, a phytotoxin used experimentally to

cause pulmonary syndrome in rats as a model for studying pulmonary hypertension in humans (Lame et al., 2000). PDI has been implicated in halothane hepatitis along with other adducted proteins (Pohl et al., 1989; Martin et al., 1993a; 1993b). Autoantibodies to PDI were detected in rats exposed to D-galactosamine, acetaminophen or carbon tetrachloride when the latter two were combined with diethylmaleate (Nagayama et al., 1994). In a proteomic study, PDI, ERp29, P5 and ERp57 were identified among seven proteins in the ER as targets for the reactive metabolites of bromobenzene (Koen and Hanzlik, 2002).

In light of the evidence pointing to the vulnerability of the active site cysteine residues of the thioredoxin superfamily in conjunction with the identification of PDI as a possible target of reactive metabolites, a question can be posed regarding the active site of PDI. Are the thiolate anions of PDI preferred targets of electrophiles in the ER or on the cell surface? PDI has been shown to be sensitive to the redox environment both in the cell and at the cell surface. Does PDI serve as a buffer for potentially harmful electrophiles or even for increases in oxidative stress? Is PDI activity in danger of becoming inhibited at the detriment of the cell under toxic insult?

2.4   PROTEOMICS AND MASS SPECTROMETRY

Proteomics is the study of the *proteome*, the protein complement of the *genome*. It is the study of multiprotein systems, in which the focus is on the interplay of multiple, distinct proteins in their roles as part of a larger system or network. This shift from studying individual genes, proteins or small cluster of related components of specific biochemical pathways to thinking about the workings of whole living systems is a result of the

techniques available. In the past, northern blots (for RNA levels) and western blots (for protein levels) were the techniques for mapping the status of a handful of genes or proteins. The development of gene and protein sequence databases paralleled with microarray technology to determine gene expression profiles and mass spectrometry to analyze complex protein mixtures has revolutionized our ability to think in terms of systems biology. The emerging collection of software that can match mass spectrometric data with specific protein databases has facilitated the evolution of proteomics.

The applications of proteomics include mining, protein-expression profiling, protein network mapping and mapping of protein modifications and can be found reviewed by Liebler (2001; 2002). Protein mining is simply identifying all the proteins in a given sample. Protein expression profiling identifies the proteins in a particular sample as a function of a particular state of the organism or cell (e.g., differentiation, developmental state, or disease state) or as a function of exposure to a drug, chemical or physical stimulus. Protein network mapping tries to determine how proteins interact with each other in living systems, such as signal-transduction cascades. Mapping of protein modifications is the task of identifying how and where proteins are modified. Modifications range from common post-translational modifications to xenobiotics and endogenous chemicals that give rise to electrophiles that covalently modify proteins. In this thesis, an attempt is made to characterize modifications targeted at the sulfhydryl groups of cysteine residues with the proteomic tools described below.

2.4.1 Mass Spectrometry of Proteins and Peptides

Mass spectrometry (MS) is a major tool used for proteomic analysis. X-ray crystallography and NMR combined with the information generated by mass spectrometry have created a powerful tool of structure function analysis of proteins. Mass spectrometers have three essential parts, the *source* which produces ions from the sample, the *mass analyzer* that resolves ions based on their mass to charge ratio (m/z) and the *detector* that detects the ions resolved by the mass analyzer (Figure 2.7). The mass spectrometric instruments used for protein and peptide analysis have high resolution or are able to distinguish ions differing in m/z values of at least 1 Da (i.e., the mass of one hydrogen atom). The instruments must be able to detect femtomole (10^{-15} mole) quantities of peptides or less (i.e., high sensitivity) and be able to measure values for peptide ions or their fragment ions as close as possible to their real values (i.e., mass accuracy). Two types of instruments are used for most proteomics MS work: the MALDI-TOF(TOF) instruments and the Electrospray ionization (ESI) tandem MS instruments.

Peptide Digest

Ion Source → Mass analyzer → Ion Detector

Peptide Mass Map

Mass (m/z)
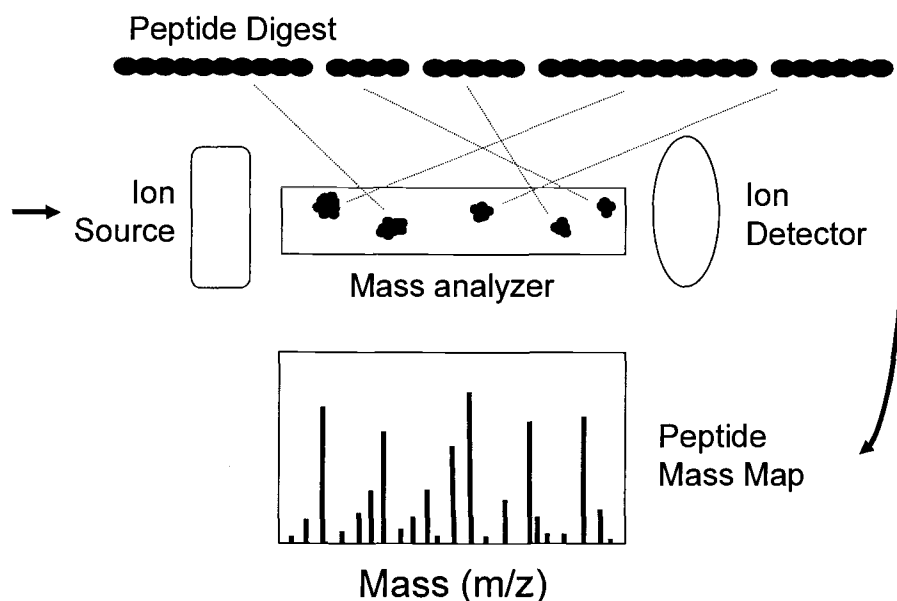
Figure 2.7 Mass spectrometry instrumentation used in protein and peptide analysis. Mass spectrometers have three essential parts, the source which produces ions from the sample, the mass analyzer which resolves ions based on their mass to charge ratio (m/z) and the detector which detects the ions resolved by the mass analyzer. The mass spectrum produced from a protein digest is a peptide mass map.

2.4.1.1   MALDI-TOF MS Instruments

MALDI-TOF is the standard acronym for matrix-assisted laser desorption ionization-time of flight. MALDI refers to the source and TOF refers to the mass analyzer. The sample to be analyzed is mixed with a chemical matrix, which typically contains a small organic molecule with a desirable chromophore that absorbs light at a specific wavelength. The mixture of sample and matrix is spotted onto a small plate and then allowed to evaporate. The resulting crystal lattice contains the integrated peptide or

protein. A laser beam is focused at the sample where the matrix absorbs photons and becomes electronically excited. This excess energy is then transferred to the peptides or proteins in the sample, which are then ejected from the target surface in the gas phase. Smaller molecules such as peptides pick up only one proton to become singly charged. Larger molecules such as proteins can pick up to as many as four protons depending on the size and display a multiply charged spectrum. The ions formed are then extracted and directed into the TOF analyzer. The TOF measures the time it takes the ions to travel from one end of the analyzer to the other and impact on the detector. The speed with which the ions travel through the analyzer tube is proportional to their m/z values. The greater the m/z, the faster they travel. The reflectron focuses ions of the same m/z values and allows them to reach the detector at the same time dramatically improving the resolution of TOF analyzers. Pulse-laser ionization with delayed extraction builds a slight delay between the laser pulse (ionization) and the direction of the ions down the flight tube.

2.4.1.2   ESI MS Instruments

Electrospray ionization (ESI) is generally accomplished by forcing a sample through a flow stream (often from the HPLC) and passing through a stainless-steel cone or needle held at high voltage. As the flow stream exits the needle, it sprays out in a fine mist of droplets. The source then separates the peptide ions from the solvent components and transfers the ions into the mass analyzer. Desolvation can occur in one of two ways. In some sources, the droplets pass through a heated capillary and the solvent evaporates. In others, a curtain of nitrogen gas passes across the spray to cause desolvation. The ions are then drawn into the mass analyzer. A unique characteristic of ESI is the production of multiply charged ions from proteins

and peptides. Many proteins/peptides bear multiple proton accepting sites and can exist as singly or multiply charged ions in solution. This multiple charging of proteins and peptides serves the added purpose of forming ions that are within the mass range of the quadrupole and ion-trap mass analyzers that have a more limited mass range than the TOF analyzers. The ESI spectrum of the intact protein appears as a so-called "multicharge" envelope in which all the charge states of the protein in solution are represented (Figure 2.8).
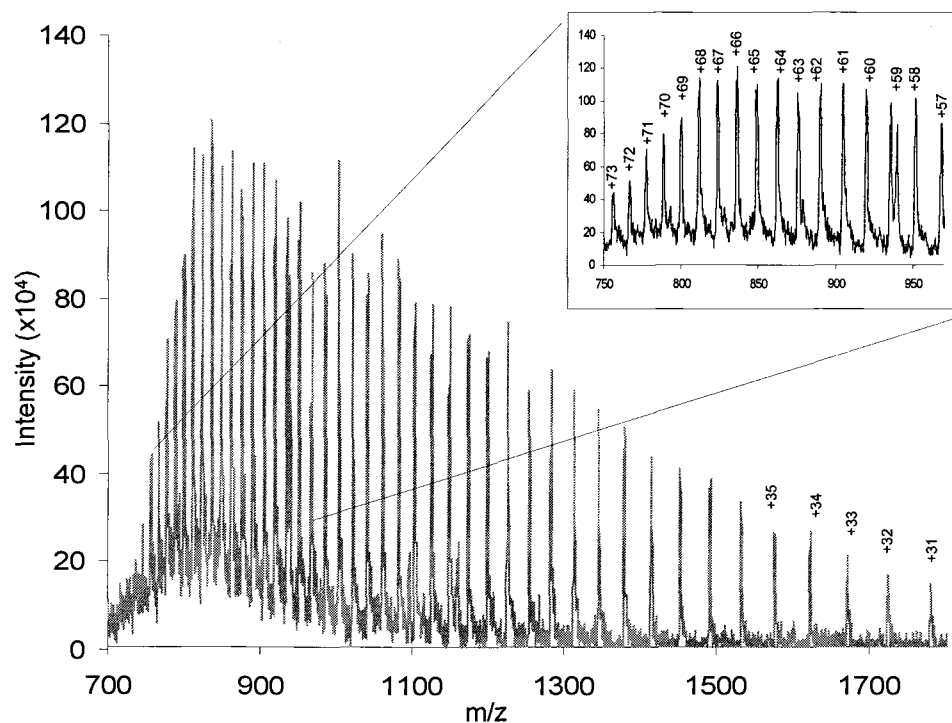
Figure 2.8   LC-MS electrospray spectrum of PDI. All of the charge states of the protein in solution are represented.

2.4.2 Tandem Mass Analyzers for Peptide Sequencing

There are four types of ESI tandem mass spectrometers: the triple quadrupole, ion trap, quadrupole-TOF (Q-TOF) and Fourier Transform-Ion Cyclotron Resonance (FT-MS). The most commonly used tandem mass spectrometers in proteomic work are the triple quadrupole and the ion trap. The MALDI-TOF/TOF can also be used to generate MS/MS spectra.

From a mixture of peptide ions generated from the ESI (or MALDI) source, the tandem MS analyzers select a single m/z species. This ion is then subjected to collision-induced dissociation (CID), which induces fragmentation of the peptide into fragment ions and neutral fragments. The fragment ions are then analyzed on the basis of their m/z to produce a product ion spectrum (Figure 2.9). For peptides and proteins, the polypeptide is fragmented in the CID cell in a predictable way giving rise to an ion series from which the sequence can be deduced. Peptides are fragmented along the protein backbone in specific places yielding diagnostic ion series such as A_n, C_n, X_n and Z_n (Figure 2.10). Nomenclature that identifies a product ion based on whether the C-terminus (y-ion) or N-terminus (b-ion) carries the charge is described by Biemann (1988) and Roepstorff and Fohlman (1984) (Figure 2.11).

Precursor ion Selection

Collision Gas

A^{++}

B^{++} Sample $\longrightarrow$ $\longrightarrow$ CID Cell $\longrightarrow$ b_2^+ $\longrightarrow$ **Fragment ion Spectrum**

C^{++}

b_1^+

b_3^+

Collision Induced Dissociation

MS-1

MS-2
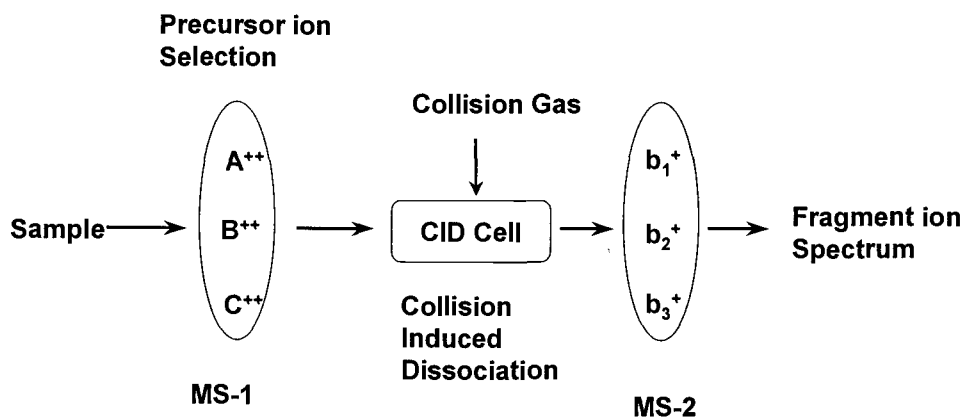
Figure 2.9   Collision induced dissociation used to identify fragment ions
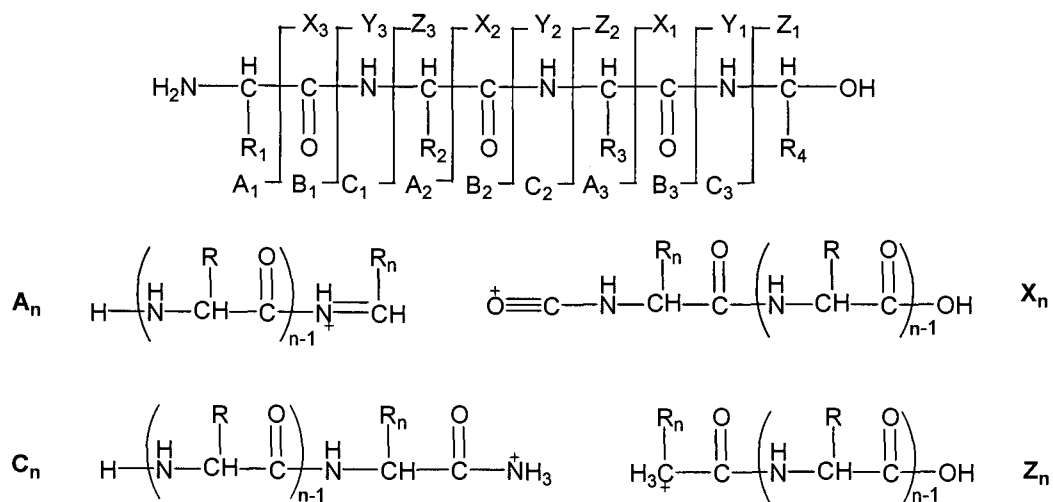
Figure 2.10   Fragment ions resulting from cleavage of peptide backbones
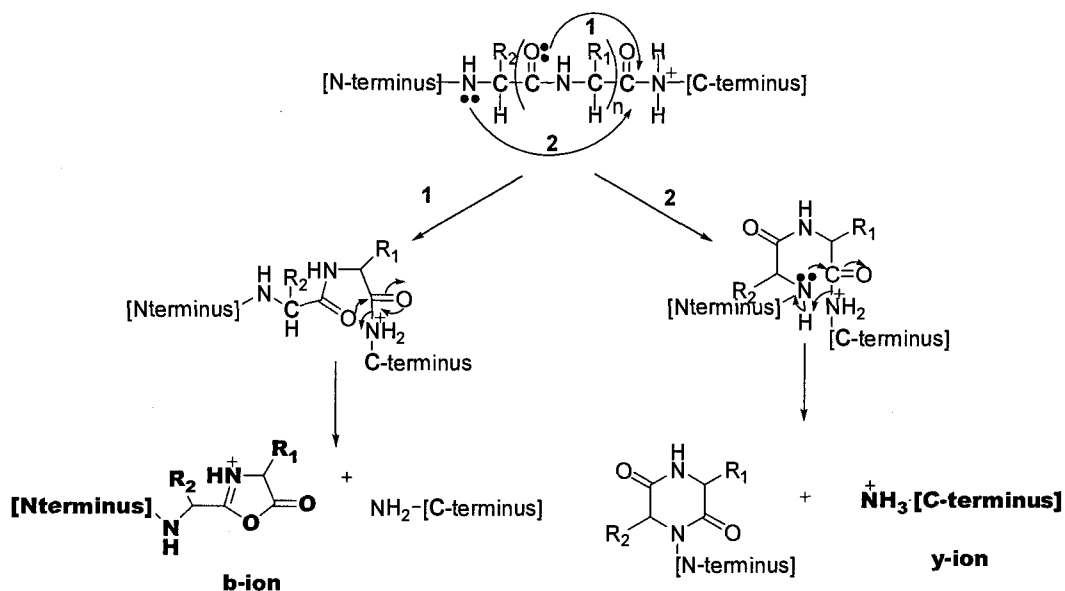
Figure 2.11. Proposed mechanism for the formation of b and y ions.

Triple quadrupole mass spectrometers were the original instruments used for tandem MS. The triple quadrupole instruments (Q1, Q2, and Q3) analyze a full spectrum of ions by passing them through all three quads. To perform MS/MS, Q1 focuses a selected ion into Q2 where collision induced dissociation occurs. The fragment ions are then separated by Q3.

The ion trap collects and stores ions in order to perform MS/MS on them. In full scan mode, the ions in the ion trap are scanned and sequentially ejected on the basis of their m/z values. This produces a full spectrum representing all of the peptide ions in the trap at any given time. Thus, unlike the triple quad, the ion trap produces a series of closely spaced analyses, rather than a continuous analysis. The ion trap detects multiply charged peptide ions formed by ESI as long as their m/z values fall within the mass range limit of the mass analyzer. The ion trap fills with ions from the source and then a particular ion of interest is selected and the trap voltages are adjusted to eject ions of all other m/z values. The remaining ions in the trap

are energized by increasing the trap voltage. This results in low energy CID of the peptide ions with the helium gas atoms in the trap resulting in fragmentation.

The Q-TOF is essentially the same as the triple quad except that the third quadrupole is replaced with a time-of-flight mass analyzer. These analyzers are very fast and capable of very high resolution. FT-ICR is analogous to an ion trap; however, the mass analyzer has a powerful magnetic field and the ions are analyzed by a Fourier transform algorithm.

Tandem mass spectra generated by MALDI-TOF can be generated in two ways. A technique called post-source decay can be used on instruments with a reflectron. The voltage of the reflectron is modulated during analysis to allow the detection of fragments of peptide ions formed during ionization and acceleration down the flight tube. This is not the best MS technique for peptide-sequence analysis. The MALDI-TOF/TOF is equipped with a second source and TOF after the first mass analyzer (TOF). This source offers high energy CID (occurring at kilovolt translational energies) that is believed to operate by electronic excitement. High energy CID differs from low energy CID in that the mass spectra show a broader range of fragment reactions and are relatively insensitive to collision conditions. Low energy CID (occurring at translational energies in the range of tens to hundreds of electron volts) used in the ion trap is believed to work by vibrational excitation and the activated precursor ions have a narrow internal energy distribution. This means the resulting product-ion mass spectra are strongly dependent on experimental conditions such as collision gas pressure and composition, collision energy, and temperature. A comparison of a tandem MS from and ESI-MS/MS versus a MALDI-TOF/TOF MS/MS is shown in Figure 2.12.
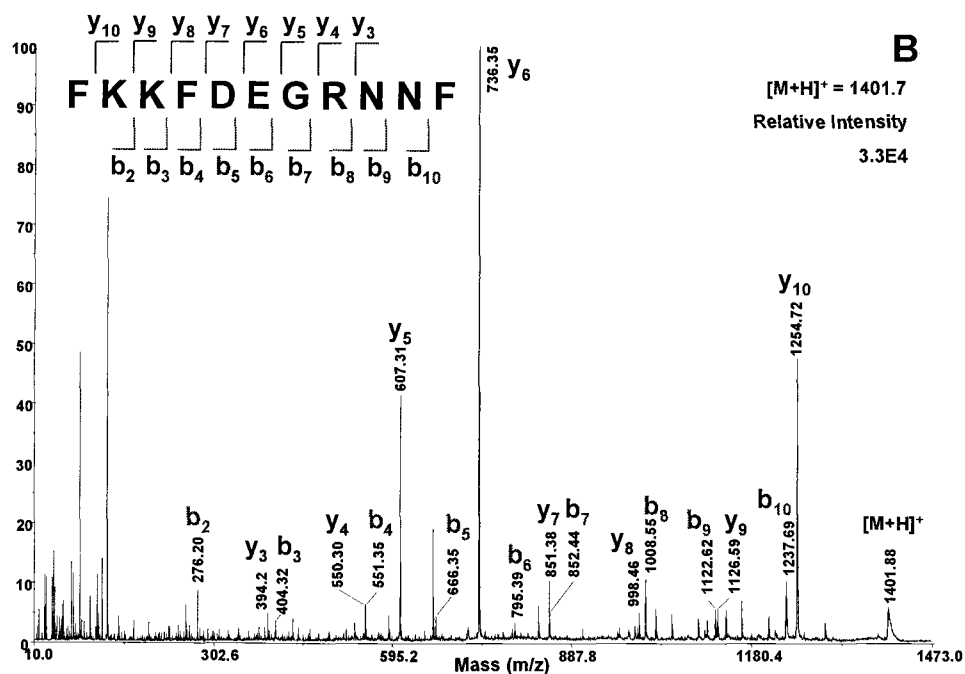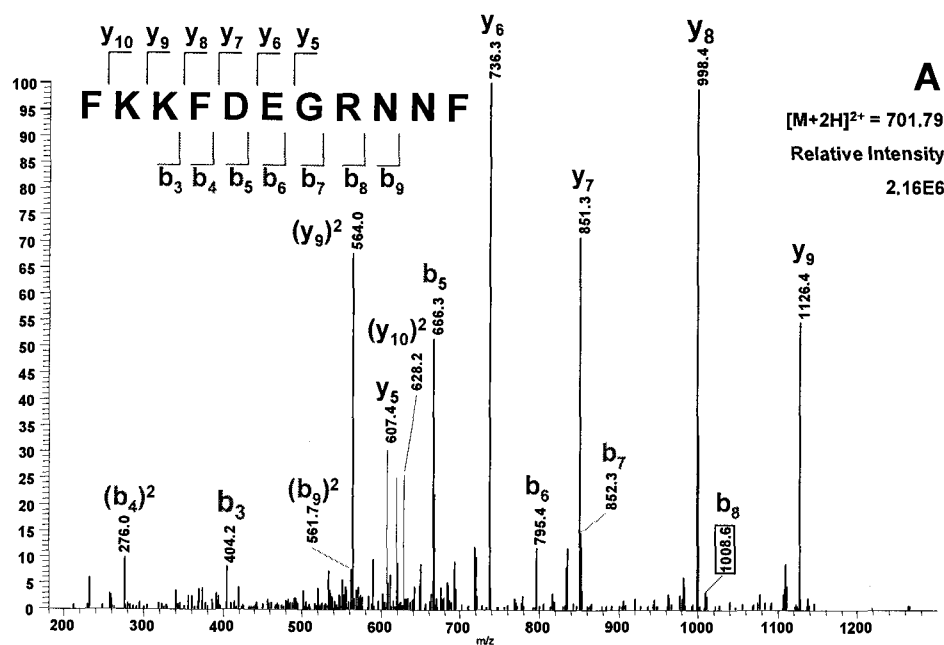
Figure 2.12   Comparison of tandem MS spectra generated from and electrospray ion trap LC-MS and MALDI-TOF/TOF MS. A) LC-MS/MS spectrum from electrospray ionization with an ion trap and B) MALDI-TOF/TOF tandem mass spectrum.

2.5   Research Goals

The thiol redox environment of intracellular and extracellular compartments is critical in the determination of protein structure, regulation of enzyme activity, cell signaling, and control of transcription factor activity and binding. Because of the abundance of PDI in the ER, the redox-nature of its two active sites, its role as a stress protein and chaperone, and its association with disease and chemically induced toxicity, the goal of this research was to investigate a mechanism through which PDI could pose as a target for biological reactive intermediates.

The two N-terminal active site cysteines, one in each catalytic domain, exist as a thiolate anion at physiological pH. The major hypothesis that this work revolves around is that these two thiolate anions are potential targets for electrophiles *in vivo*, such as the episulfonium ion of the 1,2-dichloroethane-glutathione conjugate. Further, identifying these sites as susceptible to modification implies that PDI is sensitive to not only toxic alkylating species but everyday changes in the redox environment. This may strengthen the argument that PDI can act as a control factor in a number of redox-specific cell regulations.

The specific goals of this project were (1) to determine if the catalytic properties of PDI changed after modification by a range of electrophilic compounds, (2) to identify the residues of PDI that are modified, (3) to relate the modification of the cysteine residues to other proteins that are susceptible to alkylation, and finally (4) to assess the susceptibility of the active site thiols to the bioreactive GSH conjugate of 1,2-dichloroethane. *In vitro* enzymatic analyses in addition to mass spectrometry techniques for sequencing were useful in testing the hypothesis.

3.0 USE OF ALKYLATING AGENTS TO CHARACTERIZE THE CATALYTIC ACTIVE SITE OF PROTEIN DISULFIDE ISOMERASE

3.1 ABSTRACT

The thiol redox status of intracellular and extracellular compartments is critical in the determination of protein structure, regulation of enzyme activity, cell signaling, and control of transcription factor activity and binding. It is becoming clear that proteins containing thiols at their active site play a role in the redox control of cells. Protein disulfide isomerase (PDI) is a redox active protein containing two catalytic active sites each containing the sequence –CGHC–. PDI is a multifunctional protein catalyzing the formation of disulfide bonds, acting as a molecular chaperone and being a component of the enzymes prolyl-4-hydroxylase and microsomal triglyceride transfer protein. The goal of this work was to determine the susceptibility of the thiolate anions present in each of the two active site domains of PDI. To this end, recombinant rat PDI was incubated with 1-chloro-2,4-dinitrobenzene (CDNB), iodoacetamide (IAM) and biotin-conjugated iodoacetamide (BIAM). CDNB is a thiol alkylating electrophile used as a substrate to determine glutathione transferase activity. The activity and thiol groups of PDI were affected by in $vitro$ incubation with CDNB. At the highest concentration used, 1 mM CDNB incubated with 2 μM PDI decreased reductase activity by 63% $\pm$ 13% of native PDI activity. Oxidative folding as measured by the continuous RNase refolding assay decreased 75% $\pm$ 3% of native PDI activity. We Using DTNB, 3.86 $\pm$ 0.26 moles SH/mole PDI was decreased to 1.86 $\pm$ 0.34 mole SH/mole PDI. Initial mass spectrometry experiments with PDI and weePDI (a C-terminal fragment of PDI resulting from initiation of translation at a second AUG start codon in the gene sequence) suggested that PDI was alkylated by at least two dinitrophenyl moieties of CDNB, one in each "end" of PDI as

delineated by PDI versus weePDI mass spectra. PDI was alkylated by a maximum of four CAM or BAM groups derived from IAM and BIAM. A titration of these cysteine residues showed alkylation of the first N-terminal cysteine residue (–C*GHC–) followed by alkylation at the second cysteine residue (–C*GHC*–). Modification with BIAM, a larger but similar electrophile showed the same alkylating profile indicating that size of the electrophile did not preclude alkylation. These results show that the thiolate anion is a sensitive reactive nucleophile; however, PDI is not as susceptible to alkylation by CDNB as the selenocysteine of thioredoxin reductase. The relative susceptibility of PDI to alkylating agents is discussed.

3.2   INTRODUCTION

Irreversible modification of the thiol groups of cysteine residues in proteins by biologically reactive metabolites may affect protein structure, enzyme activity, and redox environment, or interrupt normal signal transduction cascades. Thiol-containing proteins have been implicated in the redox control of the cell, and modification of the cysteine residues at the active sites of these proteins is beginning to emerge not only as a site of regulation of biological signals but as a target for toxic insult. An exploration of the mechanism by which active site cysteine residues are modified by electrophiles is at the foundation of understanding the role of thiols in the cell.

Protein disulfide isomerase (PDI) is a member of a class of enzymes called thiol-disulfide oxidoreductases that are involved in cellular thiol homeostasis through their catalysis of thiol-disulfide interchange reactions. These redox-active proteins are referred to as the thioredoxin superfamily because of their similarity to the structure of thioredoxin (Trx). The oxidizing

potential of PDI (Aslund et al., 1996) allows it to function primarily as dithiol oxidant and isomerase (Aslund et al., 1996) in the endoplasmic reticulum where it acts in the folding of newly synthesized proteins by disulfide isomerization (Gilbert, 1997; Bulleid and Freedman, 1990; Freedman et al., 1989). PDI also contains a peptide binding site which is responsible for its chaperone/antichaperone activity independent of its isomerase activity (Wang, 2002; Primm et al., 1996; Tsai et al., 2001). It is highly abundant in the lumen of the endoplasmic reticulum (ER) constituting 0.8% of the total cellular protein in liver (Freedman et al., 1994) and reaching near millimolar concentrations in some tissues (Zapun et al., 1992).

Members of the thioredoxin superfamily contain at least one catalytic active site sequence $-CX_1X_2C-$ within a thioredoxin fold motif of which PDI contains two. The modular structure of PDI is composed of four Trx fold domains which are arranged sequentially as **a, b, b',** and **a',** plus a C-terminal acidic extension, **c** (Kemmink et al., 1997). The **a** and **a'** thioredoxin domains contain the catalytically redox-active sites with the cysteine residues in the –CGHC– sequence and are directly involved in thiol-disulfide exchange reactions (Darby et al., 1996). The **b** and **b'** domains maintain the thioredoxin fold motif but do not contain the catalytic active site sequence (Kemmink et al., 1999).

The first cysteine residue (Cys[37] and Cys[381] by recombinant rat PDI numbering) of the **a** and **a'** domains has a sulfur atom that is accessible and reactive with external thiol and disulfide reagents; the second cysteine (Cys[40] and Cys[384]) is buried and unreactive (Kemmink et al., 1997), though it is believed to provide an escape mechanism, preventing PDI from becoming trapped with substrates that isomerize slowly (Walker and Gilbert, 1997; Schwaller et al., 2002). The pKa of Cys[37] (and Cys[381] by sequence

homology) in the **a** domain is 4.5 (Kortemme et al., 1996) leading to a stabilization of the thiolate anion of PDI at physiological pH. The overall redox potential of PDI ($E^{o'}$ = -178 mV) is oxidizing compared to that of the reducing thioredoxin (-270 mV) (Lundstrom and Holmgren, 1993; Krause and Holmgren, 1991). The stabilization of the two thiolate anions of PDI highlights PDI as a very good candidate for electrophilic attack by bioreactive intermediates. In an effort to determine the susceptibility of PDI to alkylation, we studied the interaction between the thiol alkylating agents 1-chloro-2,4-dinitrobenzene (CDNB), iodoacetamide (IAM) and an IAM derivative, biotin-conjugated iodoacetamide (BIAM).

CDNB has been established as an immunomodulatory agent to provoke delayed-type hypersensitivity (Ahmed and Blose, 1983) by initiating a cell mediated immune response (T1 response). CDNB is an electrophilic compound used as a substrate to determine glutathione transferase activity that is involved in elimination of CDNB *in vivo* (Habig et al., 1974). The mechanism of CDNB *in vivo* has not been established, however it has been determined to adduct proteins. CDNB irreversibly inhibits the mammalian protein, thioredoxin reductase (TR) and in the presence of NADPH induces NADPH oxidase activity in the modified enzyme (Arner et al., 1995). TR catalyzes the NADPH dependent reduction of the active site disulfide in thioredoxin, Trx-(SS), to a dithiol, Trx-(SH)$_2$. In addition to the conserved redox catalytic site –CVNVGC–, mammalian TR contains a C-terminal extension carrying a penultimate selenocysteine (SeC) residue in the conserved sequence motif –GC(SeC)G– (Zhong et al., 1998; Gladyshev et al., 1996). The investigation of PDI in these studies was initiated before the cysteine and the SeC in the C-terminal sequence were identified to be dinitrophenyl alkylated upon incubation of TR, NADPH and CDNB (Nordberg et al., 1998). This suggests that the selenol group of SeC has an unusually

high nucleophilic reactivity and a low pKa value, which makes this residue a natural target for alkylation. The neighboring cysteine residue was also found to be alkylated indicating that this thiol group might also have an unusual reactivity indicating a low pKa value. PDI does not have this selenol group but the thiolate anion present in both active sites is one of the most reactive groups known, being 1,000 - 10,000 times more reactive than a cysteine thiol group (Friedman et al., 1965; Pearson et al., 1968).

In an effort to evaluate the relative reactivity of vicinal thiols in the active sites of proteins, we investigated the sensitivity of PDI to CDNB alkylation. We wanted to know if PDI is susceptible to alkylation by CDNB considering the nucleophilic nature of the thiolate anions in the active sites. Also, is PDI as good of a target for alkylation by CDNB as TR? There is evidence that PDI and its homologues ERp29, P5, and ERp57 are targeted in bromobenzene toxicity (Koen and Hanzlik, 2002). These studies may lead to further insight on the possibility of the PDI thiolate anion as a target for biologically reactive electrophiles *in vivo*.

We have shown a decrease of PDI activity, loss of protein thiols and an increase in mass of at least two dinitrophenyl moieties derived from CDNB. To further elucidate the susceptibility of the active site thiols in PDI, a titration of the active site cysteine of PDI with IAM and the similar but larger biotin-conjugated iodoacetamide (BIAM) showed an increase in mass up to four alkylations per PDI polypeptide with both IAM and BIAM. These electrophilic agents first alkylated the N-terminal cysteine residue in each active site (–C*GHC–) followed by alkylation at the second cysteine residue (–C*GHC*–). Modification with the larger BIAM showed no difference in the alkylating profile. These findings and their implication with respect to the susceptibility of the thiolate anion of PDI are discussed.

3.3 EXPERIMENTAL PROCEDURES

3.3.1 Materials

All reagents used were purchased from Sigma unless otherwise noted. The pETPDI.2 plasmid containing the recombinant rat PDI gene was a generous gift from H.F. Gilbert. Biotinoylated iodoacetamide (N-(biotinoyl)-N'-(iodoacetyl)ethylenediamine, BIAM) was purchased from Molecular Probes. HPLC grade acetonitrile was supplied by Fisher Scientific, and water was generated with a Milli-Q Ultrapure water purification system.

3.3.2 Expression and Purification of Recombinant Rat PDI

Recombinant rat PDI was expressed in *E. coli* strain BL21(DE3) (Novagen) containing the pETPDI.2 plasmid as a soluble cytosolic protein and purified over a DEAE-Sephacel column (Amersham Pharmacia) followed by a Zn^{2+}-affinity column (Chelating Sepharose Fast Flow, Amersham Pharmacia) as described previously (Gilbert, 1998; Gilbert et al., 1991). The reduced protein was concentrated and stored in 25 mM Tris (pH 8) at 80°C in 50 µl aliquots. Protein concentration was determined according to Bradford (1976) at a final concentration ranging from 10-20 mg/mL. Care must be taken in pooling the DEAE fractions as the contaminant weePDI elutes at the end of the PDI peak. WeePDI (21 kDa) is a C-terminal fragment of PDI resulting from initiation of translation at a second AUG start codon in the gene sequence (Puig et al., 1997). Preparations containing PDI and weePDI were used in some of the mass spectrometry analyses.

3.3.3 Reduction and Covalent Modification of PDI

Stock solutions of CDNB were made in 99% ethanol and CDNB experiments were performed per the protocol in Arner et al. (1995). PDI (4 μM) in 0.5 mL was incubated for 10 minutes at room temperature with 50 mM DTT and then applied to a Sephadex G25 column (NAP-5, Amersham Pharmacia) equilibrated with 0.2 M potassium phosphate and 1 mM EDTA (pH 7.5) to remove excess DTT. The enzyme was eluted in 1 mL buffer. This sample was split and 0.45 mL ([PDI] ~ 2 μM) was combined with CDNB (0.05 to 1 mM or 25X to 500X fold excess of CDNB:PDI), ethanol as control, or 0.25 mM iodoacetamide (IAM) and incubated 30 minutes or up to 2 hours at room temperature. To assess irreversibility of inhibition, the alkylating agent was removed again with a Sephadex G25 column (Final [PDI] ~ 1 μM). Eluates were assayed for PDI activity, protein thiols, or concentrated and desalted with a Centricon-10 tube (Amicon) for mass spectrometry. Protein estimates were measured by the BCA Protein Assay (Pierce) with bovine serum albumin as the standard.

For the mass spectrometric characterization of IAM and BIAM derived adducts, PDI (0.1 mM) in 0.06 mL was incubated for 30 minutes with 4 mM tris(2-carboxyethyl)phosphine (TCEP) at 37°C and then applied to a polyacrylamide Micro Bio-Spin® column (BioRad) equilibrated with 25 mM NH$_4$HCO$_3$ (pH 8) to remove the TCEP. IAM was weighed and dissolved in 25 mM NH$_4$HCO$_3$ buffer and added to 0.05 mM of PDI in 0.06 mL aliquots to give molar ranges ranging from equimolar to 20X fold excess for 90 minutes at 37°C in the dark. BIAM was dissolved in dimethyl sulfoxide (DMSO) and diluted and applied similarly to IAM. The alkylating agents were removed with Micro Bio-Spin® columns equilibrated with 25 mM Tris (pH 8). Protein

estimates were performed with BCA Protein Assay reagent (Pierce) with serum albumin as the standard.

3.3.4 PDI Reductase Activity

PDI reductase activity was assessed by the GSH-dependent reduction of insulin by coupling the formation of GSSG to NADPH oxidation via glutathione reductase (Gilbert, 1998). Native and modified PDI (~1 μM) from the eluates were combined in a 1 mL cuvette with 0.12 mM NADPH, 4U of glutathione reductase, and 5 mM GSH and preincubated for 1 minute to reduce any contaminating GSSG. Bovine insulin (final concentration = 30 μM) was then added and oxidation of NADPH was recorded every 30 seconds for 5 minutes at 340 nm. After subtracting the background rate of uncatalyzed insulin reduction, the specific activity was calculated on the basis of $\varepsilon = 6.23$ mM^{-1}cm^{-1}. The specific activity of PDI in this assay was 0.12 ($\pm$ 0.01) μmol of GSSG formed/min/mg. Spectrophotometric measurements were performed with a Beckman DU-64 with a Kinetics soft-pac module.

3.3.5 Assay of RNase Refolding

PDI activity was measured by observing the activity due to the formation of native RNase with cCMP as a substrate (Lyles and Gilbert, 1991a and 1991b; Gilbert, 1998). The hydrolysis of cytidine 2',3'-cyclic monophosphate (cCMP) at an initial concentration of 4.5 mM was monitored continuously at 296 nm with a $\Delta\varepsilon$ of 0.19 mM^{-1}cm^{-1}. Active RNase concentration at any time was calculated from the first derivative of the absorbance versus time curve. The assay was performed at pH 8.0, 25°C in 0.1M Tris-acetate buffer containing 2 mM EDTA, a glutathione redox buffer

(1mM GSH/0.2 mM GSSG) and ~1 μM PDI. Reduced denatured RNase (Ribonuclease A from bovine pancreas, type IIIA) was reduced and denatured by the method of Gilbert (1998). Spectrophotometric measurements were performed with a Beckman DU-64 with a Kinetics soft-pac module.

3.3.6 Protein Thiols

It was necessary to increase the concentration of PDI to be in the range of detection with Elman's reagent, 5,5'-dithio-bis-2-nitrobenzoic acid (DTNB). After reduction and removal of DTT, PDI (~7 μM) was combined with 500X fold excess of CDNB (3.5 mM) as described above. A 0.9 mL aliquot of the eluate (~3 μM PDI) was combined with 1.5 mM DTNB and incubated for 20 minutes at room temperature. Absorbance was measured at 412 nm. Protein thiols were calculated on a GSH standard curve. Measurements were performed on a Kontron UV spectrophotometer. Protein estimates were performed with BCA protein reagent (Pierce) with bovine serum albumin as the standard.

3.3.7 MALDI-TOF MS of Whole Protein

MALDI-TOF MS analyses of native and modified PDI (~ 55 kDa) containing weePDI (21 kDa) were performed on a custom built time-of-flight reflector mass spectrometer equipped with a two-stage delayed extraction source. Approximately 1 μl of the concentrated sample was mixed with 3 μl of sinapinic acid or α-cyano-4-hydroxy cinnaminic acid in 40% acetonitrile (Fisher Scientific) with 0.1% trifluroacetic acid. A 1 μl droplet of this analyte/matrix solution was deposited onto a sample probe and allowed to

dry in air. Mass spectra were produced by irradiating the sample with a (355 nm) Nd:YAG laser (Spectra Physics) and operating the ion source at 23 kV with a 700 ns/1.0 kV delay. Every mass spectrum was recorded as the sum of 30 consecutive spectra each produced by a single pulse of photons. Ions from bovine serum albumin were used for mass calibration.

3.3.8 Chromatography and Mass Spectrometry of Whole Protein

Chromatography of native and modified PDI was performed on a 0.32 mm, 5A column packed with Jupiter C_4 stationary phase (Phenomenex) preceded by a Protein Microtrap (Michrom BioResources, Inc.). Solvent A was 0.03% trifluroacetic acid (TFA) in 95:5 water:acetonitrile, while solvent B contained the same acid modifier in 5:95 water:acetonitrile. A linear gradient was performed from 10 to 60% B in 20 minutes followed by a sharper gradient to 95% B in 10 minutes for a total of 30 minute runs. Mass spectra were obtained on a Perkin Elmer SCIEX API III+ triple-quadrupole mass spectrometer. The ion spray voltage was 5,000 volts and the orifice voltage was 100 volts.

3.3.9 Peptic Digestion

To denature the protein, 18 μl of 8M urea and 4 mM TCEP (dissolved in 0.1M citric acid) were added to 30 μg of PDI and incubated for 1-3 hours at 37°C. Porcine pepsin (10 μg) was dissolved in 100 μl of 5% formic acid and 3 μg (30 μl) of pepsin was added to the protein solution and digested for 2-3 hours at 37°C. Alternatively, 30 μg of native or modified PDI was combined directly with 3 μg of pepsin dissolved in 5% formic acid and digested for 2-3 hours at 37°C.

3.3.10   Chromatography and Mass Spectrometry of PDI Peptides

Chromatography was performed on a 0.17 mm column packed with Jupiter C_{18} stationary phase (Phenomenex) preceded by a Peptide Captrap (Michrom BioResources, Inc.). Solvent A for liquid chromatography was composed of 0.01% TFA and 0.1% acetic acid in 95:5 water:acetonitrile, while solvent B contained the same acid modifiers in 5:95 water:acetonitrile. A linear gradient was performed from 10 to 60% B in 70 minutes followed by a sharper gradient up to 95% B over 10 minutes for a total of 80 minute runs. Peptic digests were loaded onto the trap in 10 µl aliquots and washed with Solvent A prior to injection onto the column. Mass Spectra were obtained on a Finnegan LCQ ion trap mass spectrometer (ThermoFinnegan). In a method similar to Jones and Liebler (2000) and Mason and Liebler (2000), the scan event series included one full scan with a mass range of 400 to 2000 m/z followed by three dependent MS/MS scans of the most intense ion. Dynamic exclusion was used with a repeat count of 1 over 1 minute with a 3 minute exclusion duration window.

3.3.11   Data Analysis

SEQUEST (ThermoFinnegan) and MASCOT (Matrix Science) were used for protein and peptide identification. For both programs, the nonredundant database and a specified recombinant rat PDI sequence were searched to identify peptides. Defining analysis parameters included no endoprotease (pepsin is non-specific) and possible modifications +57 (IAM) or +327 (BIAM) m/z for Cys, His, Tyr, Ser, Thr, and N-terminus. The SEQUEST algorithm was used to analyze tandem mass spectra as previously described (Wolters et al., 2001). MASCOT was used to verify the

protein identifications found in SEQUEST and also to search for modifications (Perkins et al., 1999).

3.4   RESULTS

3.4.1 Inactivation of Activity

Using the NADPH-dependent reduction of insulin disulfide, initial experiments showed that preincubation of recombinant rat PDI with DTT followed by incubation with increasing doses of CDNB decreased the activity of PDI (Figure 3.1). After 30 minutes incubation at room temperature, 1 mM CDNB decreased the activity of 2 μM PDI by 63% ± 13%. Inactivation occurred in a dose dependent manner. Inhibition persisted after the removal of CDNB with Sephadex G25 chromatography indicating that adduct formation was the mechanism of inactivation. These experiments used a maximum of 1 mM CDNB, a 500X fold excess of CDNB over PDI. This was the maximum CDNB concentration allowable as increasing doses were not soluble under these experimental conditions, and 2000X fold excess used in the inhibition of TR (Arner et al., 1995) were not attainable with PDI. Incubation of PDI with 0.25 mM of iodoacetamide (IAM) for 30 minutes resulted in complete inhibition of reductase activity (data not shown). This assay only measured reductase capabilities of PDI; for oxidative folding activity, the continuous RNase refolding assay was used.
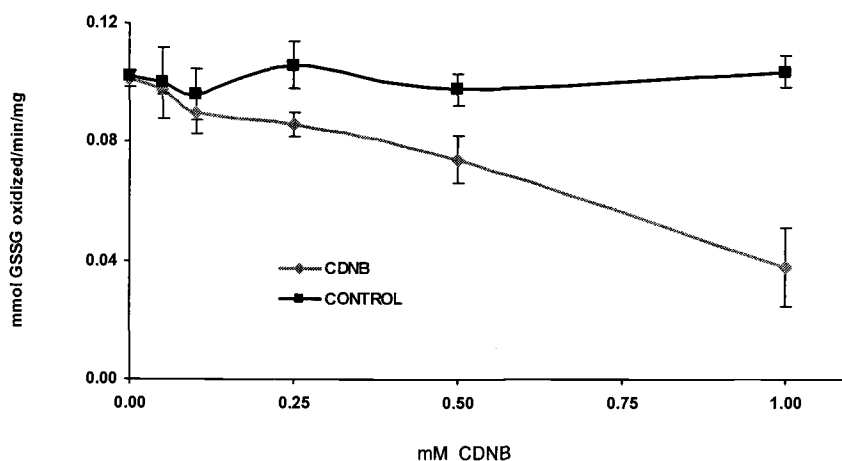
Figure 3.1 Inhibition of the NADPH-dependent reduction of insulin disulfide by PDI by varying concentrations of CDNB. Recombinant rat PDI was preincubated with CDNB or ethanol at room temperature for 30 minutes as described in the Experimental Procedures section. Each point is the average of three experiments ± standard deviation.

The isomerase activity of PDI was measured by incubating PDI with reduced denatured RNase. As PDI refolds RNase, RNase becomes capable of hydrolyzing cCMP to CMP. Monitoring the appearance of CMP over time was a direct measurement of active PDI in the sample. The absorbance change during the PDI-catalyzed refolding of reduced RNase in the presence of cCMP was compared to PDI modified by IAM (Figure 3.2). PDI incubated with 0.25 mM IAM completely inhibited the ability of PDI to refold RNase. As with reductase activity, inactivation due to increasing concentrations of CDNB occurred in a dose dependent manner (Figure 3.3). Active RNase (proportional to the amount of active PDI) at any time was calculated from the first derivative of the absorbance versus time curve. Oxidative folding activity of PDI decreased by 75% ± 3% when preincubated with 1 mM CDNB for 30 minutes. The inactivation of PDI incubated with 0.5 mM CDNB over

time showed a biphasic curve typical of a second order reaction (Figure 3.4). Complete inhibition was not achieved in the two hour time frame monitored.
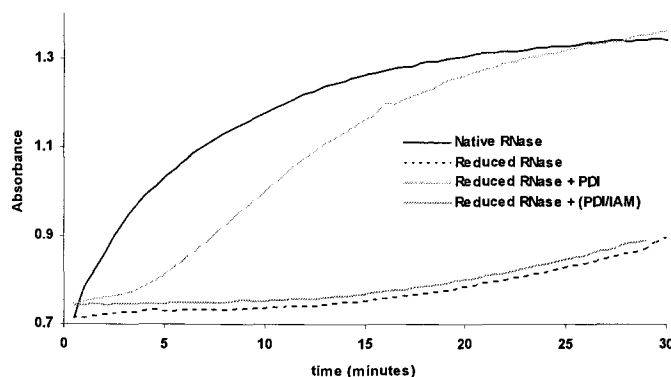
Figure 3.2 Absorbance change during the PDI-catalyzed refolding of reduced RNase in the presence of cCMP. Time course for the absorbance change at 296 nm produced by RNase-catalyzed hydrolysis of cCMP. Refolding of reduced RNase by PDI and inhibition of PDI by IAM is shown. IAM time course was representative of five experiments.
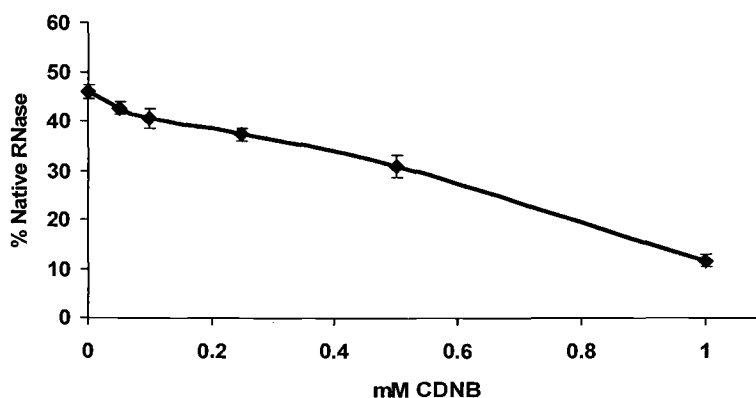
Figure 3.3   Inhibition of the ability for PDI to refold RNase in the presence of cCMP by varying concentrations of CDNB. Recombinant rat PDI was preincubated with CDNB at room temperature for 30 minutes. CDNB was removed with Sephadex-G-25 columns and analyzed as described in the Experimental Procedures section. Data is expressed as % Native RNase activity. Each point is the average of three experiments ± standard deviation.
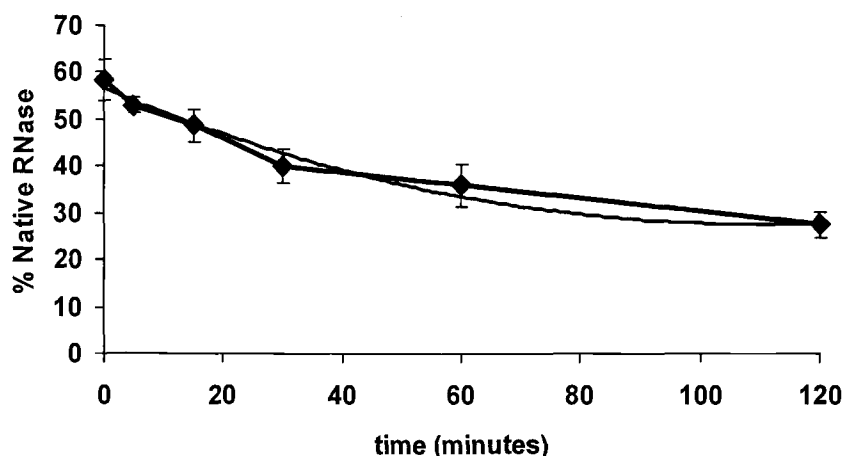
Figure 3.4   Rate of Inactivation of PDI by varying concentrations of CDNB. PDI was preincubated with 0.5 mM CDNB at room temperature for up to 120 minutes and then isolated with Sephadex G25 columns. % Native RNase is directly proportional to the concentration of active PDI. The second order rate constant curve is shown. Data shown are the mean of three experiments ± standard deviation.

3.4.2   Decrease in Protein Thiols

Ellman's reagent (DTNB) was employed to measure free protein thiols in PDI incubated with CDNB or IAM. It was necessary to increase the concentration of PDI in order to measure a loss of thiols within the range of detection. After reduction and removal of DTT, PDI (~7 μM) was combined with 500X fold excess of CDNB (3.5 mM) as described in the Experimental Procedures section. This excess of CDNB is equivalent to the molar ratio used in the 1 mM CDNB experiment. Total protein thiols of PDI ± CDNB or 0.25 mM IAM were measured at 412 nm after 20 minute incubation with DTNB (Figure 3.5).
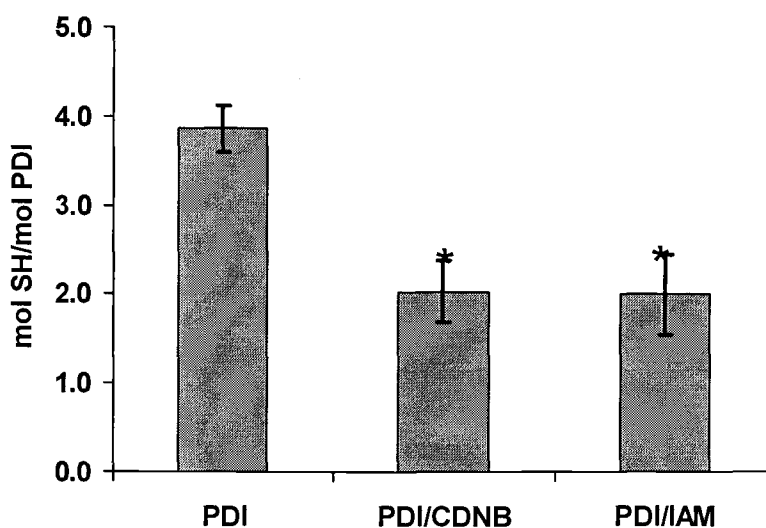
Figure 3.5   Effect of CDNB on protein thiols. After reduction with DTT, PDI was preincubated with CDNB or IAM and then the alkylating agent was removed with Sephadex G25 columns. Protein thiols of PDI (3 μM) were measured with DTNB (1.5 mM) per protocol in Experimental Procedures section. Values are the mean of three experiments ± standard deviation. * indicates p < 0.001.

Total protein thiols for native PDI were 3.86 ± 0.26 mole SH/mole PDI. Incubation with CDNB resulted in 1.82 ± 0.34 mole SH/mole PDI. This paralleled the number of thiols lost after incubation with IAM (1.86 ± 0.046). IAM induced a complete loss of both reductase and isomerase activities with a concomitant loss of two thiol groups at 0.25 mM IAM whereas CDNB (1mM) produced only a 70% loss of activity with a loss of two thiol groups. The change in mass due to a dinitrophenyl alkylation of PDI was further elucidated with MALDI-TOF mass spectrometry.

3.4.3 MALDI-TOF MS Analyses on PDI and weePDI Incubated with CDNB

MALDI-TOF MS was used to measure the increase in mass of modified PDI after incubation of PDI with CDNB to confirm the covalent modification of the dinitrophenyl moieties derived from CDNB. The molecular weight of CDNB is 202.6 and the loss of the chloride ion upon alkylation results in a dinitrophenyl moiety molecular weight of 167.1 g/mol. The MALDI-TOF MS spectra for native and modified PDI are presented in Figure 3.6. Spectrum A shows PDI with an average mass of 55032 m/z at the singly charged peak. PDI incubated with 1 mM CDNB shown in Spectrum B has an average mass of 55360 m/z representing a difference of 328 m/z equaling approximately two dinitrophenyl moieties. PDI can be seen in four charge states in both spectra. WeePDI (20927 Da), a truncated version of PDI, contains only one active site sequence from the **a'** domain. Unmodified weePDI in Figure 3.6A shows an m/z of 20933. The peak corresponding to modified weePDI (21102 m/z) shows an increase of 169 m/z equaling the mass of one dinitrophenyl moiety (Figure 3.6B). WeePDI is seen in two charge states. The latter third of PDI (corresponding to weePDI) was alkylated with one DNP moiety and the other alkylation event was located somewhere in the first two thirds of the N-terminal end of PDI.

To further elucidate the specific residues targeted by these nucleophiles we chose IAM because of the complete inhibition of reductase and oxidative folding compared to that of CDNB. We analyzed PDI modified with IAM and BIAM. The structures of CDNB, IAM and BIAM are represented in Figure 3.7. Recombinant rat PDI has two cysteine residues at positions 37 and 40 in the **a** domain, and two cysteine residues at 381 and 384 in the **a'** domain. The other two cysteine residues are in the **b'** domain and proposed to be buried within the protein structure. IAM was employed to determine if

any of these cysteine residues were targets. Biotin-conjugated to IAM (BIAM) was subsequently used to see if increase in size of the electrophile due to the biotin moiety would change its ability to alkylate PDI because of accessibility restrictions. Mass spectrometric analyses of the whole protein and then subsequent peptide sequencing by tandem mass spectrometry determined the number and location of alkylating events.
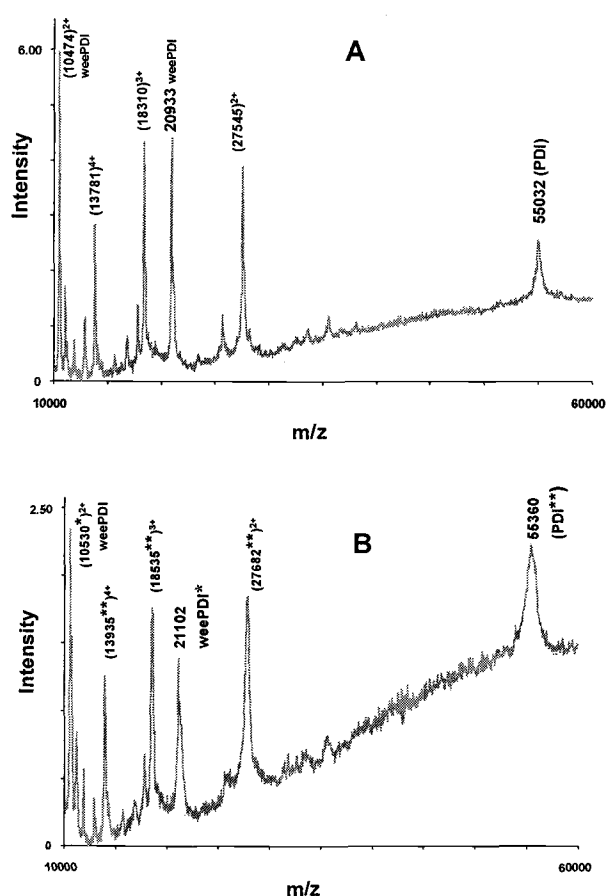
Figure 3.6   Effect of CDNB on the MALDI-TOF MS spectrum of native and modified PDI. Recombinant rat PDI and weePDI were incubated with 1 mM CDNB for 30 minutes at room temperature and then isolated with Sephadex G25 columns. After desalting and concentrating the sample MALDI-TOF MS analyses were performed as described in the Experimental Procedures section. Spectra are representative of three different experiments.

1-chloro-2,4-dinitrobenzene   iodoacetamide   N-biotinoyl)-N'-(iodoacetyl) ethylenediamine
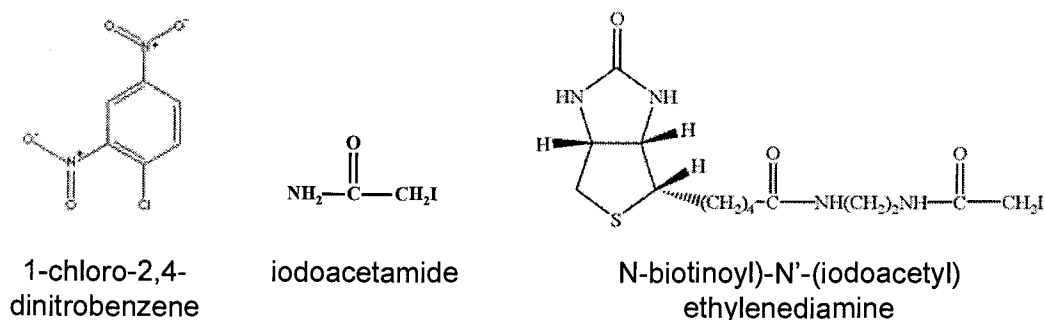
Figure 3.7   Structures of CDNB, BIAM and IAM. These electrophilic chemicals readily alkylate the thiol groups of cysteine residues.

3.4.4   Alkylation of PDI by IAM and BIAM

Native and modified PDI were analyzed by electrospray ionization (ESI) LC-MS with a triple quadrupole instrument (SCIEX). The proteins were separated by reverse chromatography on a C_4 column. A mass spectrum of unmodified PDI showing the multicharge envelope of ions is represented in Figure 3.8. The reconstructed mass of PDI after transformation of the multicharge envelope showed a m/z of 55136 ± 26 (Figure 3.9). While this was within the range of resolution of the instrument for high molecular weight assessment, the average molecular weight for recombinant PDI is 55114. The deviation in mass could have been due to the contaminant Na^{2+} (23 m/z) from inefficient desalting of the sample. Sodiated adducts have been detected in MS/MS spectra performed with the MALDI-TOF/TOF (see Chapter 4). The multicharge envelope of PDI was very large and protein ions with up to 75 charges were measured.
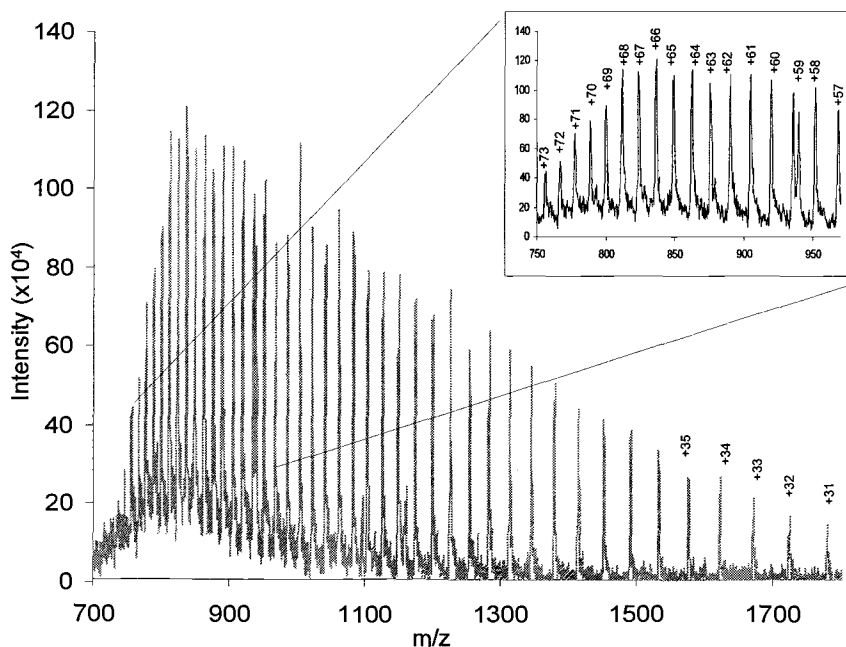
Figure 3.8   LC-MS electrospray spectrum of PDI in which all of the charge states of the protein in solution are represented.

After reducing PDI with 4 mM TCEP for 30 minutes at room temperature, TCEP was removed by micro-spin columns packed with polyacrylamide P-6 Bio-Gel (BioRad). The eluate (PDI) was combined with equimolar (1X), 2X, 4X and 10X fold excess amounts of IAM or BIAM over PDI for 30 minutes at 37°C. Adduction by IAM or BIAM did not change the protein ionization pattern in the multicharge envelope that is sometimes observed in structure changes after alkylation. Reconstructed masses of PDI modified with IAM are presented in Figure 3.10. The samples produced very consistent chromatograms monitored by total ion count and UV spectroscopy with one peak containing PDI and its modified derivatives coeluting (data not shown). Increasing excess of IAM over PDI caused a stepwise incremental

increase by 57 m/z with a maximum of four carbamidomethylations (1-CAM, 2-CAM, 3-CAM, and 4-CAM). A maximum of four CAM modifications were observed under these experimental conditions.
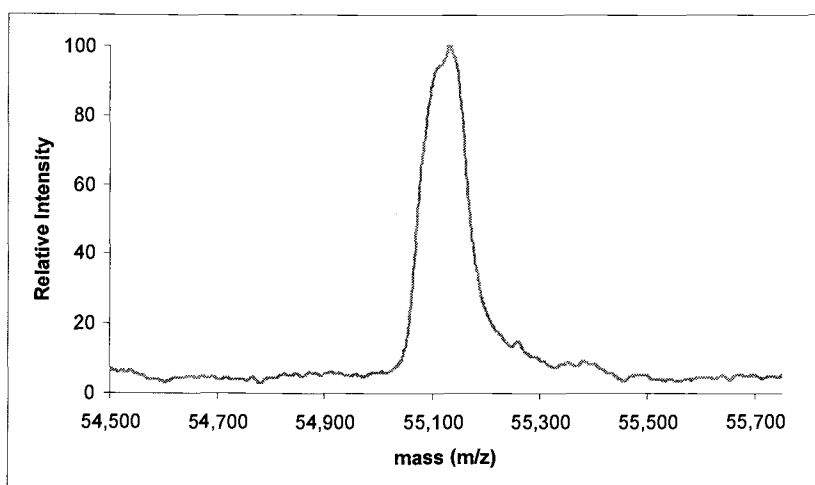
Figure 3.9   Reconstructed mass of PDI. The multicharge envelope of the electrospray LC-MS spectrum of PDI was transformed to determine the mass of PDI. The average mass was 55136 ± 26 m/z.

Interestingly, incubation with equimolar (1X) amounts of IAM with PDI showed both 1-CAM and 2-CAM species, suggesting that two alkylation events were simultaneous, not necessarily sequential. Incubations with lower concentrations of IAM with PDI (0.5X) had a majority of 1-CAM but 2-CAM adductions were still detectable (data not shown). All of the incubations except 0.5X were void of native PDI suggesting that all of the protein in incubation was alkylated by at least 1-CAM. After reduction with TCEP and incubation with BIAM (1X, 2X, 4X and 10X) LC-MS spectra resulted in up to

four biotinoylated-amidomethylated (BAM) species at each 327 m/z step increment (Figure 3.11). The signal to noise ratio was much higher in these reconstructed mass spectra as the relative intensity of these spectra were 10% of the reactions with IAM and much more difficult to quantitate. A maximum of four BAM modifications were observed under these experimental conditions. Exposure to 100X BIAM only resulted in a 4-BAM species as well (data not shown).
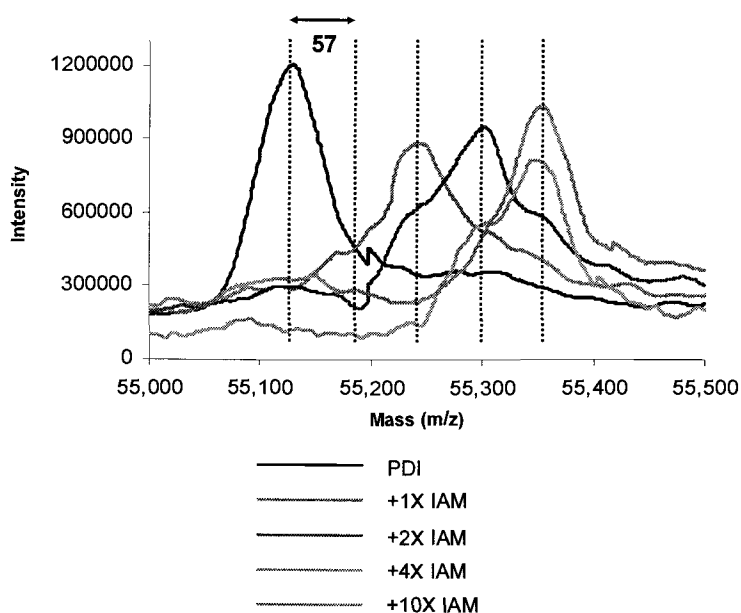
Figure 3.10   Reconstructed mass of multicharge envelope of PDI incubated with increasing doses of IAM. The mass of PDI was shifted in increments of 57 mass units. PDI did not adduct more than four carbamidomethyl (CAM) groups. Spectra are representative of three different experiments.
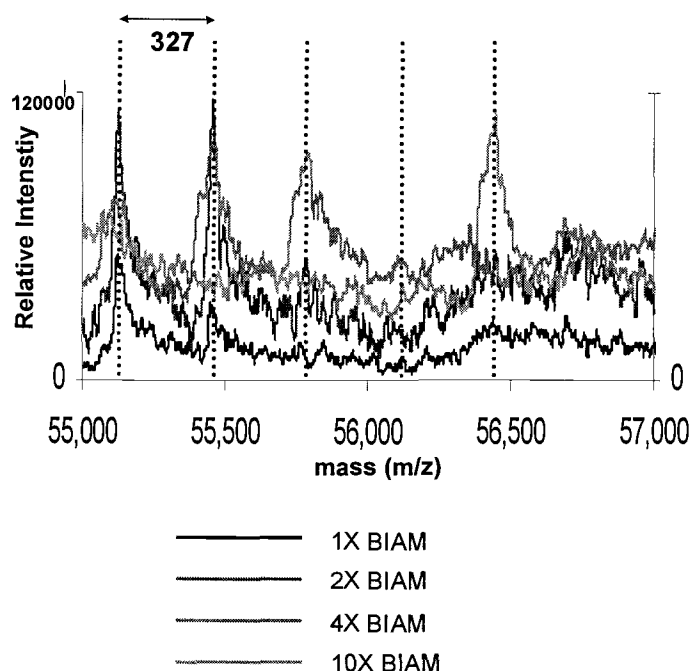
Figure 3.11 Reconstructed mass of the multicharge envelope of PDI incubated with increasing doses of biotinoylated IAM (BIAM). The overall intensity was lower than that of IAM (<10%). As resolution approaches the baseline, separation and identification of single mass species in the spectrum became difficult to delineate. Spectra were representative of three different experiments.

3.4.5   Peptide Mapping of PDI

Covalent modification of cysteine residues of PDI by IAM or BIAM was determined by ESI LC-MS/MS analysis of peptic peptides. Pepsin was chosen over the preferred proteases, trypsin and chymotrypsin, for two reasons: (1) predicted masses containing the active site sequences with trypsin or chymotrypsin were too long for singly or doubly charged molecules to be analyzed consistently in the electrospray ion trap and (2) the

nonspecific cleavage by pepsin allowed several peptides of different lengths containing the active site sequences to be generated. After digestion at ~ pH 2, pepsin generated a peptide map containing approximately 29 peptides accounting for the various permutations at the peptide ends due to pepsin (Figure 3.12).
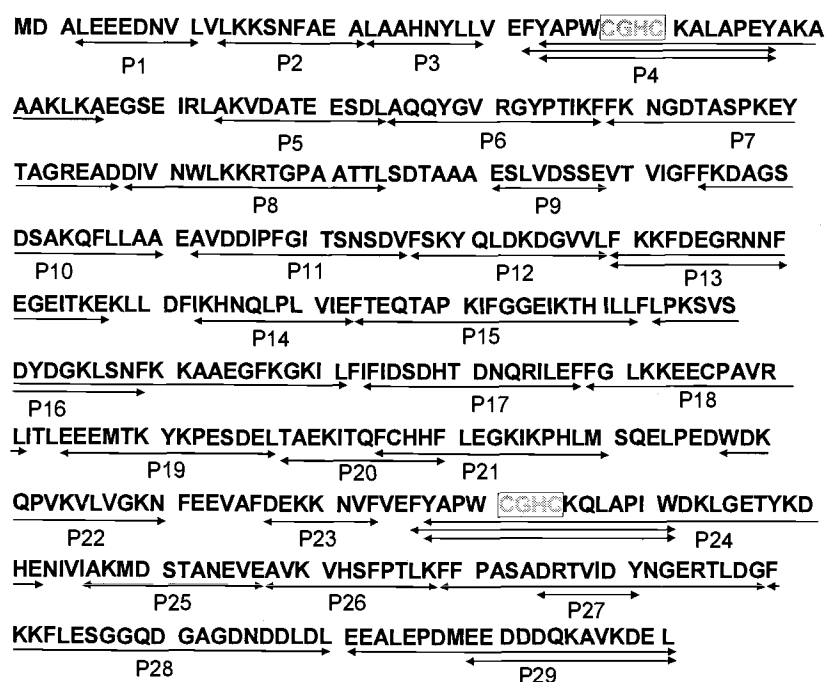
Figure 3.12   Recombinant rat PDI protein sequence showing peptic peptides. The active sites in the **a** and **a'** domains containing the two cysteine residues are highlighted in peptides P4 and P24. Protein coverage was 97%. Multiple mass peptides are shown only for the active site sequences.

The peptides containing the active site sequences in the **a** and **a'** domain were P4 (YAPWCGHCKALAPEY) and P24 (YAPWCGHCKQLAPIW)

respectively. The peptides were separated by reverse phase chromatography on a C_{18} microbore column prior to mass analysis. Abundance of the peptides P4 and P24 was low relative to other peptides and the total ion chromatogram (Figure 3.13).
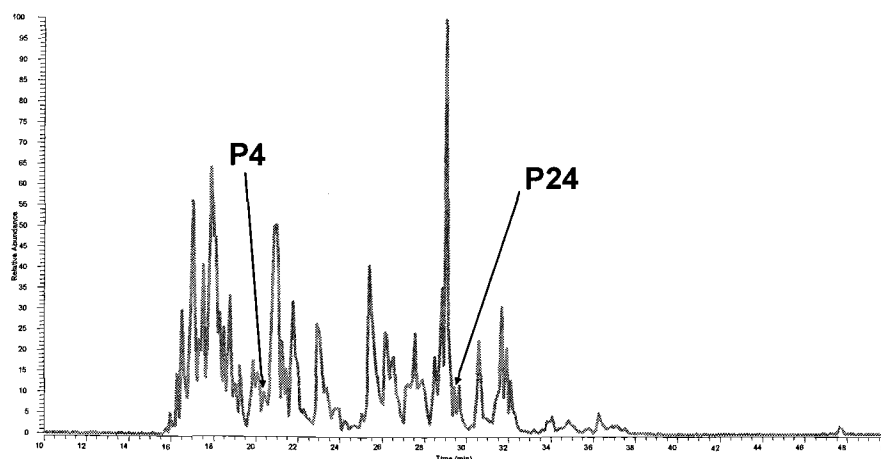
Figure 3.13 LC-MS chromatogram of PDI pepsin digest. Peptides containing catalytic active site sequences –CGHC– in the **a** (P4, YAPWCGHCKALAPEY) and **a'** (P24, YAPWCGHCKQLAPIW) domains are labeled.

Mass spectra of the singly [M+H]$^+$ and doubly [M+2H]$^{2+}$ charged ions showing incorporation of 1-CAM and 2-CAM groups derived from IAM are presented in Figure 3.14 for P4 and Figure 3.15 for P24. In the unmodified peptides P4 and P24, the intense [M+H]$^+$ masses were 1705.7 (1707.6) and 1770.6 (1772.7). The 2 m/z difference in the [M+H]$^+$ peaks were due to the presence or absence of the hydrogen atoms on the cysteine residues as reduced dithiols or an oxidized disulfide. The alkylated [M+H]$^+$ and [M+2H]$^{2+}$ for P4 ionized well (precursor ion count ~4.4 x 10^7) except for the 1-CAM

peptide $[M+2H]^{2+}([M+H]^+)$ = 884.2 (1766.5) m/z which had a lower precursor ion count (~1.6 x 10^6).

The full scan MS1 spectra containing the doubly charged ions including the addition of one and two biotinoyl-amidomethyl (BAM) groups are presented in Figure 3.16 for P4 and Figure 3.17 for P24. The incorporation of 327 m/z increased the singly charged ion beyond the mass limits set on the MS detector (2000 m/z) hence only the doubly charged ion was observed. The corresponding 1-BAM adduct of P4 ($[M+2H]^{2+}$ = 1019.1) was not the most intense ion of the MS1 and 1-BAM modified P4 coeluted with unmodified P4 at 1X and 2X fold excess incubations.
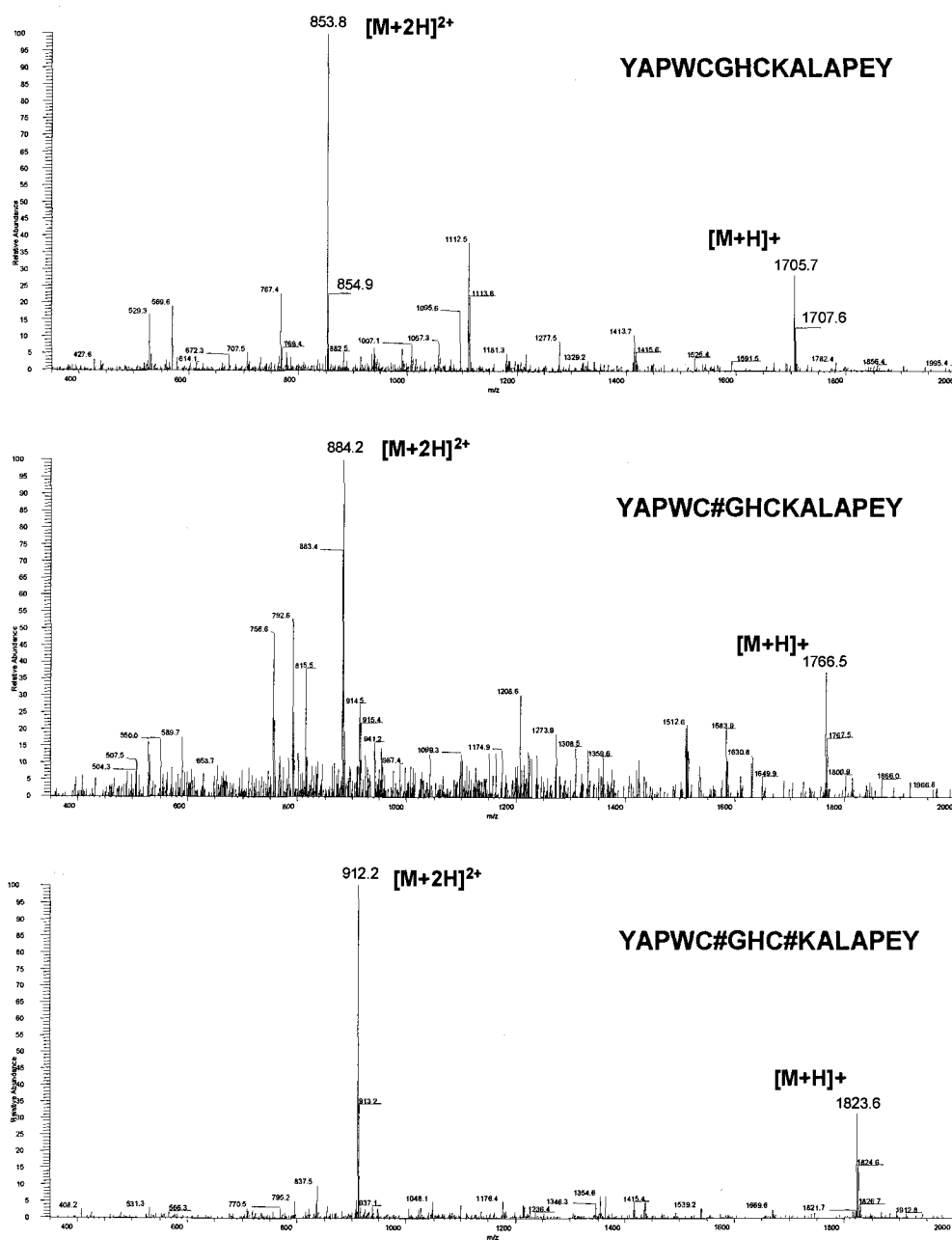
Figure 3.14   MS1 spectra showing the addition of one and two CAM modifications on the P4 peptide (YAPWCGHCKALAPEY).
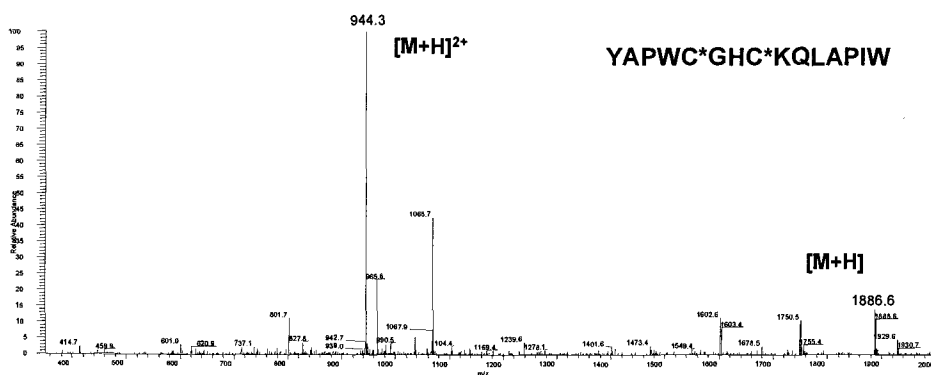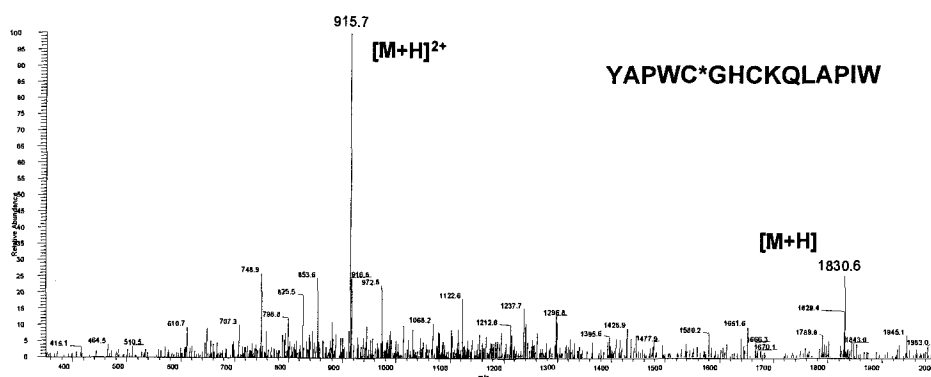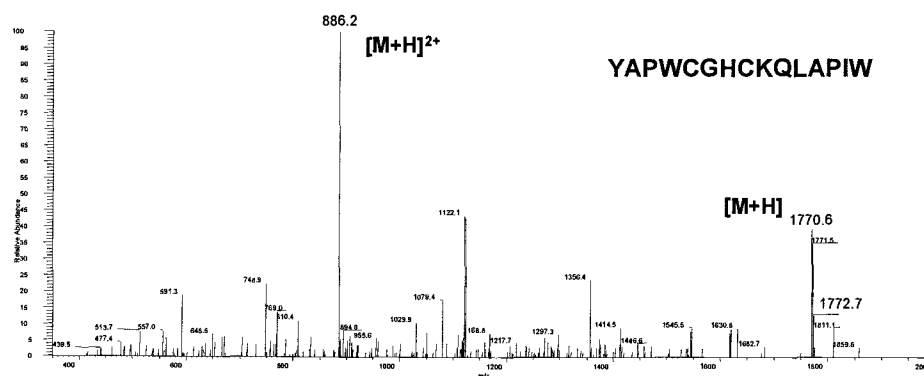
Figure 3.15   MS1 spectra showing the addition of one and two CAM modifications on the P24 peptide (YAPWCGHCKQLAPIW).
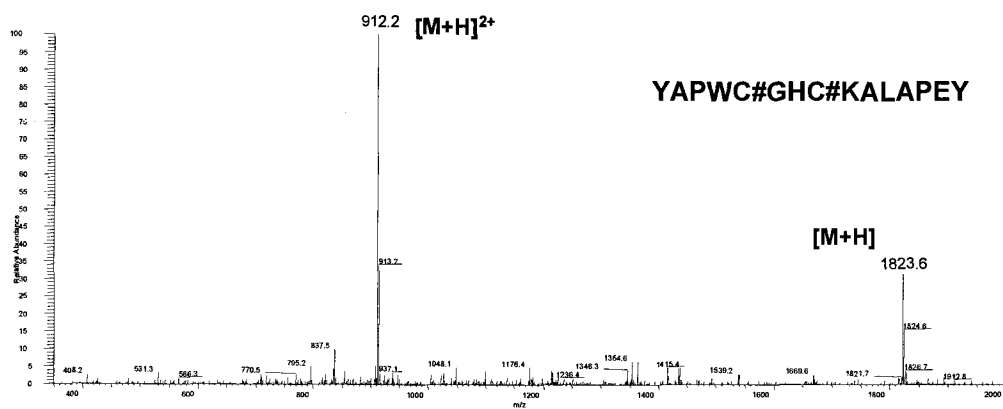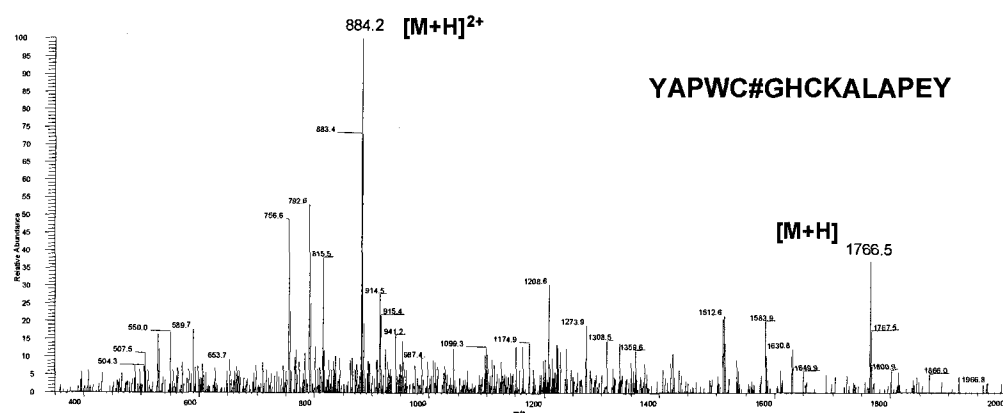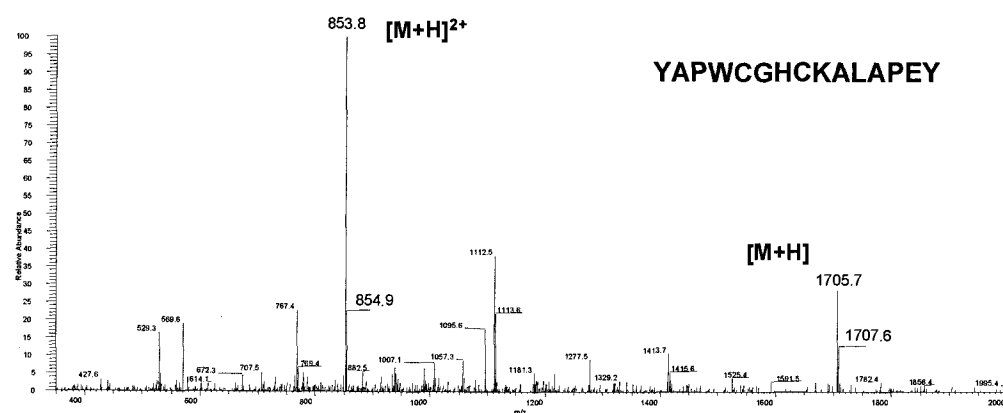
Figure 3.16   MS1 spectra showing the addition of one and two BAM modifications on the P4 peptide (YAPWCGHCKALAPEY).
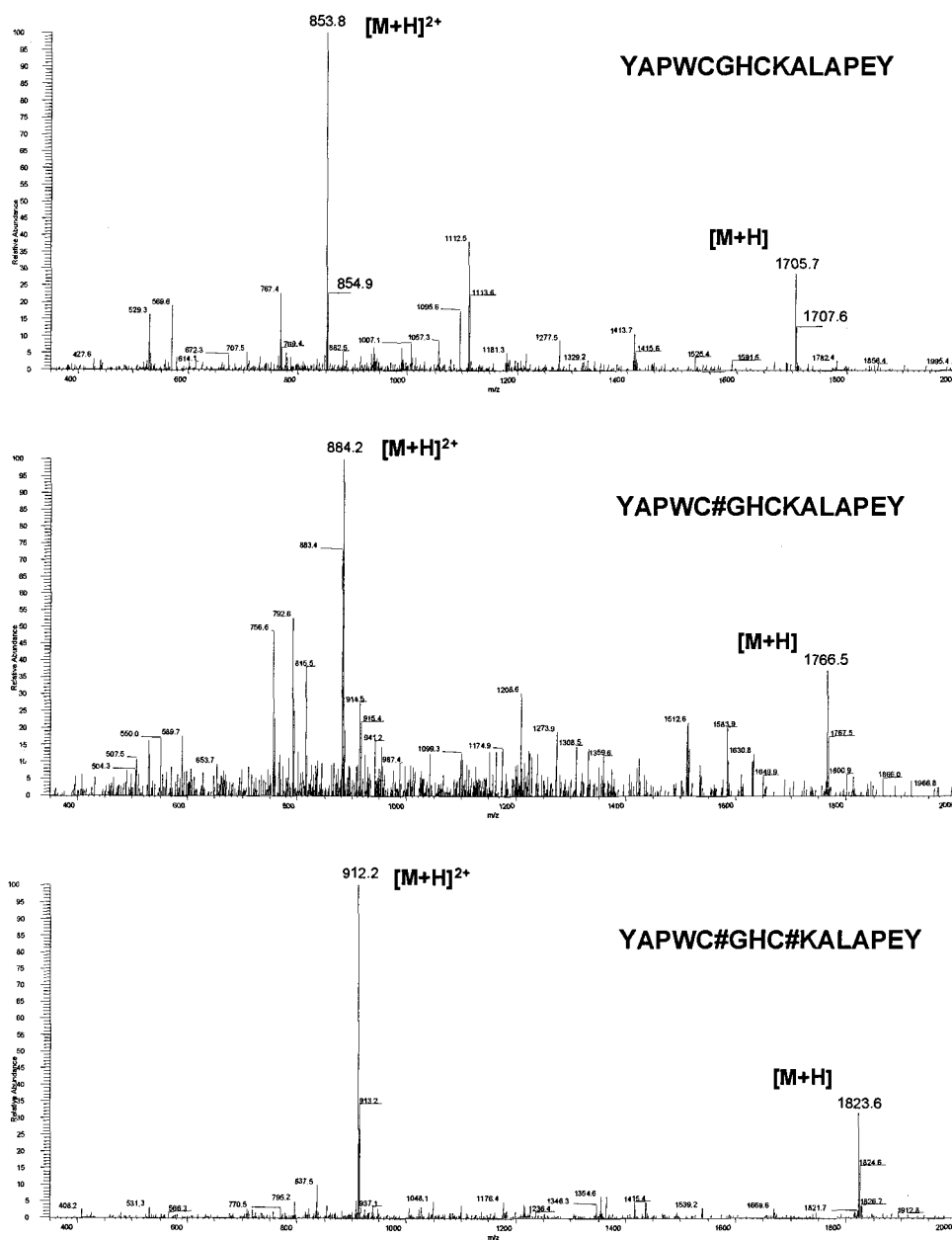
Figure 3.17   MS1 spectra showing the addition of one and two BAM modifications on the P24 peptide (YAPWCGHCKQLAPIW).

3.4.6 Sequencing Modified Peptides by CID with Tandem MS

The S-carbamidomethylation of peptide cysteine thiols was achieved by treatment with IAM and BIAM. The sequences of the peptic peptides P4 and P24 containing the two catalytic active sites were 80% homologous having only three residues that differ. The proline residues at either end of the peptides caused a specific CID fragmentation pattern as shown in the first spectrum in Figures 3.18 and 3.19. The most prominent ions were b_{12} and y_3 that dissociated at the N-terminus of the C-terminal proline. Concurrently, y_{13} at the N-terminal proline was usually detected as the doubly charged ion in most tandem mass spectra generated in the electrospray ion trap. Additionally, the internal fragment PWCGHCKALA (1065 m/z) from P4 and PWCGHCKQLA (1121 M/Z) from P24 was also detected in all of the spectra regardless of modification. These two internal ions are labeled with a dot in each of the spectra in Figures 3.18 and 3.19. Another hallmark found in these two peptides was the propensity of the unmodified cysteine-containing fragments to be present both as the disulfide m/z and dithiol form (+2 m/z) (data not shown).

Figure 3.18 presents a comparison of the MS/MS spectra of P4 (YAPWCGHCKALAPEY) and of the S-carbamidomethylated (CAM) P4. In the spectrum of the $[M+2H]^{2+}$ unmodified P4, the b-series fragment ions were not all present. The unmodified Cys^{37} which would be indicated by the b-series ion pair at 518 m/z (b_4) and 621 m/z (b_5) ion pair was not detectable in any of the spectra collected on P4. The unmodified Cys^{37} was also not detected in the y-series fragment ion pair at 1089 m/z (y_{10}) and 1192 (y_{11}). The ion pair of Cys^{40} in the b-series at 815 m/z (b_7) and 918 m/z (b_8) was only identified at b_8. Similarly, the y-series fragment ions for the ion pair

indicating Cys^{40} at 791 m/z (y_7) and 894 m/z (y_8) was only identified at y_7. Modification was observed first at Cys^{37} followed by Cys^{40}.

The fragmentation of P4 was more intense after CAM adduction and most of the y-series was identified, including the Cys^{37} shift of y_{10} and y_{11} to 1089 m/z and 1248 m/zfor 1-CAM and 1146 m/z and 1306 m/z with 2-CAM adductions. The identification of the b_5, b_6 and b_7 or y_8, y_9 and y_{10} ions was important in distinguishing the difference between the mono-alkylated – C*GHC– versus –CGHC*– peptide due to the 57 m/z equivalence of glycine and the CAM adduct. The second Cys^{40} shift was detected at 951 m/z (y_8) but not at y_7. The relative abundances of the b- and y-ion series after CID were above 10%, permitting manual sequencing by visual inspection of the spectra.

Figure 3.19 presents a comparison of the MS/MS spectra of P24 (YAPWCGHCKQLAPIW) and the CAM modifications of P24. The intensity of P24 in relation to the total ion chromatogram was greater than P4, hence the stronger signals observed in the MS/MS spectra. P24 also exhibited the same fragmentation patterns due to the prolines at either end of the peptide. The unmodified Cys^{381} was indicated by the y-series ion pair 1152 m/z (y_{10}) and 1256 (y_{11}) and Cys^{384} was indicated by the y-series ion pair 856 m/z (y_7) and 958 m/z (y_8). The ion pair of Cys^{381} in the b-series at 518 m/z (b_4) and 621 m/z (b_5) was only identified at b_4. The ion pair of Cys^{384} in the b-series at 815 m/z (b_7) and 920 m/z (b_8) was only identified at b_8. As observed with P4, modification occurred first at Cys^{381} followed by Cys^{384} and care was taken to correctly identify the 57 mass change due to CAM and not glycine. The y-series was identified in adductions including the Cys^{381} shift of y_{10} and y_{11} to 1152 m/z and 1312 m/z for 1-CAM and 1209 m/z and 1369 m/z with 2-CAM adductions. The second Cys^{384} shift was detected at 1015 m/z (y_8) but not at

y_7; however, the b-series ion pair was identified at 872 m/z (b_7) and 1161 m/z (b_8).

The fragmentation of BAM adducted P4 is shown in Figure 3.20. Cys^{37} was alkylated first and indicated by the y-series ion pair 1089 m/z (y_{10}) and 1519 m/z (y_{11}). The ion pair of Cys^{37} in the b-series at 518 m/z (b_4) and 948 m/z (b_5) was only identified at b_5. Cys^{37} did not have an ion pair identified in the 2-BAM spectrum in the y- or b-series; however, the b_5, b_6 and b_7 ions and the y_8, y_9 and y_{10} ion did indicate alkylation Cys^{37} in addition to Cys^{40}. Cys^{40} was only identified in spectra, with a Cys^{37} BAM adduct and was indicated by the b-series ion pair 1142 m/z (b_7) and 1570 m/z (b_8). The fragmentation of BAM adducted P24 is shown in Figure 3.21. In both 1-BAM and 2-BAM adducted spectra neither ion pairs in the y- or b-series were present. However, the 1-BAM P24 spectrum did not identify Cys^{384} as being alkylated and the presence of 518 m/z (b_4) and 1152 m/z (y_{10}) default Cys^{381} as the primary alkylation site. In the 2-BAM adducted P24, the modified Cys^{384} was indicated by the y-series ion pair 856 m/z (y_7) and 1284 m/z (y_8) as well as the b-series ion pair 1141 m/z (b_7) and 1570 m/z (b_8). The identification of alkylation at these four cysteine residues was confirmed by MALDI-TOF/TOF tandem MS.
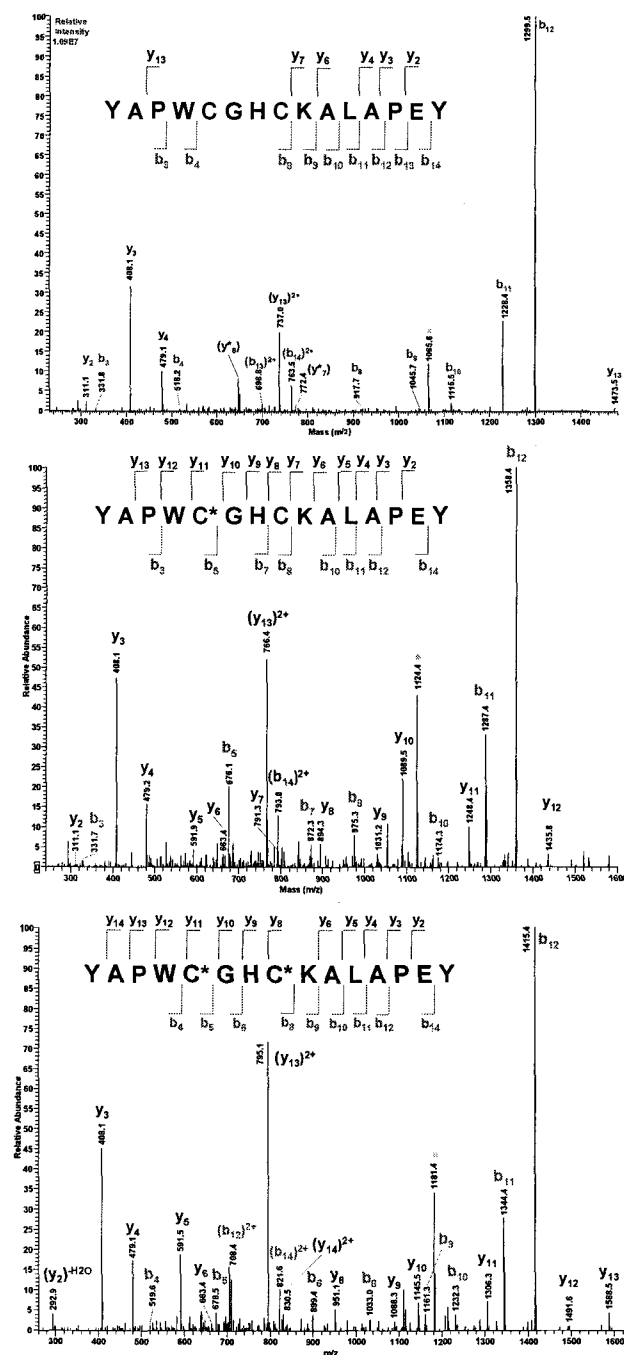
Figure 3.18 [M+2H]²⁺ CID spectra of the P4 peptide with 1-CAM adduct on the Cys³⁷ residue and 2-CAM adducts on Cys³⁷ and Cys⁴⁰ residues. Spectra of precursor ions unmodified (854 m/z), 1-CAM (884 m/z) and 2-CAM (913 m/z) are shown.
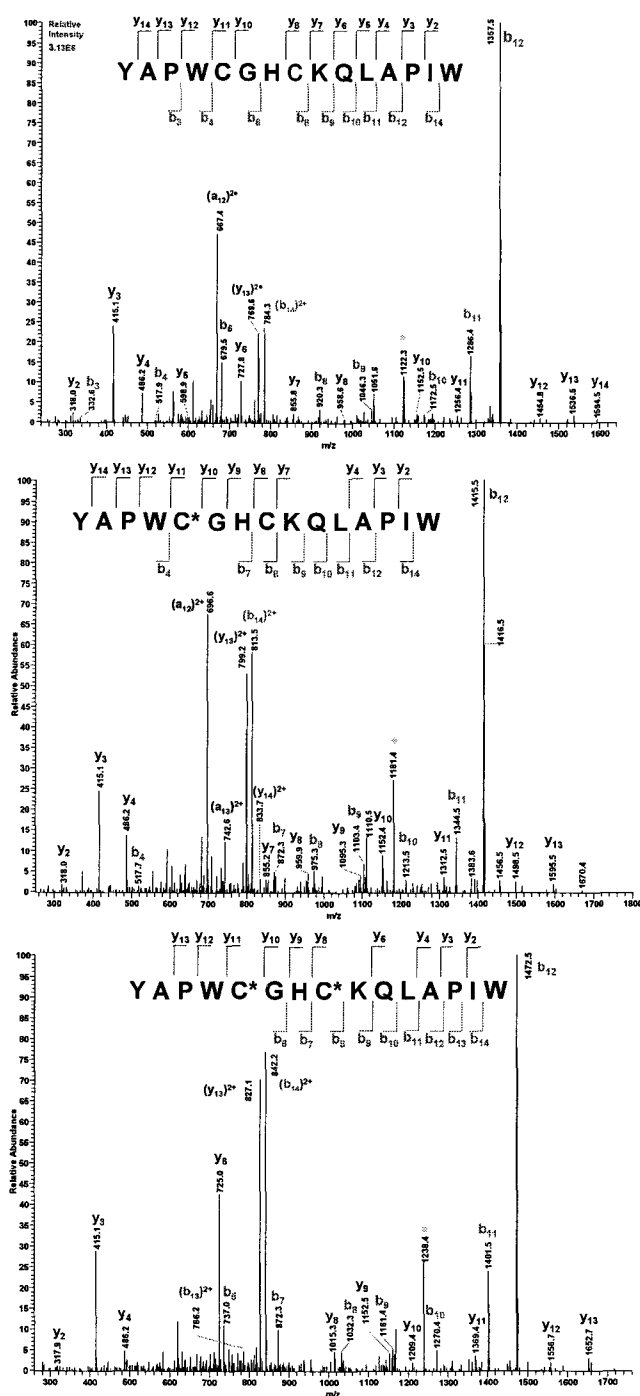
Figure 3.19 [M+2H]$^{2+}$ CID spectra of the P24 peptide with 1-CAM adduct on the Cys^{381} residue and 2-CAM adducts on Cys^{381} and Cys^{384} residues. Spectra of precursor ions of unmodified (887 m/z), 1-CAM (915 m/z) and (944 m/z) are shown.
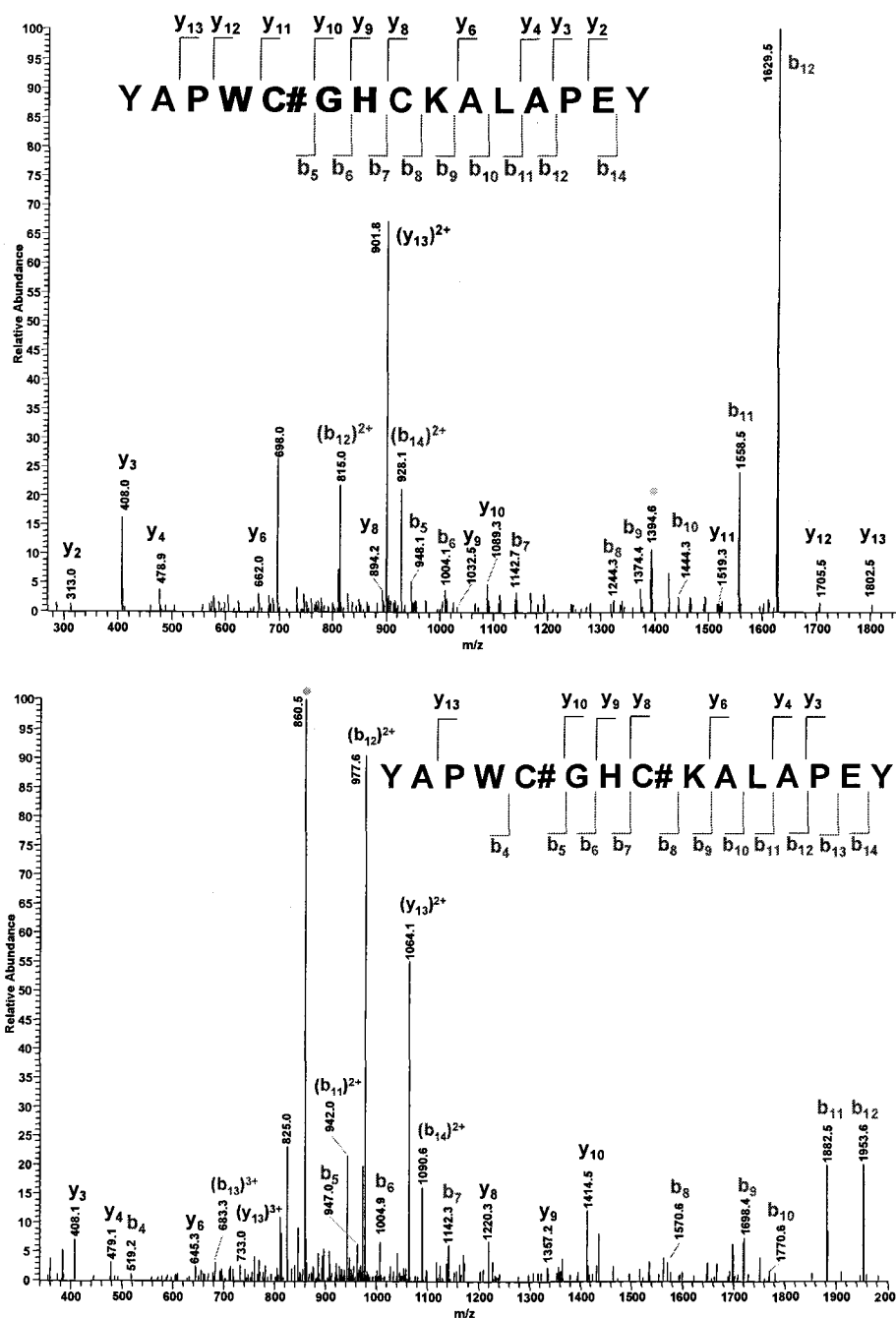
Figure 3.20   [M+2H]$^{2+}$ CID spectra of the P4 peptide with 1-BAM adduct on the Cys^{37} residue and 2-BAM adducts on Cys^{37} and Cys^{40} residues. Spectra of precursor ions 1-BAM (1018 m/z) and 2-BAM (1181 m/z) adducted peptides.
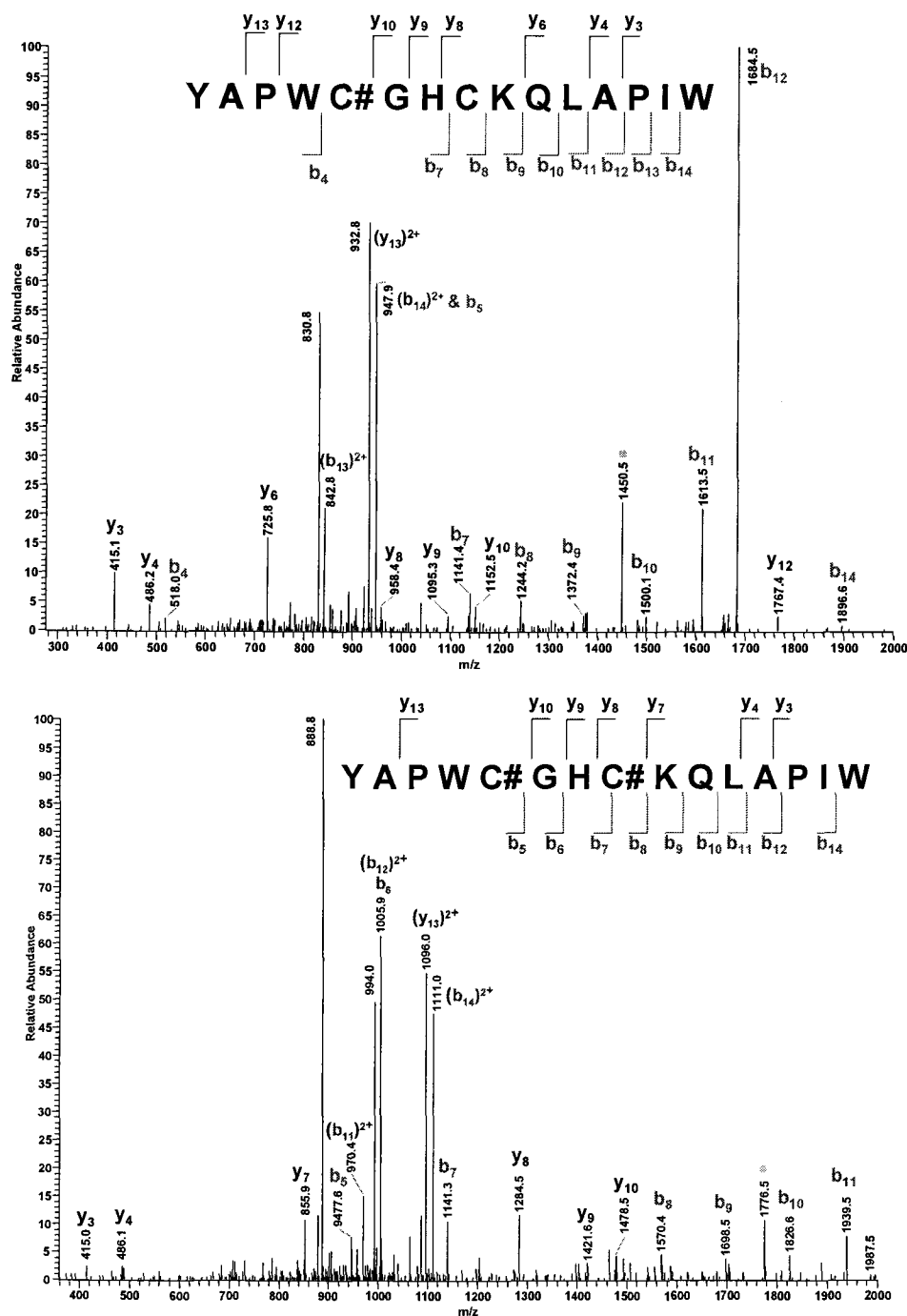
Figure 3.21   [M+2H]$^{2+}$ CID spectra of the P24 peptide with 1-BAM adduct on the Cys^{381} residue and 2-BAM adducts on Cys^{381} and Cys^{384} residues. Spectra of precursor ions of 1-BAM (1050 m/z) and 2-BAM (1213 m/z) adducted peptides.

3.5   DISCUSSION

The goal of this study was to determine the relative susceptibility of the thiolate anions in the two active sites of PDI to alkylation. PDI was incubated with increasing doses of CDNB and then the ability of PDI to reduce the disulfide of insulin and the ability to refold reduced denatured RNase was measured. There was a decrease in both reductase and oxidative folding activity; however, complete inhibition was not achieved in either assay. Four thiols of reduced PDI could be measured with DTNB and incubation with 1 mM CDNB showed a loss of two thiols after 30 minutes. PDI incubated with 0.25 mM IAM also showed a loss of two thiols after 30 minutes with a concurrent complete loss of activity. Clearly, IAM is depleting the availability of the catalytic sites of PDI more efficiently than CDNB. For this reason, IAM was used to determine the residues targeted for alkylation.

Small molar excesses of IAM over PDI were incubated, and the protein was subjected to LC-MS to determine the number of alkylation events. PDI was alkylated a maximum of four times by IAM. The carbamidomethylated (CAM) sites were identified to occur first at the N-terminal cysteine in each active site (Cys^{37} and Cys^{381}). The second cysteine residue (Cys^{40} and Cys^{384}) were modified subsequently, and only identified in spectra in which the first cysteine was also modified. The alkylation of the N-terminal cysteine of –C*GHC– in each domain was expected and can easily be explained by the chemical properties described for these two sites. The pKa of the N-terminal cysteine residues have been reported to be 4.5 (Kortemme et al., 1996; Ferrari and Soling; 1999) and the redox potential of PDI is one of the most oxidizing proteins identified (Aslund et al., 1997) second only to DsbA and DsbC, the prokaryotic homologs of PDI.

Identification of the second residue in both the **a** and **a'** domains of PDI as a third and fourth alkylated residue has not been reported in the literature. The contribution of these sites to activity was not clear. Hawkins and Freedman (1991) noted that inhibition of PDI occurred with the incorporation of only 2 moles of [^{14}C]IAA per mole of PDI polypeptide. IAM is less polar than IAA and may have been able to alkylate the buried cysteine residues with greater efficiency. The second cysteine residue in each active site domain has a higher pKa of 8.5, more representative of the pKa of free cysteine. The second cysteine in each active site domain has been reported to be required for net oxidation of substrate proteins *in vitro*, but its role *in vivo* may be to facilitate disruption of intermolecular disulfides, allowing efficient scanning of several disulfide isomers and to prevent trapping of PDI in disulfide linked complexes (Walker and Gilbert, 1997; Schwaller et al., 2002).

In regard to susceptibility to IAM alkylation, there was no preference of one active site to be alkylated before the other. The spectra representing both domains were found in each sample containing IAM. None of the IAM incubations yielded a sole mono-alkylated protein; there was always a bis-alkylated protein as well. The four alkylations were attributed to the two cysteine residues in the two active sites. Possible modifications were searched on cysteine, histidine, tyrosine, serine, and threonine residues as well as the N-terminus. There was no evidence that another residue other than cysteine was modified.

A similar titration with BIAM showed the same alkylating profile as IAM. The biotinoyl moiety conjugated to IAM increased the alkylating mass 5.7 times that of the CAM moiety. This increase in size did not hinder alkylation of either the first or second cysteine in each domain. The biotinoyl

moiety is still relatively non-polar and evidence of alkylation by more polar molecules may change the accessibility of one or both of the cysteine residues in a domain. CDNB was larger than IAM, yet it did not alkylate to the same extent as IAM or BIAM. One explanation of this may be because of the charge associated with the nitro groups of CDNB. PDI may hinder the accessibility of the active site by electrostatic forces.

The thiolate anion in each domain **a** and **a'** of PDI has shown to be susceptible to alkylation by IAM and BIAM. The second cysteine residue in each site was also susceptible to alkylation. PDI activity was reduced in the presence of CDNB with a concomitant loss of thiols. The availability of these thiolate anions is still not comparable to the rate or extent of inhibition of TR by CDNB (Arner et al., 1995). The dinitrophenyl alkylated residues of TR were identified to be the cysteine and selenocysteine of the –GC(SeC)G– C-terminal extension (Nordberg et al., 1998). Our data support the hypothesis that the SeC has an unusually high reactivity and low pKa value, which makes this residue a natural target for alkylation. PDI does not have this selenol group but the two thiolate anions are 1000 to 10000 times more reactive than a cysteine thiol group rendering PDI a very good target as well. The selenol group seems to contribute greatly to the reactivity of TR to CDNB. The carbonium ion produced after the loss of the chlorine of CDNB is distributed over a larger area compared to IAM. CDNB does alkylate PDI initially; however, the tertitary structure of PDI might have changed after one alkylation leading to a decrease in accessibility of the other domain.

Mutational studies revealed nonequivalence of the N- and C-terminal domains (Lyles and Gilbert, 1994). The **a'** domain contributes more to apparent steady-state binding, and the **a** domain contributes more to catalysis at saturating concentrations of substrate. There is also evidence of

equivalence between the active sites of domain **a** and **a'** (Vuori et al., 1992). Further mutation studies have shown differences between the oxido-reductase and isomerase activities of PDI with PDI cysteine mutants to complement a DsbA (formation of disulfide bonds) or DsbC (isomerization of disulfide bonds) deficient *E. coli* (Stafford and Lund, 2000). The requirements for the redox active cysteine residues are more stringent for oxidase activity than isomerase activity. Isomerase activity was dependent on both cysteine residues in the **a** domain, and severely reduced with mutation of either cysteine in the **a'** domain. Oxidase activity was reduced to 56% if Cys^{37} was the only cysteine available and 29% if Cys^{381} was the only cysteine available.

The use of mass spectrometry to determine the amino acid residue of alkylation in a large and complex protein proved to be insightful in beginning to assess the relative susceptibility of PDI thiols to alkylating agents. The accessibility of the active site thiols becomes an important aspect of analyzing PDI as a target for biological reactive intermediates *in vivo*. Of the seven proteins identified in the ER as targets for the reactive metabolites of bromobenzene, PDI and three of its homologues (ERp29, P5, and ERp57) were targeted (Koen and Hanzlik, 2002). Because PDI is present in such high concentrations, serves as a chaperone and has two redox-sensitive catalytic sites, the actual residue of adduction may prove to have implications on the role of PDI *in vivo*. PDI has been found to have an increased turnover rate in oxidatively stressed cells and was selectively degraded by the proteasome and new PDI was synthesized. Perhaps PDI plays a protective role for the cell or is a target simply based on its abundance. PDI is also a target for the reactive metabolites of acetaminophen and methoxychlor (Zhou et al., 1995; 1996). PDI has also been implicated in the hepatotoxicity of halothane (Martin et al., 1993a; 1993b; Pohl et al., 1989).

The mechanism through which PDI is targeted during chemically induced toxicity is still unknown. PDI is a major redox-active protein of the ER existing in high concentrations; however, isomerase activity may not be the only, or even the major, function of PDI in cells. At high concentrations, it serves as a chaperone and inhibits aggregation; however, at lower concentrations PDI can display the unusual ability to facilitate aggregation, termed anti-chaperone activity (Puig and Gilbert, 1994). Alkylation with these electrophiles did not alter the mass of peptides containing the peptide binding region in the **b'** and **a'** domains. Our findings implicate the reactivity of the thiols of PDI in chemically induced toxicity, which can lead to the possibility of PDI as an element of the redox-controlled pathways in the cell.

3.6 CONCLUSION

The activity and thiol groups of PDI were affected by *in vitro* incubation with CDNB. Initial mass spectrometry experiments suggested that PDI is alkylated by at least two dinitrophenyl moieties of CDNB, one in each "end" of PDI as delineated by PDI versus weePDI mass spectra. The CDNB concentrations required for inhibition of PDI were many fold lower than concentrations inhibiting TR suggesting that the alkylation sites of TR, i.e., the –GC*(SeC)*G– active site of TR, appear to be more nucleophilic than the thiolate anion present at the active site –C*GHC– hypothesized to be the most susceptible site of alkylation in the PDI active sites. This suggests that PDI is not as susceptible to alkylkation by CDNB as TR *in vitro*. Because of the role of oxidative folding PDI has *in vivo*, its abundance in the ER, and its identification as a target in proteomic analyses in chemically induced toxicity, the complete inhibition of activity by the thiol specific probe IAM suggests that irreversible alkylation could inactivate a critical thiol of PDI which could

have implications on PDI as a target for reactive metabolites *in vivo* such as those of CDNB.

PDI was alkylated by a maximum of four CAM or BAM groups derived from IAM and BIAM. The two cysteine residues in the two active site domains **a** and **a'** of PDI were identified as the residues modified. A titration of these cysteine residues showed alkylation of the first N-terminal cysteine residue (–C*GHC–) followed by alkylation at the second cysteine residue (–C*GHC*–). Modification with BIAM, a larger but similar electrophile, showed the same alkylating profile indicating that size does not preclude alkylation.

The next chapter discusses thiol modification as a target for the toxicity of the environmental contaminant 1,2-dichloroethane. The inhibition of activity and decrease in protein thiols of PDI *in vitro* after exposure to the glutathione conjugate of 1,2-dichlorethane, S-(2-chloroethyl)glutathione (CEG), is explored. An identification of the specific residues in PDI modified by CEG is presented.

3.7   ACKNOWLEDGEMENTS

4.0 ALKYLATION OF PROTEIN DISULFIDE ISOMERASE BY THE EPISULFONIUM ION DERIVED FROM THE GLUTATHIONE CONJUGATE OF 1,2-DICHLOROETHANE AND MASS SPECTROMETRIC CHARACTERIZATION OF THE ADDUCTS

4.1 ABSTRACT

Glutathione (GSH) can protect cells from both endogenous and exogenous electrophiles that cause cell damage. However, GSH conjugation can cause cytotoxicity by enhancing the reactivity of a number of xenobiotic chemicals, i.e., halogenated alkenes, quinones, and isothiocyanates. GSH conjugation to form S-(2-chloroethyl)glutathione (CEG) as a consequence of 1,2-dichloroethane exposure is another example of a toxification reaction. Evidence indicates that mutagenicity of 1,2-dichloroethane is due to the GSH conjugate. CEG can form an electrophilic episulfonium ion that can react with specific sites in DNA and proteins. Previous work in this laboratory has shown that *E. coli* thioredoxin alkylated by the episulfonium ion of CEG is inactivated based on the insulin reduction assay (Meyer et al., 1994). Further studies have shown that the alkylation of reduced *E. coli* thioredoxin by the episulfonium ion derived from CEG at physiological pH has resulted in alkylation primarily at the N-terminal Cys[32] site (Erve et al., 1995a). Our experiments compared the reactivity of this episulfonium ion with the catalytic sites of protein disulfide isomerase (PDI) which is a protein of the thioredoxin superfamily. PDI has two thioredoxin active sites. The redox-active site at the N-terminus contains two cysteine residues at positions Cys[37] and Cys[40] (recombinant rat PDI numbering) and the second redox-active site contains two cysteine residues at positions Cys[381] and Cys[384]. When reduced, these four cysteine residues are expected to be the major targets of alkylation by the episulfonium ion of CEG. We incubated reduced PDI for 90 minutes with

a range of concentrations from equimolar to 100 fold excess CEG to PDI. Reductase activity based on the NADPH-dependent reduction of insulin was irreversibly inhibited when incubated with a 100 fold excess of CEG. The ability of PDI to refold reduced denatured RNase was also decreased by approximately 75% with 100 fold excess of CEG. A concurrent loss of two free thiols was measured. MALDI and ESI mass spectrometry show a gain of at least two CEG derived episulfonium masses. Tandem MS spectra from electrospray LC-MS identified one alkylation event on each of the two active site peptic peptides. Sequencing by ESI tandem MS was unsuccessful due to fragmentation of the alkylating moiety from the peptide. MALDI-TOF/TOF tandem MS/MS successfully identified the N-terminal cysteine residues within each active site. Even though Cys^{37} and Cys^{381} are targeted and a loss of two thiols is observed, PDI activity was not completely inhibited. These results imply that PDI is robust and able to either maintain one unmodified active site or protect its active sites by steric constraint. Results of this study confirm that the episulfonium ion of CEG can adduct PDI at the active site and may have important toxicologic significance regarding the mechanism of 1,2-dichloroethane toxicity. (This work was supported by grants from the NIH (ES00040 and ES00210).

4.2   INTRODUCTION

1,2-Dihaloethanes have been found to be hepatotoxic, mutagenic, and carcinogenic. Exposure to these compounds leads to a substantial loss of cellular glutathione accompanied by lipid peroxidation (Albano et al., 1984), formation of DNA adducts (Cmarik et al., 1992; Guengerich et al., 1987; Inskeep et al., 1986; Koga et al., 1986), and covalent protein adduct formation (Jean and Reed, 1992; Igwe et al., 1986; Hill et al., 1978). Dihaloethanes are metabolized via two pathways, either by microsomal

oxidation via CYP2E1 to chloroacetaldehyde or direct conjugation to GSH catalyzed by glutathione-S-transferase resulting in the formation of the episulfonium ion (Figure 4.1). The oxidation versus conjugation urinary metabolites of 1,2-dibromoethane occurs at a ratio of 4:1 in the rat (van Bladeren et al., 1981; Foureman and Reed, 1987) and low levels of 2-(S-chloroethyl)glutathione (CEG) derived from 1,2-dichloroethane (DCE) in the bile indicates that uptake of CEG or its metabolites through the intestinal wall and into the plasma may play an important role in determining the overall toxicity of 1,2-dihaloethanes (Marchand and Reed, 1989). The mutagenicity of DCE has been associated with the glutathione conjugate pathway of metabolism. Investigation of the alkylating activity of the bioactive episulfonium ion derived from CEG against model compounds such as dipeptides, nucleosides and glutathione revealed that CEG preferentially alkylates cysteinyl thiol groups (Jean and Reed, 1989; Erve et al., 1995b). It is becoming clear that amino acids alkylated in a protein are not randomly targeted, but are determined by the nature of the electrophile, available nucleophiles, and steric constraints imposed by the tertiary structure of the protein.

Previously, thioredoxin (Trx) was selected as a model protein to study the susceptibility of protein thiols and possibly other amino acid residues in toxification by DCE-glutathione conjugate modification. At physiological pH, treatment of *E.coli* thioredoxin by CEG resulted in several alkylated forms of thioredoxin as determined by isoelectric focusing and matrix-assisted laser desorption ionization (MALDI) mass spectrometry with a concomitant loss of *in vitro,* enzymatic activity (Meyer et al., 1994). The site of alkylation by the episulfonium ion derived from CEG was determined to be primarily at the N-terminal cysteine residue in the active site sequence –C*PYC– with electrospray ionization mass spectrometry in the MS/MS mode (Erve et al.,

1995a; Kim et al., 2002). In an effort to determine the relative reactivity of these vicinal thiols in the active sites of proteins in the thioredoxin superfamily, protein disulfide isomerase (PDI) containing two –CGHC– active site sequences was chosen.
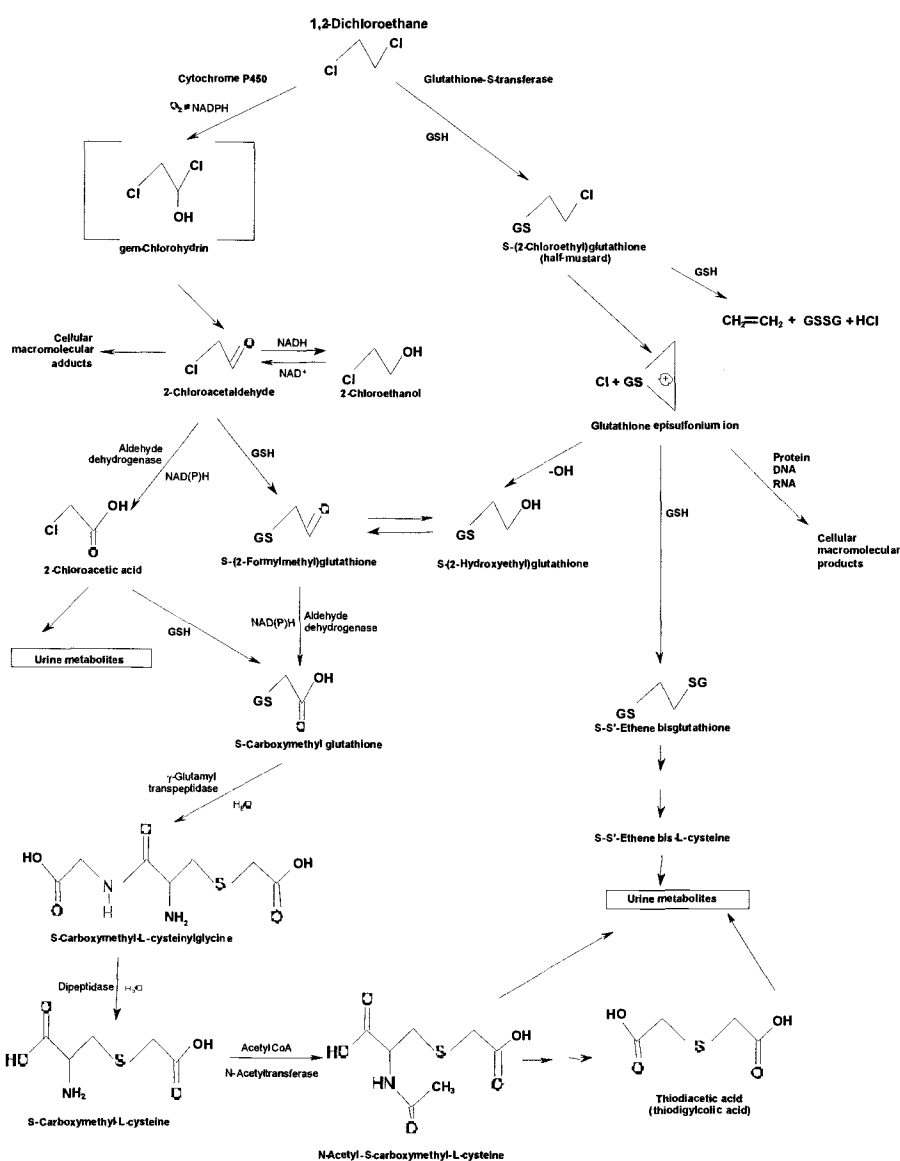
Figure 4.1 Proposed pathways for 1,2-DCE metabolism (from ASTDR, 1992)

PDI is primarily localized in the lumen of the endoplasmic reticulum, where it acts in the folding of newly synthesized proteins (Freedman et al., 1989; Gilbert, 1997). *In vitro* PDI catalyzes the oxidative formation, reduction and isomerization of disulfide bonds depending on the redox potential of the environment (Freedman et al., 1994). PDI contains a peptide binding site which is responsible for its chaperone/antichaperone activity (Wang, 2002; Primm et al., 1996; Tsai et al., 2001). The modular structure of PDI is composed of four thioredoxin fold domains which are arranged sequentially as **a, b, b'**, and **a'** followed by a C-terminal acidic extension, **c** (Kemmink et al., 1997). The thioredoxin fold structure of domains **a** and **b** have been determined by NMR (Kemmink et al., 1997; 1999) and the structures of **b'** and **a'** can be inferred from sequence homology.

The cysteine residues in the –CGHC– sequences of **a** and **a'** make up the two catalytically redox-active sites and are directly involved in thiol-disulfide exchange reactions. Only the first cysteine residue (Cys^{37} and Cys^{381} by recombinant rat PDI numbering) of **a** and **a'** has a sulfur atom that is accessible and reactive with external thiol and disulfide reagents; the second cysteine (Cys^{40} and Cys^{384}) is thought to be buried and less reactive (Lyles and Gilbert, 1994), though it is believed to provide an escape mechanism, preventing PDI from becoming trapped with substrates that isomerize slowly (Walker and Gilbert, 1997; Schwaller et al., 2002). The pKa of Cys^{37} (and Cys^{381} by sequence homology) in the **a** domain is 4.5 (Kortemme et al., 1996) leading to a stabilization of the thiolate anion of PDI at physiological pH. The overall redox potential of PDI ($E^{o'}$ = -178 mV) is oxidizing compared to that of the reducing thioredoxin (-270 mV) (Lundstrom and Holmgren, 1993; Krause and Holmgren, 1991). This propensity for the N-terminal cysteine of PDI's active sites to be ionized along with the high

millimolar concentrations of PDI in the ER *in vivo* suggest that PDI is a potential target of the episulfonium ion of the DCE-glutathione conjugate.

In chapter 3, studies were presented that describe the activity and thiol groups of PDI, which were affected by *in vitro* incubation with CDNB. Initial mass spectrometry experiments suggested that PDI is alkylated by at least two dinitrophenyl moieties of CDNB. The data show an increase in mass up to four alkylations per PDI polypeptide with both iodoacetamide (IAM) and its relative biotin-conjugated iodoacetamide (BIAM). These electrophilic agents first alkylated the N-terminal cysteine residue in each active site (–C*GHC–) followed by alkylation at the second cysteine residue (–C*GHC*–). Modification with BIAM showed no difference in alkylating profiles indicating that the accessibility of the active site was not limited by size of the alkylating agent.

The objective of this study was to determine the mechanism of inactivation of PDI by the episulfonium ion derived from CEG. *In vitro* activity measurements followed by mass measurements of whole native and modified PDI and tandem mass spectrometric analysis of peptide sequences analyses were undertaken to determine the nature of the episulfonium induced modifications. A decrease in activity and protein thiols of PDI is observed after incubation with CEG. A titration curve with CEG showed incremental increases equal to the ethyl glutathione moiety derived from the episulfonium. There were more than four increases in mass that were detected at the higher concentrations of CEG. Tandem mass spectrometry only identified two residues as modified, Cys^{37} and Cys^{384}, in both the **a** and **a'** domain active site sequence –C*GHC–.

4.3 EXPERIMENTAL PROCEDURES

4.3.1 Materials

All reagents used were purchased from Sigma unless otherwise noted. The pETPDI.2 plasmid containing the recombinant rat PDI gene was a generous gift from H.F. Gilbert. CEG was synthesized according to the method of Reed and Foureman (1986) and stored at -80°C and verified before use with FAB-MS. HPLC grade acetonitrile was supplied by Fisher Scientific and water was generated with a Milli-Q Ultrapure water purification system.

4.3.2 Expression and Purification of Recombinant Rat PDI

Rat recombinant PDI was expressed in *E. coli* strain BL21(DE3) (Novagen) containing the pETPDI.2 plasmid as a soluble cytosolic protein and purified over a DEAE-Sephacel column (Amersham Pharmacia) followed by a Zn^{2+}-affinity column (Chelating Sepharose™ Fast Flow, Amersham Pharmacia) as described previously (Gilbert, 1998; Gilbert et al., 1991). The reduced protein was concentrated and stored in 25 mM Tris (pH 8) at -80°C in 50 μl aliquots. Protein concentration was determined according to Bradford (1976) at a final concentration ranging from 10 to 20 mg/mL.

4.3.3 Reduction and Covalent Modification of PDI

PDI (0.1 mM) in 0.06 mL was incubated for 30 minutes with 2 mM tris(2-carboxyethyl)phosphine (TCEP) and then applied to a Micro Bio-Spin® column (BioRad) equilibrated with 25 mM NH_4HCO_3 (pH 8) to remove the

TCEP. CEG was weighed and dissolved in 25-50 µl of 25 mM NH_4HCO_3 buffer and quickly added to 0.05 mM of PDI in 0.06 mL aliquots to give molar concentrations ranging from equimolar to concentration of 100X fold excess. High molar excess was found necessary because water competes for the episulfonium ion in the hydrolysis of CEG. The pH dropped slightly with the addition of CEG so that the pH of the reaction was between 7.0 and 7.4. After 90 minutes at 37°C, CEG was removed with Micro Bio-Spin® columns equilibrated with 25 mM Tris (pH 8). Protein estimates were performed with BCA Protein Assay reagent (Pierce) with serum albumin as the standard.

4.3.4   PDI Reductase Activity

PDI reductase activity was assessed by the GSH-dependent reduction of insulin by coupling the formation of GSSG to NADPH oxidation via glutathione reductase (Gilbert,1998). Native and modified PDI (~1 µM) were diluted in phosphate buffer (0.2 M phosphate, 1 mM EDTA, pH 7.5) and combined in a 1 mL cuvette with 0.12 mM NADPH, 4U glutathione reductase, 5 mM GSH and preincubated for 1 minute to reduce the contaminating GSSG. Bovine insulin was then added (final concentration 30 µM) and the oxidation of NADPH was recorded every 30 seconds for 5 minutes at 340 nm. After subtracting the background rate of uncatalyzed insulin reduction, the specific activity was calculated on the basis of $\varepsilon = 6.23$ $mM^{-1}cm^{-1}$. The specific activity of PDI in this assay was 0.12 (± 0.01) µmol of GSSG formed/min/mg. Spectrophotometric measurements were performed with a Beckman DU®-64 with a Kinetics soft-pac module.

4.3.5 Assay of RNase Refolding

PDI activity was measured by observing the activity due to the formation of native RNase with cCMP as a substrate (Lyles and Gilbert, 1991a and 1991b; Gilbert, 1998). The hydrolysis of cytidine 2',3'-cyclic monophosphate (cCMP) at an initial concentration of 4.5 mM was monitored continuously at 296 nm with a $\Delta\varepsilon$ of 0.19 mM^{-1}cm^{-1}. Active RNase concentration at any time was calculated from the first derivative of the absorbance versus time curve. The assay was performed at pH 8.0, 25°C in 0.1 M Tris-acetate buffer containing 2 mM EDTA, a glutathione redox buffer (1 mM GSH/0.2mM GSSG) and 0.1 μM PDI. Reduced denatured RNase (Ribonuclease A from bovine pancreas, type IIIA) was prepared by the method of Gilbert (1998). Spectrophotometric measurements were performed with a Beckman DU$^{\circledR}$-64 with a Kinetics soft-pac module.

4.3.6 Protein Thiols

Protein thiols were measured by a Thiol Quantitation Kit (T-6060, Molecular Probes). Protein thiols reduce a disulfide inhibited derivative of papain (papain-SSCH$_3$), stoichiometrically releasing active papain. Active papain cleaves N-benzoyl-L-arginine-p-nitroanilide (L-BAPNA), releasing the p-nitrolaniline chromophore. Cysteamine is added to permit the detection of poorly accessible thiols that have high pKa values. This method of thiol quantitation is 100 fold more sensitive than Ellman's reagent (Wright and Viola, 1998; Singh et al., 1993).

4.3.7 Chromatography and Mass Spectrometry of Whole Protein

Chromatography of native and modified PDI was performed on a 0.32 mm, 5A column packed with Jupiter C_4 stationary phase (Phenomenex) proceeded by a Protein Microtrap (Michrom BioResources, Inc.). Solvent A was 0.03% trifluroacetic acid (TFA) in 95:5 water:acetonitrile, while solvent B contained the same acid modifier in 5:95 water:acetonitrile. A linear gradient was performed from 10% to 60% B in 20 minutes followed by a sharper gradient to 95% B in 10 minutes for a total of 30 minute runs. Mass spectra were obtained on a Perkin Elmer SCIEX API III+ triple-quadrupole mass spectrometer (SCIEX). The ion spray voltage was 5,000 volts and the orifice voltage was 100 volts.

4.3.8 MALDI-TOF MS Analysis of Native and Modified PDI

Matrix assisted laser desorption-time of flight mass spectrometric analysis of native and modified PDI (55114 Da) was performed on a custom built time-of-flight reflector mass spectrometer equipped with a two-stage delayed extraction source. Approximately 1 μl of sample was mixed with 3 μl of sinapinic acid or α-cyano-4-hydroxy cinnaminic acid in 40% acetonitrile with 0.1% TFA. A 1 μl droplet of this analyte/matrix solution was deposited onto a matrix pre-crystallized sample probe and allowed to dry in air. Mass spectra were produced by irradiating the sample with a (355 nm) Nd:YAG laser (Spectra Physics) and operating the ion source at 23 kV with a 700 ns/1.0 kV delay. Every mass spectrum was recorded as the sum of 30 consecutive spectra, each produced by a single pulse of photons. Ions from bovine serum albumin (66 kDa) were used for mass calibration.

4.3.9 Peptic Digestion

To denature the protein, 18 µl of 8M urea and 4 mM TCEP (dissolved in 0.1 M citric acid) was added to 30 µg of PDI and incubated for 1 hour at 37°C. Porcine pepsin (10 µg) (Sigma) was dissolved in 100 µl of 5% formic acid and 3 µg (30 µl) of pepsin was added to the protein solution. Digestion was allowed to proceed for 2-3 hours at 37°C. Alternatively, 30 µg of native or modified PDI was combined directly with 3 µg of pepsin dissolved in 5% formic acid and digested for 2-3 hours at 37°C.

4.3.10   Chromatography and Mass Spectrometry of Peptides

Chromatography was performed on a 0.17 mm column packed with Jupiter C_{18} stationary phase (Phenomenex) proceeded by a Peptide Captrap (Michrom BioResources, Inc.). Solvent A for liquid chromatography was composed of 0.01% TFA and 0.1% acetic acid in 95:5 water:acetonitrile, while solvent B contained the same acid modifiers in 5:95 water:acetonitrile. A linear gradient was performed from 10% to 60% B in 70 minutes followed by a sharper gradient up to 95% B over 10 minutes for a total of 80 minute runs. Peptic digests were loaded onto the trap in 10µl aliquots and then washed with Solvent A prior to injection onto the column. Mass spectra were obtained on a Finnegan LCQ ion trap mass spectrometer (ThermoFinnegan). In a method similar to Jones and Liebler (2000) and Mason and Liebler (2000), the scan event series included one full scan (mass range = 400 to 2000 m/z) followed by three data-dependent MS/MS scans on the most intense ion. Dynamic exclusion was used with a repeat count of 1 over 1 minute with a 3 minute exclusion duration window.

4.3.11   Data Analysis

SEQUEST (ThermoFinnegan) and MASCOT (Matrix Science) were used for protein and peptide identification. For both programs the non-redundant database and a specified recombinant rat PDI sequence were searched to identify peptides. Defining analysis parameters included no endoprotease (pepsin is non-specific) and possible modifications (+ 333 m/z) for Cys, His, Tyr, Ser, Thr, and N-terminus. The SEQUEST algorithm was used to analyze tandem mass spectra as previously described (Wolters et al., 2001). MASCOT was used to verify the protein identifications found in SEQUEST and also to search for modifications (Perkins et al., 1999). To facilitate identification and characterization of unmodified and modified PDI-derived peptides, peptide-sequence motif searches of the LC-MS/MS spectral data were analyzed with the Scoring Algorithm for Spectral Analysis (SALSA) (Hansen et al., 2001; Liebler et al., 2002).

4.3.12   MALDI-TOF/TOF Analyses

Aliquots of peptide digests were desalted and concentrated with C_{18} ZipTips (MilliPore Corporation) and mixed with saturated solution of α-cyano-4-hydroxycinnamic acid in 50% acetonitrile and 0.1% TFA and applied to a sample plate. Molecular mass analysis was performed by MALDI MS with an ABI4700 TOF/TOF (Applied Biosystems Inc., Framingham, MA). Data were acquired in the MALDI reflector mode with the internal ABI4700 Calmix calibration standard provided by Applied Biosystems. Data in the collision induced decay (CID) mode were calibrated with fragment ions from Glu[1]-fibrinopeptide B. Tandem mass spectra were generated by acceleration of precursor ions at 8 kV and selection with a timed gate with a window of ± 3

m/z. Gas pressure (air in the CID chamber) was set at 1 µTorr. Fragment ions were further accelerated by 14 kV prior to entry into the reflector. Data analysis was performed with MASCOT described above and confirmed with the ProteinProspector MS-Product tool at http://prospector.ucsf.edu.

4.4   RESULTS

4.4.1 Inactivation of Activity

Using the NADPH-dependent reduction of insulin disulfide, initial experiments showed that preincubation of recombinant rat PDI with TCEP followed by incubation for 90 minutes with increasing concentrations (1X, 5X, 10X, 50X, 75X, and 100X fold excess) of CEG over PDI inhibited reductase activity in a concentration dependent manner (Figure 4.2). The specific activity of PDI under the conditions of this experiment was 0.13 ± 0.01 µmol of GSSG formed/min/mg. Incubation of PDI with 100X fold excess CEG over PDI resulted in complete inhibition of reductase activity similar to the inhibition of PDI by 0.25 mM IAM (5X fold excess) after 30 minutes (data not shown). Inactivation persisted after removal of CEG with polyacrylamide spin columns indicating that adduct formation was the mechanism of inactivation. These experiments used a maximum of 100X fold excess of CEG, five times less than the concentrations of CDNB used to inactivate PDI without complete inhibition described in chapter 3. This assay only measured the reductase capabilities of PDI; for oxidative folding activity, the continuous RNase refolding assay was used.
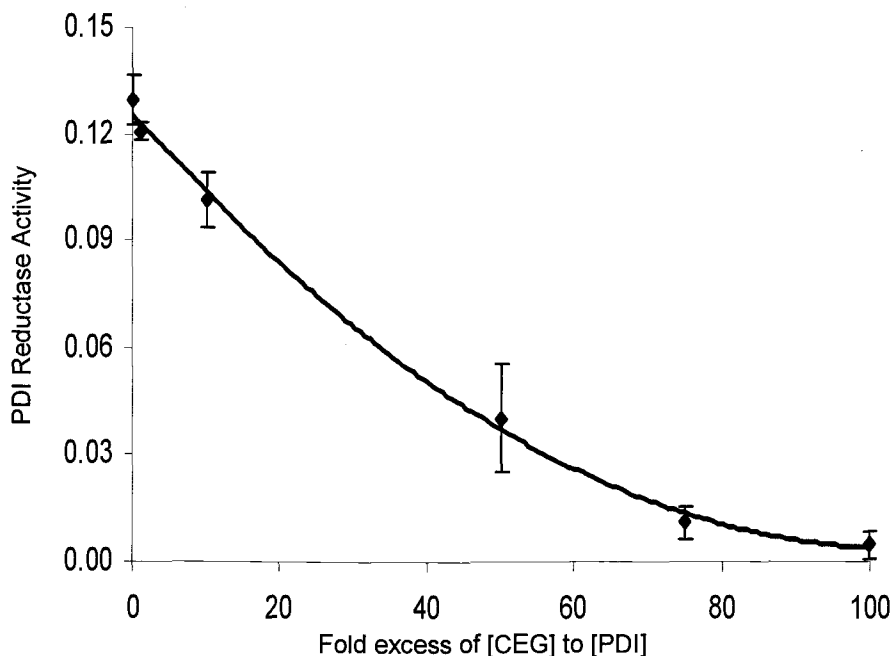
Figure 4.2   Inhibition of the NADPH-dependent reduction of insulin disulfide by varying concentrations of CEG. Reduced recombinant rat PDI was incubated with CEG at 37°C for 90 minutes then applied to polyacrylamide spin columns to remove CEG. Data points represent the mean ± standard deviation of three or four experiments.

The isomerase activity of PDI was measured by incubating PDI with reduced denatured RNase. As PDI refolds RNase, RNase is capable of hydrolyzing cCMP to CMP. Monitoring the appearance of CMP over time was a direct measurement of active PDI in the sample. Figure 4.3 is a representation of the absorbance change during the PDI catalyzed refolding of reduced denatured RNase in the presence of cCMP. Reduced PDI preincubated with 10X, 50X, 75X, and 100X excess CEG also exhibited a

dose dependent decrease in activity; however, complete inhibition was not achieved. At 100X fold excess, PDI was irreversibly decreased bt 70% of the activity observed with unmodified PDI. Further excesses of CEG above 100X caused the pH of the reaction to drop below pH 7 and resulted in precipitation of the protein.
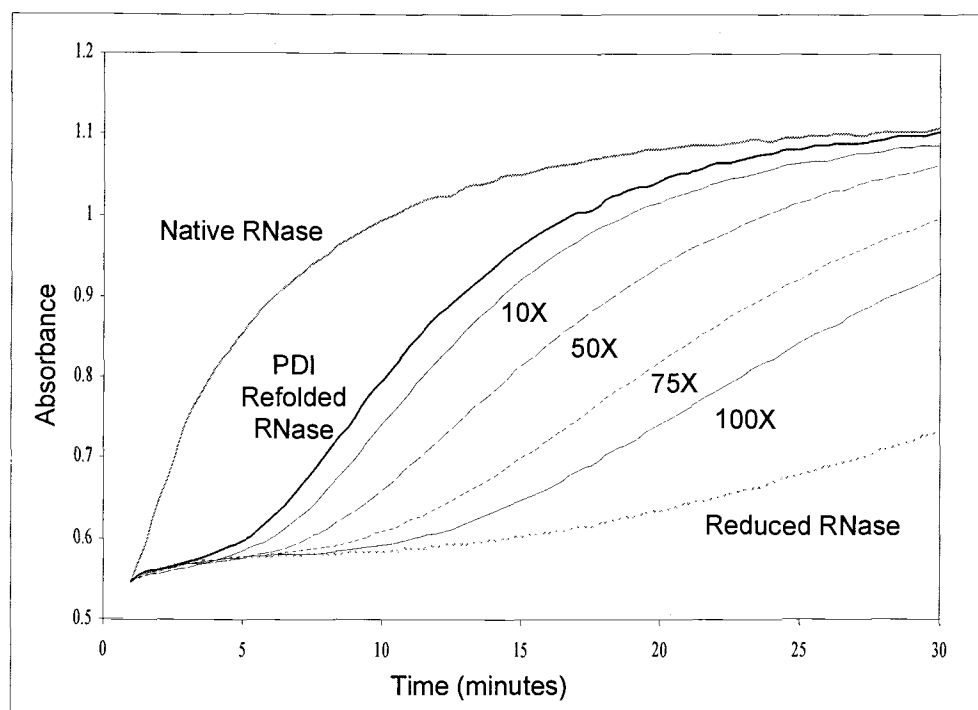
Figure 4.3   Inhibition of PDI oxidative folding activity by increased concentrations of CEG. Time course for the absorbance change at 296 nm produced by the RNase-catalyzed hydrolysis of cCMP. Refolding of RNase by modified PDI is decreased.

4.4.2   Decrease in Protein Thiols

The assay used to quantitate thiols is based on a method reported by Singh et al. (1993). The thiols or sulfides reduce a disulfide-inhibited derivative of papain, stoichiometrically releasing the active enzyme. Activity of the enzyme is then measured by the chromogenic papain substrate L-BAPNA. Although thiols and inorganic sulfides can also be quantitated by 5,5'-dithiobis-(2-nitrobenzoic acid) (DTNB or Ellman's reagent), the enzymatic amplification employed in this assay yields a sensitivity for detection of thiols or sulfides of approximately 100-fold better than that obtained with DTNB. Thiols in proteins and potentially other high molecular weight molecules can be detected indirectly by incorporating the disulfide cystamine into the reaction mixture. Cystamine undergoes an exchange reaction with protein thiols, yielding 2-mercaptoethylamine (cysteamine), which then releases active papain. Of the six cysteine residues in PDI, only 4.12 ± 0.54 mole SH/mole PDI could be measured, similar to our experiments with DTNB (described in chapter 3). Increasing amounts of CEG (1X, 5X, 10X, 50X, 75X and 100X) preincubated had a maximum loss of 2.31 moles SH/mole PDI (Figure 4.4). The protein thiols of PDI after incubation with 100X fold excess of CEG over PDI was measured at 1.81 ± 0.45 mole SH/mole PDI. After a 90 minute incubation of PDI with 100X CEG, IAM was added for 30 minutes to completely alkylate any cysteine residues not affected by the episulfonium. IAM incubation resulted in a further decrease in measured thiols to 1.21 ± 0.21 mole/mole PDI (data not shown).
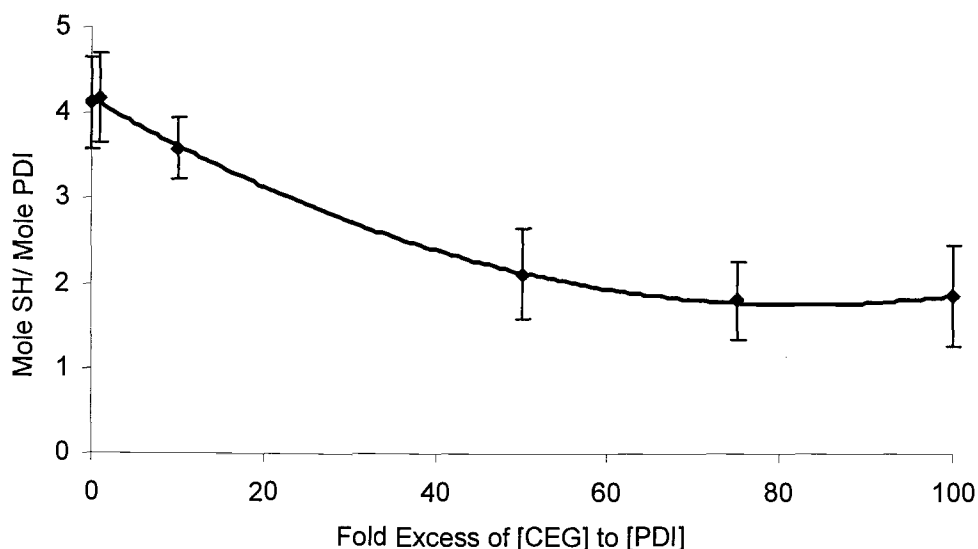
Figure 4.4 Effect of CEG on protein thiols. After reduction with TCEP, PDI was incubated with CEG then separated by polyacrylamide spin columns. Protein thiols were measured by the disulfide inhibited derivative of papain and L-BAPNA per protocol.

4.4.3 Mass Analysis of Native and Modified PDI

MALDI-TOF was initially used to characterize unmodified and undigested PDI. Analysis of the freshly purified enzyme gave a spectrum with an $[M+H]^+$ ion that corresponded to ~55114 m/z ratio for PDI in Figure 4.5. The mass accuracy of the MALDI-TOF MS at high molecular weights greater than 25,000 was estimated to be at ± 30 m/z. The molecular weight of CEG is 369 g/mol. When it loses the chlorine during the formation of the episulfonium ion, the resulting molecular weight is 334 g/mol. The episulfonium ion causes an increase of 333 m/z on a cysteine residue due to the loss of the cysteine hydrogen. Equimolar concentrations of CEG to PDI

resulted in no mass change. A 10X fold excess of CEG over PDI induced the appearance of one modified species with an increase of 327 m/z. With 50X, 75X, and 100X fold excess of CEG to PDI, two modified protein adducts or more were detected. In the MALDI-TOF spectrum representing PDI incubated with 75X fold excess CEG over PDI, native PDI is measured at 55093 m/z. A mono-alkylated (55442 m/z) and bis-alkylated protein adducts were identified which represented an increase of 328 m/z and 684 m/z, respectively. A peak also was detected at 56107 m/z which could represent a tris-alkylated protein adduct. At high CEG excesses (50X and above), it was not possible to delineate a peak due to alkylation versus the additional satellite peaks of sinapinic acid adduct ion (~214 m/z) used as the matrix. Adductions of greater than three alkylations are difficult to determine by this method. We employed a SCIEX III+ triple quadrupole electrospray ionization mass spectrometer to better determine the extent of alkylation.

Bis-alkylated PDI (55798) (56107) ?

Mono-alkylated PDI (55442) Tris-alkylated PDI

native PDI (55093)

75X CEG

Mono-alkylated PDI (55435)

native PDI (55107)

10X CEG

native PDI (55092)

1X CEG

native PDI (55114)

50000 m/z 60000
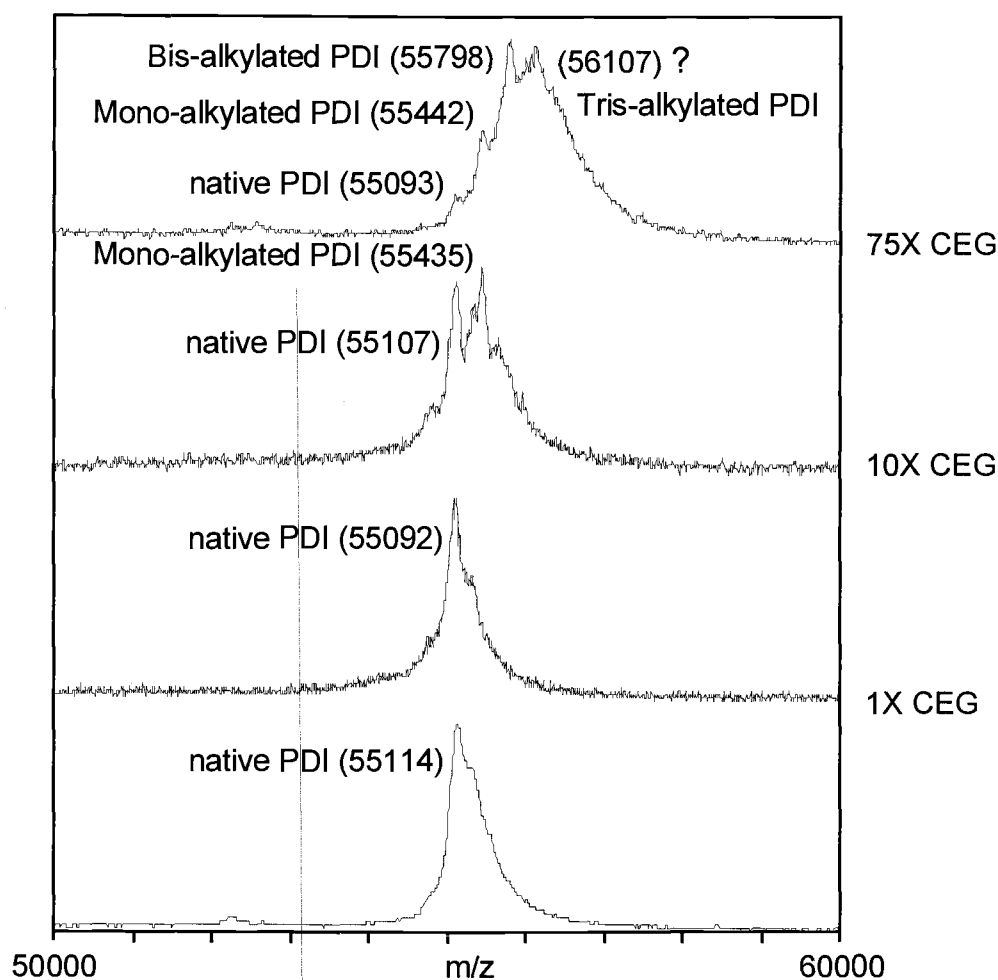
Figure 4.5   MALDI-TOF mass spectra of nativePDI and PDI modified with 1X, 10X and 75X fold excess of CEG over PDI.

The masses of native PDI and its CEG modified derivatives were also determined by electrospray ionization LC-MS. Figure 4.6 contains the reconstructed masses of PDI incubated with equimolar (1X), 2X, 5X, 10X and 50X fold excess of CEG over PDI. A peak representing mono-alkylated PDI was immediately observed in the 2X incubation with an emergence of a bis-alkylated PDI. A 5X fold excess of CEG over PDI showed two modified species. The sensitivity of PDI to CEG at such low concentrations indicated a specific site(s) of alkylation. More than one alkylated species began to

emerge at a 10X fold excess and at excesses above 50X, four alkylations were observed. The emergence of multiply alkylated species did occur and possibly six modifications can be delineated from the baseline; however, the total concentration of PDI used was spread too thin and the multicharge envelope with 6+ protein adducts became too complicated to quantitate. Clearly, PDI was alkylated in several places. There was still mono-alkylated PDI within the mixture that could account for the reductase and oxidative folding activity observed in the 50X fold excess incubations. Reductase activity was not inhibited until 100X fold concentrations of CEG were used which may correspond the total loss of native and mono-alkylated species.
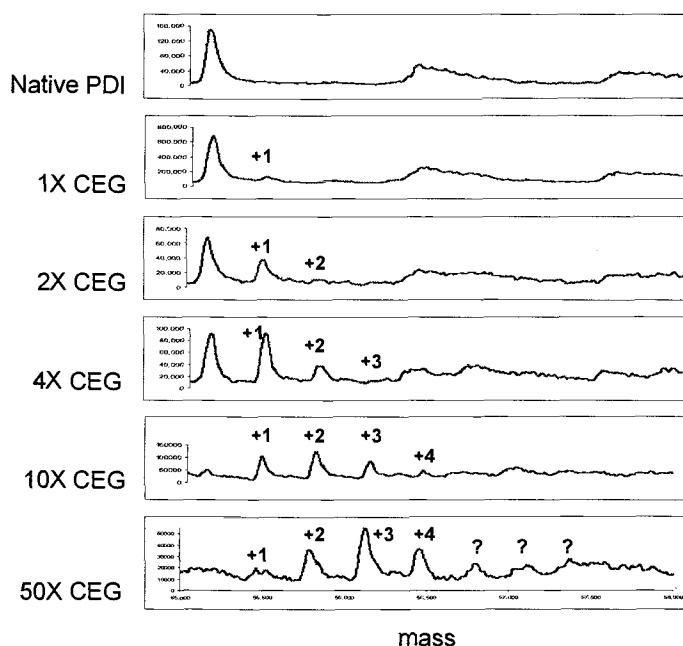
mass

Figure 4.6   Reconstructed mass of the multicharge envelope of native PDI and PDI incubated with 1X, 2X, 5X 10X, and 50X fold excess of CEG over PDI. The difference between peaks is equal to 333 m/z (an ethyl glutathione moiety derived from the episulfonium ion of CEG).

4.4.4 Peptide Mapping and Tandem Mass Spectrometry

In order to further elucidate the actual residues of alkylation by the episulfonium ion onto PDI, we obtained a peptide map that was used to sequence specific residues. In choosing a proteolytic enzyme, we found that trypsin and chymotrypsin generated a peptide map with high peptide coverage; however, the specific peptides containing the –CGHC– sequences in question were too large or became too large after alkylation to be seen easily in the doubly charged state. Pepsin was successfully employed for two reasons. First, the digest would contain the two peptides in a reasonable mass range for the LCQ electrospray ion trap, and second, the non-specificity of pepsin allowed for better coverage of the active site sequences due to multiple protease sites on each end of the peptides. After digestion at ~ pH 2, pepsin generated a peptide map containing approximately 29 peptides accounting for the various permutations at the peptide ends due to pepsin (Figure 3.12). The peptides containing the two active site sequences in the **a** and **a'** domain were P4 (YAPWCGHCKALAPEY, 1707.8 m/z) and P24 (YAPWCGHCKQLAPIW, 1772.8 m/z).

The peptides were separated by reverse phase chromatography on a C_{18} microbore column prior to mass analysis. Abundance of the peptides P4 and P24 was low relative to the other peptides and the total ion chromatogram (Figure 3.13). The MS1 full spectrum of the $[M+H]^+$ and $[M+2H]^{2+}$ unmodified P4 and P24 peptide ions are in the first spectra in Figures 3.13 and 3.14. The intense masses of P4 and P24 were 1705.7 (1707.6) and 1770.6 (1772.7). The 2 m/z difference in the [M+H]+ peaks are due to the presence or absence of the hydrogen atoms on the cysteine residues as reduced dithiols or an oxidized disulfide identified in the MS/MS spectra. SEQUEST and MASCOT identified peptide masses that

corresponded to the bis-alkylated P4 and P24, but these peptides had such low scores that they could not be sequenced. The MS1 full spectrum of the $[M+2H]^{2+}$ spectra for the mono-alkylated P4 (1021.6 m/z) and P24 (1054.3 m/z) peptides are shown in Figure 4.7. The incorporation of 333 m/z increased the singly charged ion beyond the mass limits set on the MS detector (2000 m/z) and hence only the double charged ion was present. The relative intensity of the MS1 spectra was high; however, the intensity of modified $[M+2H]^{2+}$ P4~ (1021.6 m/z) and P24~ (1054.3 m/z) was much lower (~6.2 x 10^5) and they were not the predominant ion within their respective spectra. These alkylated peptides were identified in CEG excess incubations of 5X to 100X with increasing frequency and intensity. Masses corresponding to bis-alkylated P4 and P24 were not identified.
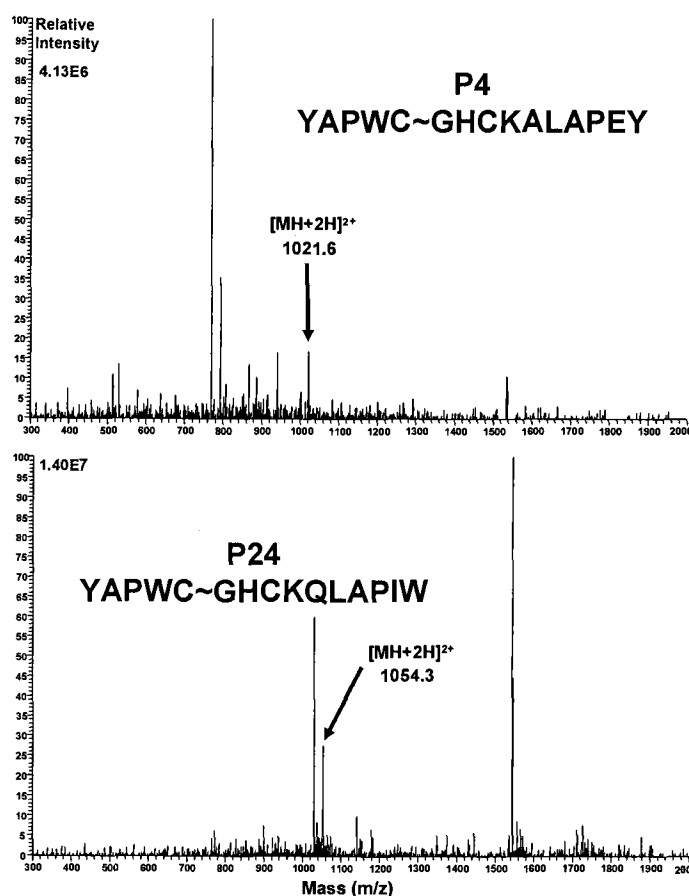
Figure 4.7   MS1 spectra showing the adduction of the episulfonium ion derived from CEG on the P4 and P24 peptides.

4.4.5 Sequencing Modified Peptides by CID with MS/MS

Collision induced dissociation (CID) was performed in an electrospray Finnegan LCQ ion trap mass spectrometer. The scan event series included one full scan followed by three data-dependent MS/MS scans on the most intense ion. Dynamic exclusion was enabled in order to fragment the low abundance peptides such as P4 and P24. The CID spectra of P4 and P24

are presented in Figures 4.8 and 4.9. Their fragment patterns are described extensively in chapter 3. Briefly, the proline residues on either end of P4 (YAPWCGHCKALAPEY) and P24 (YAPWCGHCKQLAPIW) caused fragmentation energies to focus near them resulting in strong ionization of the b_{12} and y_3 fragment ions on the C-terminal proline and the y_{13} on the N-terminal proline. Additionally, the internal fragments PWCGHCKALA and PWCGHCKQLA of P4 and P24 were present in every unmodified peptide spectrum as well as P4 modified with IAM or biotin-conjugated IAM described in chapter 3.

The only modified peptides that could be identified with SEQUEST and MASCOT peptide sequencing search engines were P4~ and P24~. Possible modifications for + 334 m/z on the following residues were searched: Cys, His Tyr, Ser, Thr and the N-terminus. Over-alkylation of peptides during digestion with iodoacetamide has been established at these residues with protein trypsin digests (Boja and Fales, 2001). The identification of modified P4~ and P24~ by SEQUEST and MASCOT was facilitated with peptide-sequence motif searches of the MS/MS spectra data in SALSA. The GSH conjugate alkylated onto these peptides had a propensity to lose its glutamate moiety, resulting in a major peak representing the neutral ion loss of 129 m/z. The peptide sequence motif combined with the ability to search for neutral losses in SALSA identified modified P4~ and P24~.
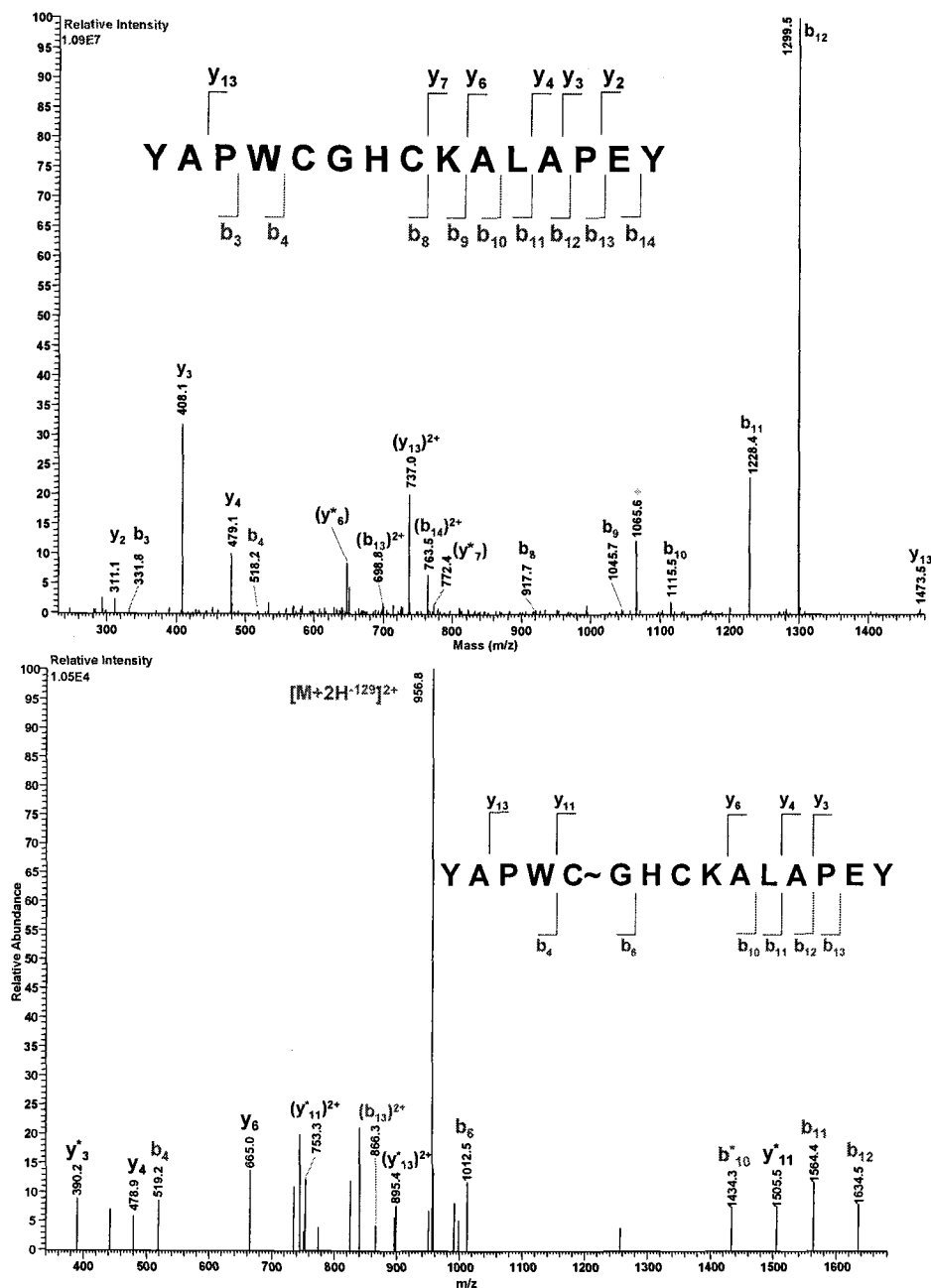
Figure 4.8 [M+2H]$^{2+}$ CID spectra of the P4 peptide modified by the episulfonium ion derived fromCEG incubation with PDI showing the major neutral ion loss of 129 m/z.
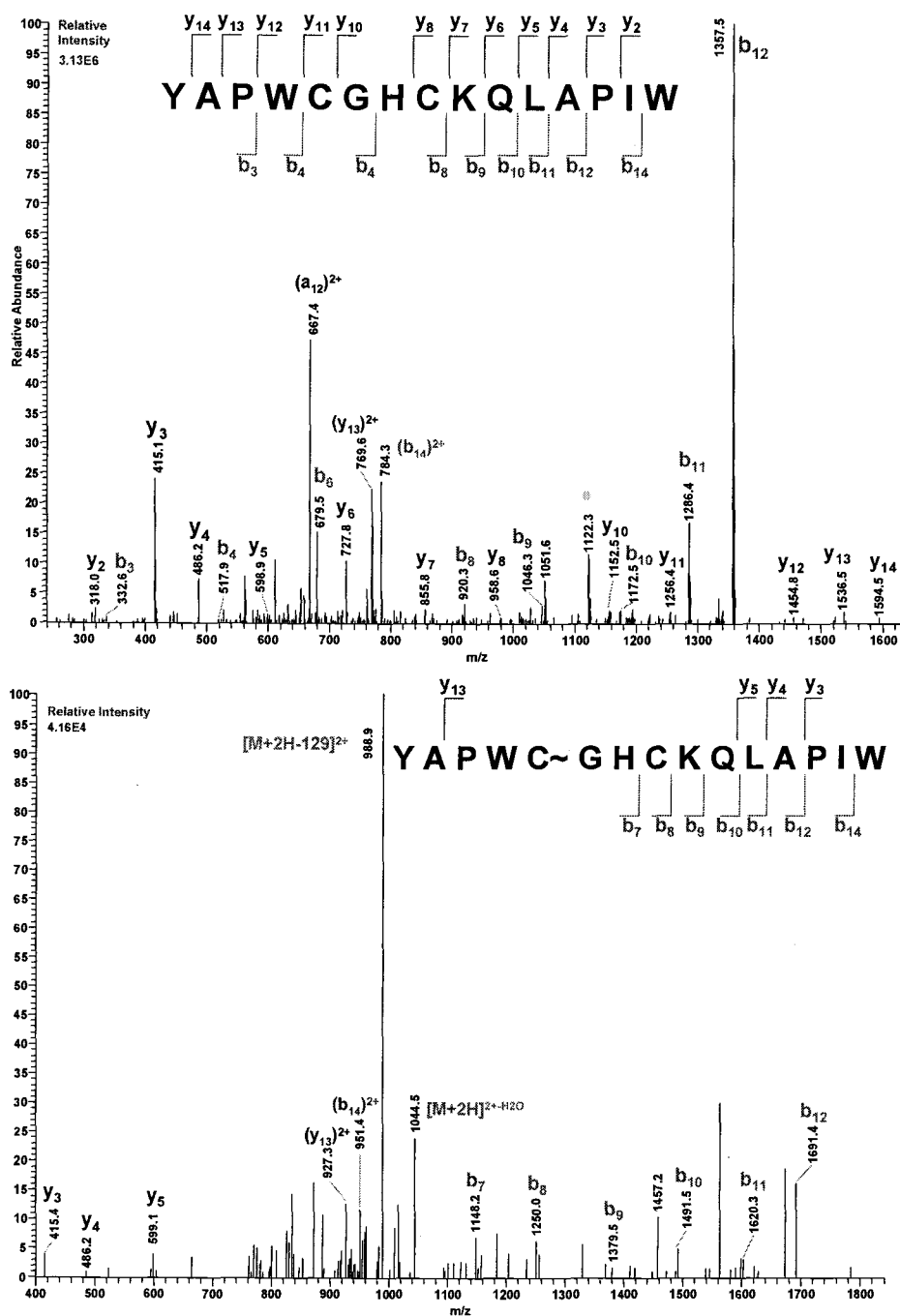
Figure 4.9 [M+2H]$^{2+}$ CID spectra of the P24 peptide modified by the episulfonium ion derived from CEG incubation with PDI showing the major neutral ion loss of 129 m/z.

The glutamate residue of GSH has been shown to be very susceptible to fragmentation in tandem MS studies such as in CEG alkylation of thioredoxin (Erve et al., 1995a; Kim et al., 2001) and glutathionylation of glutathione-S-transferase (Lantum et al., 2002). Figure 4.8 shows the $[M+2H]^{2+}$ CID of P4~ with the major ion (957 m/z) representing the neutral loss of -129. The relative intensity of this CID spectrum was very low (1.05 x 10^4), yet the b_{12}, y_3 and y_{13} ions were detectable.

Figure 4.9 presents the $[M+2H]^{2+}$ CID spectra of P24~ with one modification due to CEG modification. Again the major ion is 989 m/z, which corresponded to the -129 loss of glutamate. Again b_{12}, y_3 and y_{13} were present and 1148 m/z (b_7) and 1250 m/z (b_8) ion identified Cys^{40} as not being modified, but Cys^{37} could not be identified as the site of modification. The $[M+2H]^{2+}$ presence of 1021.6 m/z and 1054.3 m/z of the MS1 spectra, the loss of glutamate after CID with these precursor ions, and the presence of several b-series and y-series ions led to partial sequencing of P4 and P24; however, the actual residues of modification were not identified. The difference in the type of energy used in the CID of parent ions with MALDI-TOF/TOF made it possible to determine the exact residues modified.

4.4.6 Sequencing Modified Peptides by CID with MALDI-TOF/TOF

The difference in the type of collision energy applied to the parent ions provided a different array of ion coverage. The MALDI source offers high energy CID (occurring at kilovolt energies) which is believed to operate by electronic excitement. High energy CID differs from low energy CID in that the mass spectra show a broader range of fragment reactions and are relatively insensitive to collision conditions. Low energy CID (occurring at

energies in the range of tens to hundreds of electron volts) used in the ion trap is believed to work by vibrational excitation and the activated precursor ions have a narrow internal energy distribution. This means the resulting product-ion mass spectra are strongly dependent on experimental conditions such as collision gas pressure and composition, collision energy, and temperature. A MALDI-TOF/TOF unmodified control peptide digest is shown in Figure 4.10. Spectra from increasing PDI incubations with increasing fold excess of CEG are represented as well. The MALDI-TOF/TOF generated intense unmodified peptide peaks at 1709 and 1773 and modified peaks at 2042 and 2106 compared to the low intensity peptide ions generated in the ion trap after LC-MS. Among the most intense parent ions were P4 and P24 unlike the full spectrum of parent ions obtained in the LC-ESI-MS (Figure 3.13). The precursor ion was present only as a singly charged species and the loss of glutamate is not observed in the high energy CID in MALDI-TOF/TOF tandem MS.
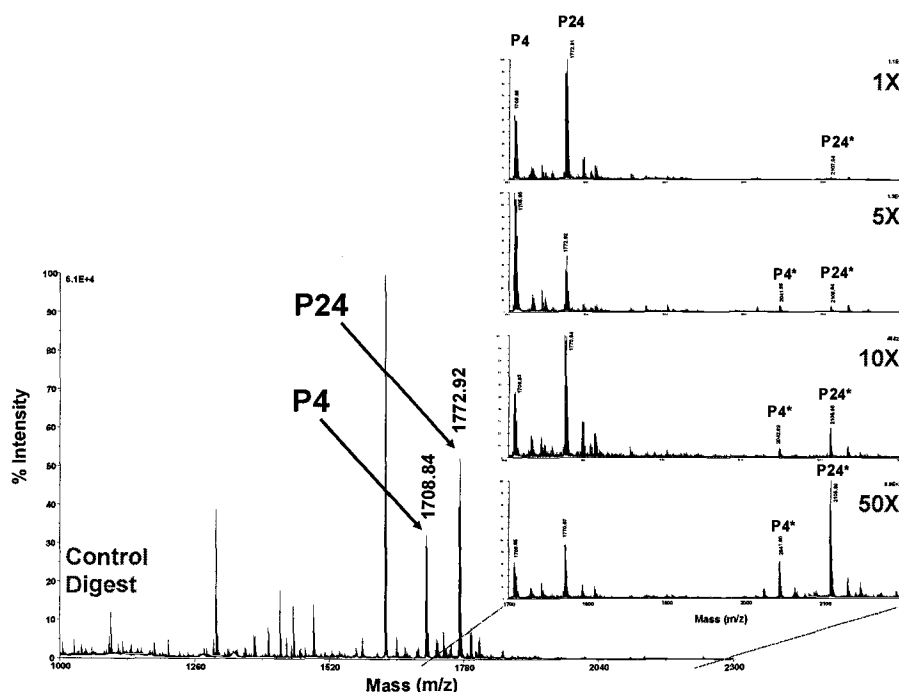
Figure 4.10   MALDI-TOF/TOF mass spectra of peptic digests generated from PDI with 1X, 5X, 10X and 50X fold excess of CEG over PDI. The inlay shows magnified spectra including peptides that are modified by one moiety of ethyl glutathione.

In the PDI peptic digest spectrum generated by MALDI-TOF/TOF a range of concentrations from 1X to 50X CEG:PDI is presented showing the emergence of alkylated peptides (Figure 4.10). Incubation of PDI with equimolar CEG (1X) resulted in a spectrum that only identified the P24~ 2106 m/z modified peptide. This suggests that the **a'** domain active site was more susceptible to alkylation than was of the **a** domain active site. Intensity of the 2106 m/z precursor ion was greater than the precursor ion 2042 m/z in all of the spectra generated from both the ESI LC-MS and the MALDI-TOF/TOF. Parent ions equaling a mass that would represent double alkylation (e.g., an ethyl glutathione moiety on each cysteine residue of a single active site) were not observed. Parent ion peaks of the unmodified and modified peptides did show corresponding peaks of sodiated (+ 23 m/z) and

potassiated (+38 m/z) peptides of the same sequences. Peaks from other peptides containing the –CGHC– active sites were also observed due to the nonspecific nature of pepsin.

The MALDI-TOF/TOF tandem mass spectra of the native and modified P4 (YAPWCGHCKALAPEY) peptide are presented in Figure 4.11. In the CID [M+H]$^+$ 1708.7 m/z spectrum of the unmodified P4, the b-series fragment ions were present from b_5 to b_{14} in a characteristic pattern of these peptides. The y-series was not as strong; however, 1475 m/z (y_{13}) and 408 m/z (y_3) fragmenting N-terminally of the prolines were identified. All of the larger unlabeled peaks were identified as internal ions. The CID spectrum of modified P4 identified Cys^{40} as the residue not modified by the y-series pair 791 m/z (y_7) and 894 (y_8). There was not an ion pair in the b-series or the y-series identifying Cys^{37} as the modified residue; however, the presence of 332 m/z (b_3) and 1088 (y_{10}) narrowed the possible sites to Trp^{36} or Cys^{37}.

Figure 4.12 presents a comparison of the spectra of unmodified P24 (YAPWCGHCKQLAPIW) and the episulfonium-modified P24. The CID [M+H]$^+$ 1773 m/z spectrum of the unmodified P24 exhibited the same fragmentation patterns due to the prolines at either ends of the peptide. The unmodified Cys^{381} was indicated by the y-series ion pair 1152 m/z (y_{10}) and 1257 m/z (y_{11}) and Cys^{384} was indicated by the y-series ion pair 855 m/z (y_7) and 958 m/z (y_8) in addition to the b-series ion pair 815 m/z (b_7) and 916 m/z (b_8). In the modified spectrum, Cys^{384} was identified as the residue not modified by both the 855 m/z (y_7) and 958.3 m/z (y_8) ion pair and the 1148 m/z (b_7) and 1251 m/z (b_8) ion pair. Cys^{381}. In a similar pattern to P4, the modified Cys^{381} did not show a y- or b-series ion pair, but the 332 m/z (b_3), 1152 m/z (y_{10}) and 321 m/z (b_5) ions did indicate that the modification was either on Trp^{380} or Cys^{381}.
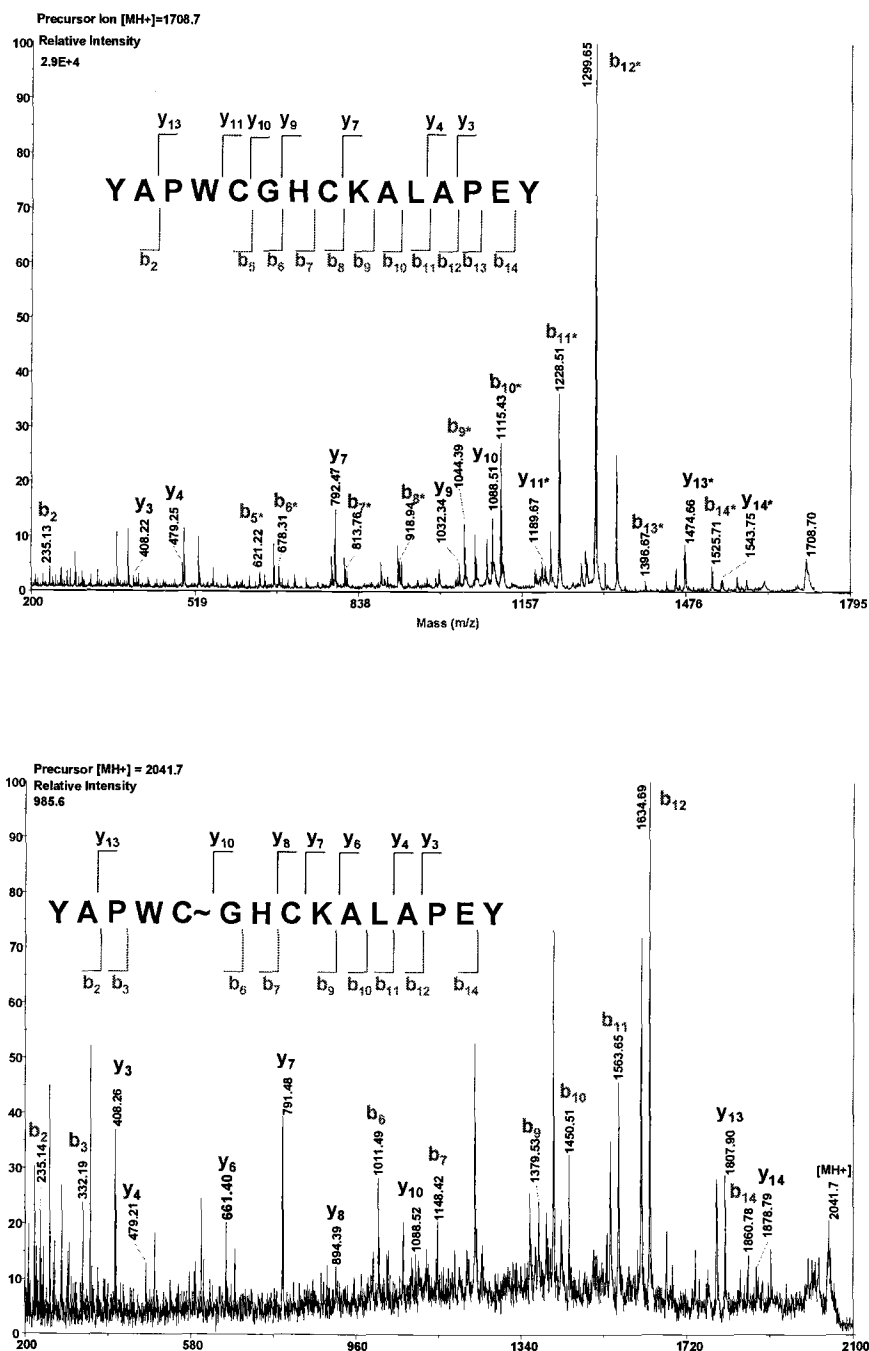
Figure 4.11   MALDI-TOF/TOF tandem mass spectra of the [M+H]$^+$ of the P4 peptide (YAPWCGHCKALAPEY) identifying Cys^{37} as the residue modified by the episulfonium ion derived from CEG.
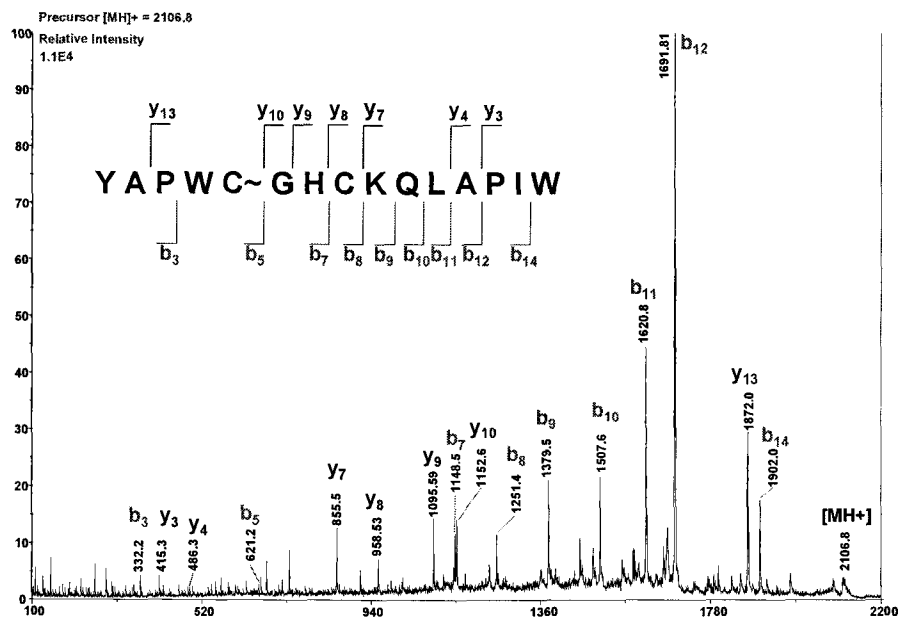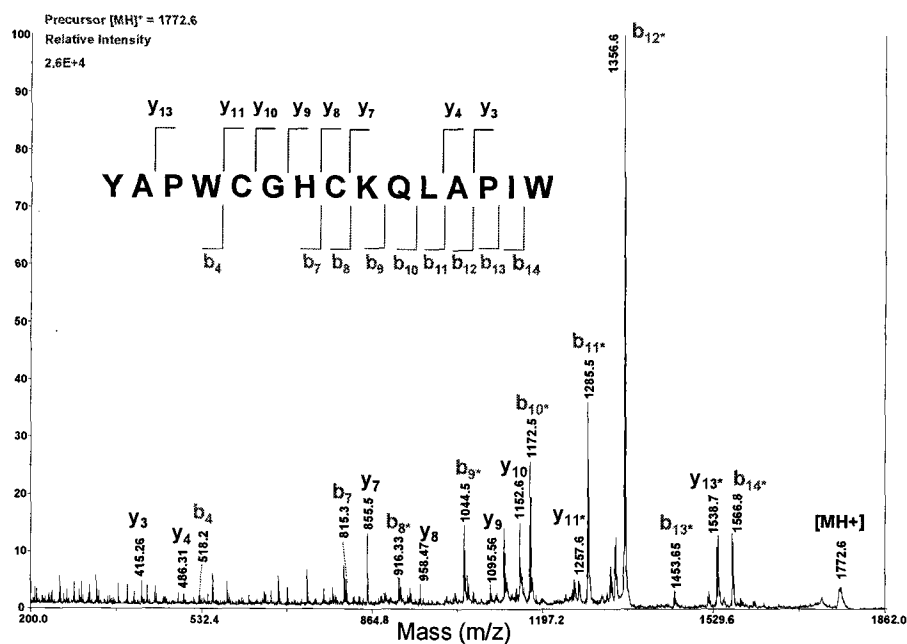
Figure 4.12   MALDI-TOF/TOF tandem mass spectra of the [M+H]+ of the P24 peptide (YAPWCGHCKQLAPIW) identifying Cys[381] as the residue modified by the episulfonium ion derived from CEG.

4.5 DISCUSSION

The mass spectrometry methods of analysis used in this study demonstrated that CEG treatment of PDI at physiological pH resulted in modification of the protein. Electrospray LC-MS suggested the production of two PDI adducts at reaction concentrations as low as 5X fold excess CEG over PDI. MALDI-TOF MS and ESI LC-MS of the whole protein indicated that increasing concentrations of CEG resulted in the formation of tris- and tetra-alkylated PDI. The potential number of protein adducts that could be observed was up to possibly six or seven with the ESI LC-MS instrumentation. Sequencing of the peptides generated from these alkylated PDI species was not possible with ESI tandem MS because of their low abundance, multiple charge states and fragmentation of the alkylating moiety from the peptide. Because of the differences in collision energies, MALDI-TOF/TOF tandem MS identified two residues that were alkylated in the lower fold concentrations of CEG over PDI. These adducts were identified on the N-terminal cysteine residue of the **a** and **a'** domain active site sequence – C̰GHC– (Cys^{37} and Cys^{381}).

The third and fourth alkylations were proposed to be on the Cys^{40} and Cys^{385}, the second cysteine residues of the active site sequence –C̰GHC̰–; however, these residues were not identified with the electrospray LC-MS ion trap or MALDI-TOF/TOF tandem MS. Peptide masses equaling bis-alkylated P4 and P24 were observed in the MS1 spectra; however the SEQUEST and MASCOT scores were so low that the sequence and therefore the residues of alkylation could not be inferred. Erve et al. (1995a) reported the appearance of adducts at low CEG fold incubations with Trx, and determined the mono-alkylated site of *E. coli* thioredoxin to be Cys^{32}, the N-terminal cysteine of the Trx active site –CPYC–. The pKa of the two cysteine residues

of Trx have been reported as approximately 6.7 and 9.0 (Kallis and Holmgren, 1980) and 7.1 and 7.9 (Li et al., 1993). Alkylation at the Trx Cys[32] confirmed the increased reactivity due to the depressed pKa of the cysteine. The corresponding cysteine residues in PDI (Cys[37] and Cys[381]) also have a depressed pKa and tandem mass spectrometry identified these residues as targeted by the episulfonium ion.

Of the six cysteine residues in PDI, four are located in the two active site domains and the other two are located in the **b'** domain and have been reported to be buried and unreactive (Lundstrom and Holmgren, 1990). Peptic peptides containing these cysteine residues (P18 and P20) were observed and sequenced with no indication of modification under the conditions of alkylation that we studied. The alkylation of PDI at more than four sites was unexpected because cysteine-containing dipeptides were at least 10-fold more reactive to CEG than other functional groups (Jean and Reed, 1989). Intentional searches were made for adductions onto Cys, His, Tyr, Ser, Thr and the N-terminus because these residues have been shown to be sensitive to overalkylation with IAM (Boja and Fales, 2001). MASCOT did not identify any O- or N-alkylations in these studies.

Among the candidates for alkylation one of the residues of PDI that could be a possible target is Tyr[398]. This tyrosine residue is homologous to the Trx tyrosine residue suspected to be the bis-adduct after incubation with CEG (Erve et al., 1995a). As in Trx, Tyr[398] exists in an equal number of residues from the N-terminal cysteine of the **a'** domain and was contained within a peptic permutation of P24. We could not identify this residue as modified with either ESI or MALDI-TOF/TOF tandem MS. Another possible candidate that could accept the episulfonium ion under these experimental conditions is one of the 11 histidine residues in recombinant rat PDI. The

histidine residue present within each of the active sites, –CGHC–, has been identified as necessary for isomerase activity (Stafford and Lund, 2000) and could be a target although our studies never identified it as alkylated. Searches with SEQUEST and MASCOT could not identify any of these modifications with CEG or the previous alkylating agents discussed in chapter 3, IAM or BIAM.

Of the four thiols measured, a decrease of 2.31 mole SH/mole PDI was observed after incubation of PDI with 100X excess of CEG. IAM decreased this value further by 0.6 mole SH/mole of PDI. Incubation of PDI with increasing doses of CEG for 90 minutes at 37°C caused a concentration dependent inhibition of reductase activity with complete inhibition measured at 100X fold excess CEG over PDI. A decrease in the oxidative folding of reduced denatured RNase was also measured, with a 70% inhibition of activity at 100X fold excess compared to native PDI. These results indicate a change in the active site of PDI caused decreased catalytic activity.

We confirmed our hypothesis that the N-terminal cysteine residue (–C~GHC–) in each of the two active sites of domains **a** and **a'** were subject to modification by the episulfonium ion of PDI. These residues are proposed to exist in the thiolate anion form due to their lowered pKa relative to that of free cysteine (Kortemme and Creighton, 1995). The measured loss of at least two thiol groups concurrent with the MS data identifying Cys[37] and Cys[381] demonstrated the relative susceptibility of these cysteine residues. Hawkins and Freedman (1991) noted that inhibition of isomerase activity measured by the scrambled RNase assay was concurrent with the incorporation of only 2 moles of [^{14}C]IAA per mole of PDI polypeptide.

Our data show that although Cys^{37} and Cys^{381} were alkylated by the episulfonium ion, only a partial loss of oxidase activity as measured by the oxidative folding of reduced denatured RNase activity was observed. This is in contrast to the complete inhibition of isomerase activity measured by the isomerization of scrambled RNase into native RNase studies performed with [^{14}C]IAA. Mutation studies have shown a difference between oxidase activity versus isomerase activity of PDI. Cysteine mutants of PDI were used to complement DsbA (oxidase activity or formation of disulfide bonds) or DsbC (isomerase activity or isomerization of disulfide bonds) deficient *E. coli* strains (Stafford and Lund, 2000). Their results were twofold. First, they demonstrated that the requirements for redox active cysteine residues for isomerase activity are clearly more stringent than for oxidase activity. Second, the **a** domain is more important than the **a'** domain with regard to isomerase activity. These studies supported prior findings that the two domains, **a** and **a'**, do not contribute equally to catalysis. The **a** domain contributes more catalysis at saturating conditions whereas the **a'** domain affects substrate recognition and steady-state binding of the substrate (Lyles and Gilbert, 1994). This unequal contribution to folding by these domains (equal in redox character) indicates that the tertiary/quaternary structures bestow unique characteristics to chemically equal domains. The emergence of the alkylated Cys^{381} (2106 m/z) over Cys^{37} (2042) in Figure 4.10 may be a function of the structures of these different sites. Trx alkylated by the episulfonium ion at Cys^{32} has been shown to affect the structure of loops close to the active site (Kim et al., 2001). It may be that alkylation of PDI also results in conformational changes of the protein. Structure changes due to alkylation by the episulfonium ion may force a reaction exposing previously inaccessible thiols or other residues.

Incubations with the highly reactive thiol alkylating agent iodoacetamide and its biotin-conjugate with PDI resulted in a maximum of four protein adducts localized on the two cysteine residues found on each active site of the **a** and **a'** domains (chapter 3) and a concurrent loss of reductase and oxidative folding activity. Thiol-alkylating agents such as Cd^{2+} (Noiva et al., 1993), maleimides (Novia et al., 1993; Schwaller et al., 2002; Essex et al., 2001), iodoacetamide (Hawkins et al., 1991a) and iodoacetic acid (Hawkins and Freedman, 1991) have been shown to inhibit the activities of PDI. The possibility that alkylation at the second cysteine residues of the two active sites was not ruled out in these studies. Some studies have suggested that the second cysteine provides an escape mechanism, preventing PDI from becoming trapped with substrates that it isomerizes slowly (Walker and Gilbert, 1997; Schwaller et al., 2002). A higher pH may increase the ability for the second cysteine to be ionized, facilitating the turnover of PDI.

It is noteworthy to mention that efforts with in-gel trypsin digests were useful in identifying PDI spots from polyacrylamide gels; however, the proteolytic sites do not allow extraction of the cysteine containing active sites from the gel presumably due to their size. This is useful information, as in-gel trypsin digests are commonplace in proteomic work applied to reactive metabolite protein identification. Identification of the active sites of PDI as the target will necessitate use of pepsin or other protease specific to sizing the active site sequences appropriately. The difference in MALDI-TOF/TOF applications to the glutathione-conjugate adducted peptides greatly improved fragment ion coverage due to the high energy CID preventing the major loss of 129 m/z glutamate and presence of only the singly charged precursor ion. The use of mass spectrometry to determine the site of alkylation in a large

and complex protein proved to be insightful in beginning to assess the relative susceptibility of the thiols of PDI to CEG.

The accessibility of the active site thiols becomes an important aspect of analyzing PDI as a target for biological reactive intermediates *in vivo*. Of the seven proteins identified in the ER as targets for the reactive metabolites of bromobenzene, PDI and three of its homologs (ERp29, P5, and ERp57) were targeted. Because PDI is present in such high concentrations, serves as a chaperone, and has a redox sensitive active site, the site of adduction may prove to have implications on the role of PDI *in vivo*. PDI has been found to have an increased turnover rate in oxidatively stressed cells and was selectively degraded by the proteasome and new PDI was synthesized. Perhaps PDI plays a protective role for the cell or is a target simply based on its abundance. PDI is also a target for the reactive metabolites of acetaminophen and methoxychlor (Zhou et al., 1996; 1995). PDI has also been implicated in the hepatotoxicity of halothane (Martin et al., 1993a; 1993b; Pohl et al., 1989).

The toxicity of 1,2-DCE is strongly correlated with the covalent binding of chemically reactive metabolites to cellular proteins; however, few protein targets of these reactive metabolites have been identified. We have shown that the episulfonium ion of CEG modified PDI *in vitro* at the N-terminal cysteine of each –CGHC– active site sequence. The results from this study paralleled prior findings of Cys[32] alkylation in the active site of Trx (Erve et al., 1995a) that the episulfonium ion of CEG is a chemically reactive species capable of alkylating the N-terminal thiolate anions of the two active sites in PDI at physiological pH. PDI, however, did not lose all of its oxidative folding capability and perhaps exhibits a conformational change upon alkylation that is protective of the protein. The focus of the present investigation was to

identify the specific amino acids that undergo alkylation when adducts are formed between the episulfonium of CEG and PDI. Even at high CEG concentrations in excess of PDI, the only two residues that could be identified were those which exist in a thiolate anion form.

4.6   CONCLUSION

Complete inhibition of reductase activity and a major decrease in oxidative folding activity accompanied by a loss of two thiols per PDI polypeptide was observed after incubation with CEG. A titration curve of PDI incubated with CEG showed incremental mass increases equal to the ethyl glutathione moiety derived from the episulfonium. There were at least six increases in mass that were detected at the highest concentration of CEG. However, the data showed only one ethyl glutathione moiety covalently modified to the N-terminal cysteine residue in both the **a** and **a'** domain active site sequence –C*GHC–; other modification sites could not be identified. Although PDI was susceptible to alkylation, it was able to maintain oxidative folding activity indicating that it may not be as sensitive to redox control as suspected.

4.7   ACKNOWLEDGEMENTS

spectrometry facility with Elisabeth Barofsky performing MALDI-TOF mass analyses and Brian Arbogast for their assistance with LC-MS.

5.0   CONCLUSION

5.1   SUMMARY

Based on the work of John Erve, it was shown that the episulfonium ion derived from S-(2-chloroethyl)glutathione, the glutathione conjugate of 1,2-dichloroethane, alkylated the first cysteine (Cys^{32}) in the active site sequence –C*PYC– of E. coli of thioredoxin (Trx). The investigations described in my dissertation have extended this work to show that CEG can also react with homologous cysteine residues present in protein disulfide isomerase (PDI), a member of the thioredoxin superfamily containing two thioredoxin domains with an active site sequence, –CGHC–. First, the relative susceptibility of the thiols of PDI to the thiol alkylating agent 1-chloro-2,4-dinitrobenzene (CDNB) indicated that PDI was alkylated by two dinitrophenyl moieties derived from CDNB with a concurrent loss of two of the four measured thiols, and a partial loss in reductase and oxidative folding activity. The N-terminal cysteine residues of the active sites of PDI have a lower pKa, resulting in a thiolate anion at physiological pH. It is these two thiolate anions that are proposed to be alkylated. CDNB had been shown to inhibit thioredoxin reductase and induce oxidase activity. PDI was not as sensitive to CDNB alkylation as thioredoxin reductase, and it was determined during these studies that the conserved C-terminal extension containing a penultimate selenocysteine –GC(SeC)G– was targeted for dinitrophenyl adducts. The selenocysteine and cysteine residues targeted were more reactive to alkylation, yet the thiolate anions of PDI are some of the most reactive groups known amongst proteins. Because iodoacetamide (IAM) was able to completely inhibit reductase and oxidative folding activity, it was used to titrate the active site cysteine residues to determine the extent of alkylation and relative susceptibility to alkylation. A maximum of four

carbamidomethylations adducted to PDI were observed by electrospray ionization mass spectrometry (ESI-MS). Sequencing the peptic peptides of native and modified PDI with ESI LC-MS ion trap instrumentation identified the first cysteine of each active site sequence (–C*GHC–) being modified followed by modification at the second cysteine (–C*GHC*–). From our data it appears that the two active site domains were alkylated equally. Biotin-conjugated IAM (BIAM) was reacted with PDI to determine if the increase in mass hindered the accessibility of either of these cysteine residues to alkylation. BIAM exhibited the same alkylating profile indicating that there is not a size restraint of the active site in either active site sequence.

After determining the relative susceptibility of PDI to these electrophiles, studies were initiated with CEG. Incubations of several fold excesses of CEG over PDI resulted in a complete loss of reductase activity but only partial loss of oxidative folding activity. Again a loss of two of the four measured thiols was shown. MALDI-TOF and ESI LC-MS of native and modified PDI suggested the production of two protein adducts at concentrations as low as 5X fold excess of CEG over PDI. Increasing concentrations of CEG resulted in tris- and tetra-adducted protein, with additional ethyl glutathione adducts beyond these. Sequencing of peptic peptides with ESI LC tandem MS generated from the alkylated species was not possible due to their low abundance, multiple charge states and fragmentation of the alkylating moiety from the peptide. Because of the difference in collision energies, MALDI-TOF/TOF tandem MS identified the same two cysteine residues first alkylated by IAM (–C*GHC–). The identification of these modifications with MALDI-TOF/TOF was encouraging as difficulties in MS analysis of glutathione related adducts has often been plagued with fragmentation of glutathione moiety. An attempt to identify other

sites of alkylation was made by searching for N-, O-, and N-terminal amino alkylation in addition to S-alkylation but without success.

The significance of the finding that proteins can be alkylated by CEG *in vitro* at physiological pH indicates that protein alkylation may be an important facet of the hepatotoxic and nephrotoxic effects observed for 1,2-dichloroethane (DCE) *in vivo*. Modification and loss of critical thiols has increased in the implication of redox control of the cell. The thiol redox environment of intracellular and extracellular compartments is critical in the determination of protein structure, regulation of enzyme activity, cell signaling, and control of transcription factor activity and binding. Recent proteomic work regarding the toxicity of bromobenzene has identified PDI and four of its homologs in the endoplasmic reticulum as reactive metabolite targets (Koen and Hanzlik, 2002). The finding that an active site cysteine is the major amino acid target of another protein of the thioredoxin superfamily *in vitro* at molar levels of CEG only slightly higher than that of the enzyme, suggests that irreversible alkylation could inactivate a critical cytosolic or endoplasmic reticulum enzyme having a nucleophilic center. It remains to be seen whether a major portion of toxicity of DCE *in vivo* is associated with the loss of this specific protein function to this alkylation event. Nevertheless, understanding the toxicologic significance of protein covalent binding requires not only identification of the target protein, but also the amino acid residue that has been modified as well. The use of tandem mass spectrometry, especially MALDI-TOF/TOF instrumentation in analyzing glutathione-related adducts will enhance the work done with these metabolites.

5.2   FUTURE WORK

Based on the results of the reactivity of rat PDI alkylation and what is known about this enzyme in other chemically induced toxicities (e.g., bromobenzene), a holistic proteomic approach to DCE toxicity including radiolabeled DCE treatment in animals, hepatocytes or cultured cells, preparation of subcellular fractions of target tissues, protein precipitation and determination of covalently bound radiolabeled protein followed by two-dimensional gel electrophoresis will separate the proteins. In-gel digestion followed by tandem MS and database searching to sequence the peptides removed from the gel will identify the adducted proteins. Further peptide extraction by different proteases may prove useful in identifying the amino acid residue(s) adducted.

The use of mass spectrometry to identify the protein adducts of a specific chemical has a very global appeal to it. Advances in databases, algorithm software for searching the databases and the automation of assessing gel spots and running mass spectrometers have made this once daunting task of western blot detection a feasible approach.

BIBLIOGRAPHY

Ahmed AR, Blose DA. Delayed-type hypersensitivity skin testing. A review. Arch Dermatol. 1983 Nov;119(11):934-45.

ATSDR (Agency for Toxic Substances and Disease Registry). 1992. *Toxicological Profile for 1,2-Dichloroethane, Update*. October, 1992. Draft report. U.S. Public Health Service, Agency for Toxic Substances and Disease Registry, Atlanta, GA, 131 pp.

Akagi S, Yamamoto A, Yoshimori T, Masaki R, Ogawa R, Tashiro Y. Distribution of protein disulfide isomerase in rat hepatocytes. J Histochem Cytochem. 1988 Dec;36(12):1533-42.

Albano E, Poli G, Tomasi A, Bini A, Vannini V, Dianzani MU. Toxicity of 1,2-dibromoethane in isolated hepatocytes: role of lipid peroxidation. Chem Biol Interact. 1984 Aug;50(3):255-65.

Arner ES, Bjornstedt M, Holmgren A. 1-Chloro-2,4-dinitrobenzene is an irreversible inhibitor of human thioredoxin reductase. Loss of thioredoxin disulfide reductase activity is accompanied by a large increase in NADPH oxidase activity. J Biol Chem. 1995 Feb 24;270(8):3479-82.

Arner ES, Nakamura H, Sasada T, Yodoi J, Holmgren A, Spyrou G. Analysis of the inhibition of mammalian thioredoxin, thioredoxin reductase, and glutaredoxin by *cis*-diamminedichloroplatinum (II) and its major metabolite, the glutathione-platinum complex. Free Radic Biol Med. 2001 Nov 15;31(10):1170-8.

Aslund F, Berndt KD, Holmgren A. Redox potentials of glutaredoxins and other thiol-disulfide oxidoreductases of the thioredoxin superfamily determined by direct protein-protein redox equilibria. J Biol Chem. 1997 Dec 5;272(49):30780-6.

Aslund F, Ehn B, Miranda-Vizuete A, Pueyo C, Holmgren A. Two additional glutaredoxins exist in *Escherichia coli:* glutaredoxin 3 is a hydrogen donor for ribonucleotide reductase in a thioredoxin/glutaredoxin 1 double mutant. Proc Natl Acad Sci U S A. 1994 Oct 11;91(21):9813-7.

Aslund F, Nordstrand K, Berndt KD, Nikkola M, Bergman T, Ponstingl H, Jornvall H, Otting G, Holmgren A. Glutaredoxin-3 from *Escherichia coli.* Amino acid sequence, 1H AND 15N NMR assignments, and structural analysis. J Biol Chem. 1996 Mar 22;271(12):6736-45.

Bader M, Muse W, Ballou DP, Gassner C, Bardwell JC. Oxidative protein folding is driven by the electron transport system. Cell. 1999 Jul 23;98(2):217-27

Bandyopadhyay S, Starke DW, Mieyal JJ, Gronostajski RM. Thioltransferase (glutaredoxin) reactivates the DNA-binding activity of oxidation-inactivated nuclear factor I. J Biol Chem. 1998 Jan 2;273(1):392-7.

Bessette PH, Cotto JJ, Gilbert HF, Georgiou G. In vivo and in vitro function of the Escherichia coli periplasmic cysteine oxidoreductase DsbG. J Biol Chem. 1999 Mar 19;274(12):7784-92.

Biemann K. Contributions of mass spectrometry to peptide and protein structure. Biomed Environ Mass Spectrom. 1988 Oct;16(1-12):99-111.

Bini L, Magi B, Marzocchi B, Arcuri F, Tripodi S, Cintorino M, Sanchez JC, Frutiger S, Hughes G, Pallini V, Hochstrasser DF, Tosi P. Protein expression profiles in human breast ductal carcinoma and histologically normal tissue. Electrophoresis. 1997 Dec;18(15):2832-41.

Biswal S, Acquaah-Mensah G, Datta K, Wu X, Kehrer JP. Inhibition of cell proliferation and AP-1 activity by acrolein in human A549 lung adenocarcinoma cells due to thiol imbalance and covalent modifications. Chem Res Toxicol. 2002 Feb;15(2):180-6.

Boja ES, Fales HM. Overalkylation of a protein digest with iodoacetamide. Anal Chem. 2001 Aug 1;73(15):3576-82.

Boston RS, Viitanen PV, Vierling E. Molecular chaperones and protein folding in plants. Plant Mol Biol. 1996 Oct;32(1-2):191-222.

Bradford MM. A rapid and sensitive method for the quantitation of microgram quantities of protein utilizing the principle of protein-dye binding. Anal Biochem. 1976 May 7;72:248-54.

Brodie AE, Reed DJ. Reversible oxidation of glyceraldehyde 3-phosphate dehydrogenase thiols in human lung carcinoma cells by hydrogen peroxide. Biochem Biophys Res Commun. 1987 Oct 14;148(1):120-5.

Bulleid NJ, Freedman RB. Defective co-translational formation of disulphide bonds in protein disulphide-isomerase-deficient microsomes. Nature. 1988 Oct 13;335(6191):649-51.

Bulleid NJ, Freedman RB. Cotranslational glycosylation of proteins in systems depleted of protein disulphide isomerase. EMBO J. 1990 Nov;9(11):3527-32.

Bushweller JH, Aslund F, Wuthrich K, Holmgren A. Structural and functional characterization of the mutant Escherichia coli glutaredoxin (C14-S) and its mixed disulfide with glutathione. Biochemistry. 1992 Sep 29;31(38):9288-93.

Bushweller JH, Billeter M, Holmgren A, Wuthrich K. The nuclear magnetic resonance solution structure of the mixed disulfide between Escherichia coli glutaredoxin(C14S) and glutathione. J Mol Biol. 1994 Feb 4;235(5):1585-97.

Cai H, Wang CC, Tsou CL. Chaperone-like activity of protein disulfide isomerase in the refolding of a protein with no disulfide bonds. J Biol Chem. 1994 Oct 7;269(40):24550-2.

Chai YC, Hendrich S, Thomas JA. Protein S-thiolation in hepatocytes stimulated by t-butyl hydroperoxide, menadione, and neutrophils. Arch Biochem Biophys. 1994 Apr;310(1):264-72.

Chrestensen CA, Starke DW, Mieyal JJ. Acute cadmium exposure inactivates thioltransferase (Glutaredoxin), inhibits intracellular reduction of protein-glutathionyl-mixed disulfides, and initiates apoptosis. J Biol Chem. 2000 Aug 25;275(34):26556-65.

Claiborne A, Miller H, Parsonage D, Ross RP. Protein-sulfenic acid stabilization and function in enzyme catalysis and gene regulation. FASEB J. 1993 Dec;7(15):1483-90.

Claiborne A, Yeh JI, Mallett TC, Luba J, Crane EJ 3rd, Charrier V, Parsonage D. Protein-sulfenic acids: diverse roles for an unlikely player in enzyme catalysis and redox regulation. Biochemistry. 1999 Nov 23;38(47):15407-16.

Cmarik JL, Humphreys WG, Bruner KL, Lloyd RS, Tibbetts C, Guengerich FP. Mutation spectrum and sequence alkylation selectivity resulting from modification of bacteriophage M13mp18 DNA with S-(2-chloroethyl)glutathione. Evidence for a role of S-(2-(N7-guanyl)ethyl)glutathione as a mutagenic lesion formed from ethylene dibromide. J Biol Chem. 1992 Apr 5;267(10):6672-9.

Collet JF, Bardwell JC. Oxidative protein folding in bacteria. Mol Microbiol. 2002 Apr;44(1):1-8.

Couët J, de Bernard S, Loosfelt H, Saunier B, Milgrom E, Misrahi M. Cell surface protein disulfide-isomerase is involved in the shedding of human thyrotropin receptor ectodomain. Biochemistry. 1996 Nov 26;35(47):14800-5.

Darby NJ, Kemmink J, Creighton TE. Identifying and characterizing a structural domain of protein disulfide isomerase. Biochemistry. 1996 Aug 13;35(32):10517-28.

Davis DA, Newcomb FM, Starke DW, Ott DE, Mieyal JJ, Yarchoan R. Thioltransferase (glutaredoxin) is detected within HIV-1 and can regulate the activity of glutathionylated HIV-1 protease *in vitro*. J Biol Chem. 1997 Oct 10;272(41):25935-40.

Delom F, Mallet B, Carayon P, Lejeune PJ. Role of extracellular molecular chaperones in the folding of oxidized proteins. Refolding of colloidal thyroglobulin by protein disulfide isomerase and immunoglobulin heavy chain-binding protein. J Biol Chem. 2001 Jun 15;276(24):21337-42.

Deneke SM. Thiol-based antioxidants. Curr Top Cell Regul. 2000;36:151-80.

Dillet V, Dyson HJ, Bashford D. Calculations of electrostatic interactions and pKas in the active site of *Escherichia coli* thioredoxin. Biochemistry. 1998 Jul 14;37(28):10298-306.

Dyson HJ, Jeng MF, Tennant LL, Slaby I, Lindell M, Cui DS, Kuprin S, Holmgren A. Effects of buried charged groups on cysteine thiol ionization and reactivity in *Escherichia coli* thioredoxin: structural and functional characterization of mutants of Asp 26 and Lys 57. Biochemistry. 1997 Mar 4;36(9):2622-36.

Ejiri SI, Weissbach H, Brot N. Reduction of methionine sulfoxide to methionine by *Escherichia coli*. J Bacteriol. 1979 Jul;139(1):161-4.

Erve JC, Barofsky E, Barofsky DF, Deinzer ML, Reed DJ. Alkylation of Escherichia coli thioredoxin by S-(2-chloroethyl)glutathione and identification of the adduct on the active site cysteine-32 by mass spectrometry. Chem Res Toxicol. 1995a Oct-Nov;8(7):934-41.

Erve JC, Deinzer ML, Reed DJ. Alkylation of oxytocin by S-(2-chloroethyl)glutathione and characterization of adducts by tandem mass spectrometry and Edman degradation. Chem Res Toxicol. 1995b Apr-May;8(3):414-21.

Essex DW, Chen K, Swiatkowska M. Localization of protein disulfide isomerase to the external surface of the platelet plasma membrane. Blood. 1995 Sep 15;86(6):2168-73.

Essex DW, Li M, Miller A, Feinman RD. Protein disulfide isomerase and sulfhydryl-dependent pathways in platelet activation. Biochemistry. 2001 May 22;40(20):6070-5.

Ferrari DM, Soling HD. The protein disulphide-isomerase family: unravelling a string of folds. Biochem J. 1999 Apr 1;339 (Pt 1):1-10.

Foureman GL, Reed DJ. Formation of S-[2-(N7-guanyl)ethyl] adducts by the postulated S-(2-chloroethyl)cysteinyl and S-(2-chloroethyl)glutathionyl conjugates of 1,2-dichloroethane. Biochemistry. 1987 Apr 7;26(7):2028-33.

Frand AR, Kaiser CA. Ero1p oxidizes protein disulfide isomerase in a pathway for disulfide bond formation in the endoplasmic reticulum. Mol Cell. 1999 Oct;4(4):469-77.

Fratelli M, Demol H, Puype M, Casagrande S, Eberini I, Salmona M, Bonetto V, Mengozzi M, Duffieux F, Miclet E, Bachi A, Vandekerckhove J, Gianazza E, Ghezzi P. Identification by redox proteomics of glutathionylated proteins in oxidatively stressed human T lymphocytes. Proc Natl Acad Sci U S A. 2002 Mar 19;99(6):3505-10.

Freedman RB. Linking catalysts to chemistry. Nature. 1999 Nov 4;402(6757):27, 29.

Freedman RB, Bulleid NJ, Hawkins HC, Paver JL. Role of protein disulphide-isomerase in the expression of native proteins. Biochem Soc Symp. 1989;55:167-92.

Freedman RB, Hirst TR, Tuite MF. Protein disulphide isomerase: building bridges in protein folding. Trends Biochem Sci. 1994 Aug;19(8):331-6.

Friedman M, Cavins JF, Wall JS. Relative nucleophilic reactivities of amino groups and mercaptide ions in addition reactions with a,b-unsaturated compounds. 1965 J Am Chem Soc 87:3672-82.

Fry DW, Bridges AJ, Denny WA, Doherty A, Greis KD, Hicks JL, Hook KE, Keller PR, Leopold WR, Loo JA, McNamara DJ, Nelson JM, Sherwood V, Smaill JB, Trumpp-Kallmeyer S, Dobrusin EM. Specific, irreversible inactivation of the epidermal growth factor receptor and erbB2, by a new class of tyrosine kinase inhibitor. Proc Natl Acad Sci U S A. 1998 Sep 29;95(20):12022-7.

Gan ZR, Wells WW. Identification and reactivity of the catalytic site of pig liver thioltransferase. J Biol Chem. 1987 May 15;262(14):6704-7.

Gasdaska PY, Oblong JE, Cotgreave IA, Powis G. The predicted amino acid sequence of human thioredoxin is identical to that of the autocrine growth factor human adult T-cell derived factor (ADF): thioredoxin mRNA is elevated in some human tumors. Biochim Biophys Acta. 1994 Aug 2;1218(3):292-6.

Gerner C, Holzmann K, Meissner M, Gotzmann J, Grimm R, Sauermann G. Reassembling proteins and chaperones in human nuclear matrix protein fractions. J Cell Biochem. 1999 Aug 1;74(2):145-51.

Gilbert HF. Molecular and cellular aspects of thiol-disulfide exchange. Adv Enzymol Relat Areas Mol Biol. 1990;63:69-172.

Gilbert HF. Protein disulfide isomerase and assisted protein folding. J Biol Chem. 1997 Nov 21;272(47):29399-402.

Gilbert HF. Protein disulfide isomerase. Methods Enzymol. 1998;290:26-50.

Gilbert HF, Kruzel ML, Lyles MM, Harper JW. Expression and purification of recombinant rat protein disulfide isomerase from *Escherichia coli*. Protein Expr Purif. 1991 Apr-Jun;2(2-3):194-8.

Gladyshev VN, Jeang KT, Stadtman TC. Selenocysteine, identified as the penultimate C-terminal residue in human T-cell thioredoxin reductase, corresponds to TGA in the human placental gene. Proc Natl Acad Sci U S A. 1996 Jun 11;93(12):6146-51.

Gladyshev VN, Kryukov GV. Evolution of selenocysteine-containing proteins: significance of identification and functional characterization of selenoproteins. Biofactors. 2001;14(1-4):87-92.

Gorlatov SN, Stadtman TC. Human thioredoxin reductase from HeLa cells: selective alkylation of selenocysteine in the protein inhibits enzyme activity and reduction with NADPH influences affinity to heparin. Proc Natl Acad Sci U S A. 1998 Jul 21;95(15):8520-5.

Grauschopf U, Winther JR, Korber P, Zander T, Dallinger P, Bardwell JC. Why is DsbA such an oxidizing disulfide catalyst? Cell. 1995 Dec 15;83(6):947-55.

Gravina SA, Mieyal JJ. Thioltransferase is a specific glutathionyl mixed disulfide oxidoreductase. Biochemistry. 1993 Apr 6;32(13):3368-76.

Guengerich FP, Peterson LA, Cmarik JL, Koga N, Inskeep PB. Activation of dihaloalkanes by glutathione conjugation and formation of DNA adducts. Environ Health Perspect. 1987 Dec;76:15-8.

Guthapfel R, Gueguen P, Quemeneur E. Reexamination of hormone-binding properties of protein disulfide-isomerase. Eur J Biochem. 1996 Dec 1;242(2):315-9.

Habig WH, Pabst MJ, Fleischner G, Gatmaitan Z, Arias IM, Jakoby WB. The identity of glutathione S-transferase B with ligandin, a major binding protein of liver. Proc Natl Acad Sci U S A. 1974 Oct;71(10):3879-82.

Hansen BT, Jones JA, Mason DE, Liebler DC. SALSA: a pattern recognition algorithm to detect electrophile-adducted peptides by automated evaluation of CID spectra in LC-MS-MS analyses. Anal Chem. 2001 Apr 15;73(8):1676-83.

Hawkins HC, Freedman RB. The reactivities and ionization properties of the active-site dithiol groups of mammalian protein disulphide-isomerase. Biochem J. 1991 Apr 15;275 (Pt 2):335-9.

Hawkins HC, de Nardi M, Freedman RB. Redox properties and cross-linking of the dithiol/disulphide active sites of mammalian protein disulphide-isomerase. Biochem J. 1991a Apr 15;275 (Pt 2):341-8.

Hill DL, Shih TW, Johnston TP, Struck RF. Macromolecular binding and metabolism of the carcinogen 1,2-dibromoethane. Cancer Res. 1978 Aug;38(8):2438-42.

Hirota K, Murata M, Sachi Y, Nakamura H, Takeuchi J, Mori K, Yodoi J. Distinct roles of thioredoxin in the cytoplasm and in the nucleus. A two-step mechanism of redox regulation of transcription factor NF-kappaB. J Biol Chem. 1999 Sep 24;274(39):27891-7.

Holmgren A. Hydrogen donor system for *Escherichia coli* ribonucleoside-diphosphate reductase dependent upon glutathione. Proc Natl Acad Sci U S A. 1976 Jul;73(7):2275-2281.

Holmgren A. Glutaredoxin from *Escherichia coli* and calf thymus. Methods Enzymol. 1985;113:525-40.

Holmgren A. Thioredoxin and glutaredoxin systems. J Biol Chem. 1989 Aug 25;264(24):13963-6.

Holmgren A. Thioredoxin structure and mechanism: conformational changes on oxidation of the active-site sulfhydryls to a disulfide. Structure. 1995 Mar 15;3(3):239-43.

Holmgren A, Bjornstedt M. Thioredoxin and thioredoxin reductase. Methods Enzymol. 1995 252:199-208.

Holst B, Tachibana C, Winther JR. Active site mutations in yeast protein disulfide isomerase cause dithiothreitol sensitivity and a reduced rate

of protein folding in the endoplasmic reticulum. J Cell Biol. 1997 Sep 22;138(6):1229-38.

Hoog JO, Jornvall H, Holmgren A, Carlquist M, Persson M. The primary structure of *Escherichia coli* glutaredoxin. Distant homology with thioredoxins in a superfamily of small proteins with a redox-active cystine disulfide/cysteine dithiol. Eur J Biochem. 1983 Oct 17;136(1):223-32.

Horton ND, Biswal SS, Corrigan LL, Bratta J, Kehrer JP. Acrolein causes inhibitor kappaB-independent decreases in nuclear factor kappaB activation in human lung adenocarcinoma (A549) cells. J Biol Chem. 1999 Apr 2;274(14):9200-6.

Hotchkiss KA, Matthias LJ, Hogg PJ. Exposure of the cryptic Arg-Gly-Asp sequence in thrombospondin-1 by protein disulfide isomerase. Biochim Biophys Acta. 1998 Nov 10;1388(2):478-88.

Hu Y, Jin X, Snow ET. Effect of arsenic on transcription factor AP-1 and NF-kappaB DNA binding activity and related gene expression. Toxicol Lett. 2002 Jul 7;133(1):33-45.

Huang KP, Huang FL. Glutathionylation of proteins by glutathione disulfide S-oxide. Biochem Pharmacol. 2002 Sep;64(5-6):1049-56.

Hwang C, Sinskey AJ, Lodish HF. Oxidized redox state of glutathione in the endoplasmic reticulum. Science. 1992 Sep 11;257(5076):1496-502.

Igwe OJ, Que Hee SS, Wagner WD. Effect of disulfiram pretreatment on the tissue distribution, macromolecular binding, and excretion of [U-1,2-14C]dichloroethane in the rat. Drug Metab Dispos. 1986 Jan-Feb;14(1):65-72.

Inskeep PB, Koga N, Cmarik JL, Guengerich FP. Covalent binding of 1,2-dihaloalkanes to DNA and stability of the major DNA adduct, S-[2-(N7-guanyl)ethyl]glutathione. Cancer Res. 1986 Jun;46(6):2839-44

Jean PA, Reed DJ. *In vitro* dipeptide, nucleoside, and glutathione alkylation by S-(2-chloroethyl)glutathione and S-(2-chloroethyl)-L-cysteine. Chem Res Toxicol. 1989 Nov-Dec;2(6):455-60.

Jean PA, Reed DJ. Utilization of glutathione during 1,2-dihaloethane metabolism in rat hepatocytes. Chem Res Toxicol. 1992 May-Jun;5(3):386-91.

Jiang XR, Wrona MZ, Dryhurst G. Tryptamine-4,5-dione, a putative endotoxic metabolite of the superoxide-mediated oxidation of serotonin, is a mitochondrial toxin: possible implications in neurodegenerative brain disorders. Chem Res Toxicol. 1999 May;12(5):429-36.

Jones JA, Liebler DC. Tandem MS analysis of model peptide adducts from reactive metabolites of the hepatotoxin 1,1-dichloroethylene. Chem Res Toxicol. 2000 Dec;13(12):1302-12.

Kallis GB, Holmgren A. Differential reactivity of the functional sulfhydryl groups of cysteine-32 and cysteine-35 present in the reduced form of thioredoxin from *Escherichia coli*. J Biol Chem. 1980 Nov 10;255(21):10261-5.

Kanai S, Toh H, Hayano T, Kikuchi M. Molecular evolution of the domain structures of protein disulfide isomerases. J Mol Evol. 1998 Aug;47(2):200-10.

Katti SK, Robbins AH, Yang Y, Wells WW. Crystal structure of thioltransferase at 2.2 A resolution. Protein Sci. 1995 Oct;4(10):1998-2005.

Kemmink J, Darby NJ, Dijkstra K, Nilges M, Creighton TE. Structure determination of the N-terminal thioredoxin-like domain of protein disulfide isomerase using multidimensional heteronuclear 13C/15N NMR spectroscopy. Biochemistry. 1996 Jun 18;35(24):7684-91.

Kemmink J, Darby NJ, Dijkstra K, Nilges M, Creighton TE. The folding catalyst protein disulfide isomerase is constructed of active and inactive thioredoxin modules. Curr Biol. 1997 Apr 1;7(4):239-45.

Kemmink J, Dijkstra K, Mariani M, Scheek RM, Penka E, Nilges M, Darby NJ. The structure in solution of the b domain of protein disulfide isomerase. J Biomol NMR. 1999 Apr;13(4):357-68.

Kim JR, Yoon HW, Kwon KS, Lee SR, Rhee SG. Identification of proteins containing cysteine residues that are sensitive to oxidation by hydrogen peroxide at neutral pH. Anal Biochem. 2000 Aug 1;283(2):214-21.

Kim MY, Maier CS, Reed DJ, Ho PS, Deinzer ML. Intramolecular interactions in chemically modified Escherichia coli thioredoxin monitored by hydrogen/deuterium exchange and electrospray ionization mass spectrometry. Biochemistry. 2001 Dec 4;40(48):14413-21.

Kim MY, Maier CS, Reed DJ, Deinzer ML. Conformational changes in chemically modified Escherichia coli thioredoxin monitored by H/D exchange and electrospray ionization mass spectrometry. Protein Sci. 2002 Jun;11(6):1320-9.

Klappa P, Koivunen P, Pirneskoski A, Karvonen P, Ruddock LW, Kivirikko KI, Freedman RB. Mutations that destabilize the a' domain of human protein-disulfide isomerase indirectly affect peptide binding. J Biol Chem. 2000 May 5;275(18):13213-8.

Klappa P, Ruddock LW, Darby NJ, Freedman RB. The b' domain provides the principal peptide-binding site of protein disulfide isomerase but all domains contribute to binding of misfolded proteins. EMBO J. 1998 Feb 16;17(4):927-35.

Koen YM, Hanzlik RP. Identification of seven proteins in the endoplasmic reticulum as targets for reactive metabolites of bromobenzene. Chem Res Toxicol. 2002 May;15(5):699-706.

Koga N, Inskeep PB, Harris TM, Guengerich FP. S-[2-(N7-guanyl)ethyl] glutathione, the major DNA adduct formed from 1,2-dibromoethane. Biochemistry. 1986 Apr 22;25(8):2192-8.

Kortemme T, Creighton TE. Ionisation of cysteine residues at the termini of model alpha-helical peptides. Relevance to unusual thiol pKa values in proteins of the thioredoxin family. J Mol Biol. 1995 Nov 10;253(5):799-812.

Kortemme T, Darby NJ, Creighton TE. Electrostatic interactions in the active site of the N-terminal thioredoxin-like domain of protein disulfide isomerase. Biochemistry. 1996 Nov 19;35(46):14503-11.

Krause G, Holmgren A. Substitution of the conserved tryptophan 31 in Escherichia coli thioredoxin by site-directed mutagenesis and structure-function analysis. J Biol Chem. 1991 Mar 5;266(7):4056-66.

Kroning H, Thiel U, Ansorge S. Induction of protein disulphide-isomerase and immunoglobulins by pokeweed mitogen in human lymphocytes. Hybridoma. 1991 Dec;10(6):651-7.

Lambert N, Freedman RB. Structural properties of homogeneous protein disulphide-isomerase from bovine liver purified by a rapid high-yielding procedure. Biochem J. 1983 Jul 1;213(1):225-34.

Lame MW, Jones AD, Wilson DW, Dunston SK, Segall HJ. Protein targets of monocrotaline pyrrole in pulmonary artery endothelial cells. J Biol Chem. 2000 Sep 15;275(37):29091-9.

Lantum HB, Liebler DC, Board PG, Anders MW. Alkylation and inactivation of human glutathione transferase zeta (hGSTZ1-1) by maleylacetone and fumarylacetone. Chem Res Toxicol. 2002 May;15(5):707-16.

Laurent TC, Moore EC. Reichard P. Enzymatic synthesis of deoxyribonucleotides VI. Isolation and characterization of thioredoxin, the hydrogen donor from Escherichia coli B. J. Biol. Chem. 1964. 239:3436-44.

Leesnitzer LM, Parks DJ, Bledsoe RK, Cobb JE, Collins JL, Consler TG, Davis RG, Hull-Ryde EA, Lenhard JM, Patel L, Plunket KD, Shenk JL, Stimmel JB, Therapontos C, Willson TM, Blanchard SG. Functional consequences of cysteine modification in the ligand binding sites of peroxisome proliferator activated receptors by GW9662. Biochemistry. 2002 May 28;41(21):6640-50.

Li H, Hanson C, Fuchs JA, Woodward C, Thomas GJ Jr. Determination of the pKa values of active-center cysteines, cysteines-32 and -35, in *Escherichia coli* thioredoxin by Raman spectroscopy. Biochemistry. 1993 Jun 8;32(22):5800-8.

Liebler DC. Introduction to Proteomics: Tools for a New Biology. Humana Press. 2001. 198 pages.

Liebler DC. Proteomic approaches to characterize protein modifications: new tools to study the effects of environmental exposures. Environ Health Perspect. 2002 Feb;110 (Suppl 1):3-9.

Liebler DC, Hansen BT, Davey SW, Tiscareno L, Mason DE. Peptide sequence motif analysis of tandem MS data with the SALSA algorithm. Anal Chem. 2002 Jan 1;74(1):203-10.

Li CJ, Haller B, Fuchs JA. Thioredoxin is the bacterial protein encoded by fip that is required for filamentous bacteriophage f1 assembly. J Bacteriol. 1985 Feb;161(2):799-802.

Lumb RA, Bulleid NJ. Is protein disulfide isomerase a redox-dependent molecular chaperone? EMBO J. 2002 Dec 16;21(24):6763-70.

Lundstrom J, Holmgren A. Determination of the reduction-oxidation potential of the thioredoxin-like domains of protein disulfide-isomerase from the equilibrium with glutathione and thioredoxin. Biochemistry. 1993 Jul 6;32(26):6649-55.

Lundstrom J, Holmgren A. Protein disulfide-isomerase is a substrate for thioredoxin reductase and has thioredoxin-like activity.J Biol Chem. 1990 Jun 5;265(16):9114-20

Luthman M, Holmgren A. Rat liver thioredoxin and thioredoxin reductase: purification and characterization. Biochemistry. 1982 Dec 21;21(26):6628-33.

Lyles MM, Gilbert HF. Catalysis of the oxidative folding of ribonuclease A by protein disulfide isomerase: dependence of the rate on the composition of the redox buffer. Biochemistry. 1991a Jan 22;30(3):613-9.

Lyles MM, Gilbert HF. Catalysis of the oxidative folding of ribonuclease A by protein disulfide isomerase: pre-steady-state kinetics and the utilization of the oxidizing equivalents of the isomerase. Biochemistry. 1991b Jan 22;30(3):619-25.

Lyles MM, Gilbert HF. Mutations in the thioredoxin sites of protein disulfide isomerase reveal functional nonequivalence of the N- and C-terminal domains. J Biol Chem. 1994 Dec 9;269(49):30946-52.

Maithal K, Ravindra G, Balaram H, Balaram P. Inhibition of plasmodium falciparum triose-phosphate isomerase by chemical modification of an interface cysteine. Electrospray ionization mass spectrometric analysis of differential cysteine reactivities. J Biol Chem. 2002 Jul 12;277(28):25106-14.

Marchand DH, Reed DJ. Identification of the reactive glutathione conjugate S-(2-chloroethyl)glutathione in the bile of 1-bromo-2-chloroethane-treated rats by high-pressure liquid chromatography and precolumn derivatization with o-phthalaldehyde. Chem Res Toxicol. 1989 Nov-Dec;2(6):449-54.

Martin JL, Kenna JG, Martin BM, Thomassen D, Reed GF, Pohl LR. Halothane hepatitis patients have serum antibodies that react with protein disulfide isomerase. Hepatology. 1993a Oct;18(4):858-63.

Martin JL, Reed GF, Pohl LR. Association of anti-58 kDa endoplasmic reticulum antibodies with halothane hepatitis. Biochem Pharmacol. 1993b Oct 5;46(7):1247-50.

Martin JL. Thioredoxin--a fold for all reasons. Structure. 1995 Mar 15;3(3):245-50.

Mason DE, Liebler DC. Characterization of benzoquinone-peptide adducts by electrospray mass spectrometry. Chem Res Toxicol. 2000 Oct;13(10):976-82.

McArthur AG, Knodler LA, Silberman JD, Davids BJ, Gillin FD, Sogin ML. The evolutionary origins of eukaryotic protein disulfide isomerase domains: new evidence from the Amitochondriate protist *Giardia lamblia*. Mol Biol Evol. 2001 Aug;18(8):1455-63.

Meyer M, Jensen ON, Barofsky E, Barofsky DF, Reed DJ. Thioredoxin alkylation by a dihaloethane-glutathione conjugate. Chem Res Toxicol. 1994 Sep-Oct;7(5):659-65.

Modrich P, Richardson CC. Bacteriophage T7 deoxyribonucleic acid replication *in vitro*. Bacteriophage T7 DNA polymerase: an an emzyme composed of phage- and host-specific subunits. J Biol Chem. 1975 Jul 25;250(14):5515-22.

Moridani MY, Cheon SS, Khan S, O'Brien PJ. Metabolic activation of 4-hydroxyanisole by isolated rat hepatocytes. Drug Metab Dispos. 2002 Oct;30(10):1063-9.

Myllyla R, Kaska DD, Kivirikko KI. The catalytic mechanism of the hydroxylation reaction of peptidyl proline and lysine does not require protein disulphide-isomerase activity. Biochem J. 1989 Oct 15;263(2):609-11.

Nagayama S, Yokoi T, Kawaguchi Y, Kamataki T. Occurrence of autoantibody to protein disulfide isomerase in rats with xenobiotic-induced hepatitis. J Toxicol Sci. 1994 Aug;19(3):155-61.

Nakamura H, Nakamura K, Yodoi J. Redox regulation of cellular activation. Annu Rev Immunol. 1997;15:351-69.

Nelson JW, Creighton TE. Reactivity and ionization of the active site cysteine residues of DsbA, a protein required for disulfide bond formation *in vivo*. Biochemistry. 1994 May 17;33(19):5974-83.

Noiva R. Enzymatic catalysis of disulfide formation. Protein Expr Purif. 1994 Feb;5(1):1-13.

Noiva R, Freedman RB, Lennarz WJ. Peptide binding to protein disulfide isomerase occurs at a site distinct from the active sites. J Biol Chem. 1993 Sep 15;268(26):19210-7.

Nordberg J, Zhong L, Holmgren A, Arner ES. Mammalian thioredoxin reductase is irreversibly inhibited by dinitrohalobenzenes by alkylation of both the redox active selenocysteine and its neighboring cysteine residue. J Biol Chem. 1998 May 1;273(18):10835-42.

Padilla CA, Martinez-Galisteo E, Barcena JA, Spyrou G, Holmgren A. Purification from placenta, amino acid sequence, structure comparisons and cDNA cloning of human glutaredoxin. Eur J Biochem. 1995 Jan 15;227(1-2):27-34.

Papayannopoulos IA, Gan ZR, Wells WW, Biemann K. A revised sequence of calf thymus glutaredoxin. Biochem Biophys Res Commun. 1989 Mar 31;159(3):1448-54

Pearson RG, Sobel H, Songstad J. Nucleophilic reactivity constants toward methyl iodide and trans-[Pt(py)2Cl2]. 1968 J Am Chem Soc. 90:319-326.

Percival MD, Ouellet M, Campagnolo C, Claveau D, Li C. Inhibition of cathepsin K by nitric oxide donors: evidence for the formation of mixed disulfides and a sulfenic acid. Biochemistry. 1999 Oct 12;38(41):13574-83.

Perkins DN, Pappin DJ, Creasy DM, Cottrell JS. Probability-based protein identification by searching sequence databases using mass spectrometry data. Electrophoresis. 1999 Dec;20(18):3551-67.

Pihlajaniemi T, Helaakoski T, Tasanen K, Myllyla R, Huhtala ML, Koivu J, Kivirikko KI. Molecular cloning of the beta-subunit of human prolyl 4-hydroxylase. This subunit and protein disulphide isomerase are products of the same gene. EMBO J. 1987 Mar;6(3):643-9.

Pirneskoski A, Ruddock LW, Klappa P, Freedman RB, Kivirikko KI, Koivunen P. Domains b' and a' of protein disulfide isomerase fulfill the minimum requirement for function as a subunit of prolyl 4-hydroxylase. The N-terminal domains a and b enhances this function and can be substituted in part by those of ERp57. J Biol Chem. 2001 Apr 6;276(14):11287-93.

Pohl LR, Kenna JG, Satoh H, Christ D, Martin JL. Neoantigens associated with halothane hepatitis. Drug Metab Rev. 1989;20(2-4):203-17.

Poole LB. Protein sulfenic acids Current Protocols of Toxicology. Ed MD Maines. Wiley Publishers, New Jersey 2002. 17:1-30.

Powis G, Montfort WR. Properties and biological activities of thioredoxins. Annu Rev Pharmacol Toxicol. 2001;41:261-95.

Powis G, Briehl M, Oblong J. Redox signalling and the control of cell growth and death. Pharmacol Ther. 1995;68(1):149-73.

Primm TP, Walker KW, Gilbert HF. Facilitated protein aggregation. Effects of calcium on the chaperone and anti-chaperone activity of protein disulfide-isomerase. J Biol Chem. 1996 Dec 27;271(52):33664-9

Primm TP, Gilbert HF. Hormone binding by protein disulfide isomerase, a high capacity hormone reservoir of the endoplasmic reticulum. J Biol Chem. 2001 Jan 5;276(1):281-6.

Puig A, Gilbert HF. Protein disulfide isomerase exhibits chaperone and anti-chaperone activity in the oxidative refolding of lysozyme. J Biol Chem. 1994 Mar 11;269(10):7764-71.

Puig A, Lyles MM, Noiva R, Gilbert HF. The role of the thiol/disulfide centers and peptide binding site in the chaperone and anti-chaperone activities of protein disulfide isomerase. J Biol Chem. 1994 Jul 22;269(29):19128-35.

Puig A, Primm TP, Surendran R, Lee JC, Ballard KD, Orkiszewski RS, Makarov V, Gilbert HF. A 21-kDa C-terminal fragment of protein-disulfide isomerase has isomerase, chaperone, and anti-chaperone activities. J Biol Chem. 1997 Dec 26;272(52):32988-94.

Qin J, Yang Y, Velyvis A, Gronenborn A. Molecular views of redox regulation: three-dimensional structures of redox regulatory proteins and protein complexes. Antioxid Redox Signal. 2000 Winter;2(4):827-40.

Quan H, Fan G, Wang CC. Independence of the chaperone activity of protein disulfide isomerase from its thioredoxin-like active site. J Biol Chem. 1995 Jul 21;270(29):17078-80.

Rahman I, Li XY, Donaldson K, Harrison DJ, MacNee W. Glutathione homeostasis in alveolar epithelial cells in vitro and lung in vivo under oxidative stress. Am J Physiol. 1995 Sep;269(3 Pt 1):L285-92.

Reed DJ. Cellular defense mechanisms against reactive metabolites. Bioactivation of foreign compounds. Ed. MS Anders. New York: Academic Press, 1985. 71-108.

Reed DJ, Foureman GL. A comparison of the alkylating capabilities of the cysteinyl and glutathionyl conjugates of 1,2-dichloroethane. Adv Exp Med Biol. 1986;197:469-75.

Rietsch A, Beckwith J. The genetics of disulfide bond metabolism. Annu Rev Genet. 1998;32:163-84.

Rietsch A, Bessette P, Georgiou G, Beckwith J. Reduction of the periplasmic disulfide bond isomerase, DsbC, occurs by passage of electrons from cytoplasmic thioredoxin. J Bacteriol. 1997 Nov;179(21):6602-8

Rigobello MP, Donella-Deana A, Cesaro L, Bindoli A. Isolation, purification, and characterization of a rat liver mitochondrial protein disulfide isomerase. Free Radic Biol Med. 2000 Jan 15;28(2):266-72

Rigobello MP, Donella-Deana A, Cesaro L, Bindoli A. Distribution of protein disulphide isomerase in rat liver mitochondria. Biochem J. 2001 Jun 1;356(Pt 2):567-70.

Rodriguez-Manzaneque MT, Tamarit J, Belli G, Ros J, Herrero E. Grx5 is a mitochondrial glutaredoxin required for the activity of iron/sulfur enzymes. Mol Biol Cell. 2002 Apr;13(4):1109-21

Roepstorff P, Fohlman J. Proposal for a common nomenclature for sequence ions in mass spectra of peptides. Biomed Mass Spectrom. 1984 Nov;11(11):601.

Rokutan K, Johnston RB Jr, Kawai K. Oxidative stress induces S-thiolation of specific proteins in cultured gastric mucosal cells. Am J Physiol. 1994 Feb;266(2 Pt 1):G247-54

Russel M, Model P. Thioredoxin is required for filamentous phage assembly. Proc Natl Acad Sci U S A. 1985 Jan;82(1):29-33

Sahrawy M, Hecht V, Lopez-Jaramillo J, Chueca A, Chartier Y, Meyer Y. Intron position as an evolutionary marker of thioredoxins and thioredoxin domains. J Mol Evol. 1996 Apr;42(4):422-31

Sandalova T, Zhong L, Lindqvist Y, Holmgren A, Schneider G. Three-dimensional structure of a mammalian thioredoxin reductase: implications for mechanism and evolution of a selenocysteine-dependent enzyme. Proc Natl Acad Sci U S A. 2001 Aug 14;98(17):9533-8

Schenk H, Klein M, Erdbrugger W, Droge W, Schulze-Osthoff K. Distinct effects of thioredoxin and antioxidants on the activation of transcription factors NF-kappa B and AP-1. Proc Natl Acad Sci U S A. 1994 Mar 1;91(5):1672-6

Schirra HJ, Renner C, Czisch M, Huber-Wunderlich M, Holak TA, Glockshuber R. Structure of reduced DsbA from *Escherichia coli* in solution. Biochemistry. 1998 May 5;37(18):6263-76

Schwaller MF, Wilkinson B, Gilbert H. Reduction/reoxidation cycles contribute to catalysis of disulfide isomerization by protein disulfide isomerase. J Biol Chem. 2003 Feb 28;278(9):7154-9.

Shaked Z, Szajewski RP, Whitesides GM. Rates of thiol-disulfide interchange reactions involving proteins and kinetic measurements of thiol pKa values. Biochemistry. 1980 Sep 2;19(18):4156-66.

Simon DI, Mullins ME, Jia L, Gaston B, Singel DJ, Stamler JS. Polynitrosylated proteins: characterization, bioactivity, and functional consequences. Proc Natl Acad Sci U S A. 1996 May 14;93(10):4736-41.

Singh R, Blattler WA, Collinson AR. An amplified assay for thiols based on reactivation of papain. Anal Biochem. 1993 Aug 15;213(1):49-56.

Stadtman ER. Protein oxidation in aging and age-related diseases. Ann N Y Acad Sci. 2001 Apr;928:22-38.

Stafford SL, Lund PL. Mutagenic studies on human protein disulfide isomerase by complementation of Escherichia coli dsbA and dsbC mutants. 2000 FEBS Letters 466:317-22.

Stamler JS. S-nitrosothiols and the bioregulatory actions of nitrogen oxides through reactions with thiol groups. Curr Top Microbiol Immunol. 1995;196:19-36.

Stamler JS, Toone EJ, Lipton SA, Sucher NJ. S-NO signals: translocation, regulation, and a consensus motif. Neuron. 1997 May;18(5):691-6.

Stamler JS, Hausladen A. Oxidative modifications in nitrosative stress. Nat Struct Biol. 1998 Apr;5(4):247-9.

Sun C, Berardi MJ, Bushweller JH. The NMR solution structure of human glutaredoxin in the fully reduced form. J Mol Biol. 1998 Jul 24;280(4):687-701.

Terada K, Manchikalapudi P, Noiva R, Jauregui HO, Stockert RJ, Schilsky ML. Secretion, surface localization, turnover, and steady state expression of protein disulfide isomerase in rat hepatocytes. J Biol Chem. 1995 Sep 1;270(35):20410-6.

Tremblay JM, Li H, Yarbrough LR, Helmkamp GM. Modification of cysteine residues in the solution and membrane-associated conformations of phospatidylinositol transfer protein have differential effects on lipid transfer acitivity. Biochemistry. 2001 40:9151-8.

Tsai B, Rodighiero C, Lencer WI, Rapoport TA. Protein disulfide isomerase acts as a redox-dependent chaperone to unfold cholera toxin. Cell. 2001 Mar 23;104(6):937-48.

Tsang ML, Schiff JA. Sulfate-reducing pathway in Escherichia coli involving bound intermediates. J Bacteriol. 1976 Mar;125(3):923-33.

Turano C, Coppari S, Altieri F, Ferraro A. Proteins of the PDI family: unpredicted non-ER locations and functions. J Cell Physiol. 2002 Nov;193(2):154-63.

Ueno M, Masutani H, Arai RJ, Yamauchi A, Hirota K, Sakai T, Inamoto T, Yamaoka Y, Yodoi J, Nikaido T. Thioredoxin-dependent redox regulation of p53-mediated p21 activation. J Biol Chem. 1999 Dec 10;274(50):35809-15.

van Bladeren PJ, Breimer DD, Rotteveel-Smijs GM, Hoogeterp JJ, Mohn GR, de Groot A, van Zeeland AA, van der Gen A. The activating role of glutathione in the mutagenicity of 1,2-dibromoethane. Adv Exp Med Biol. 1981;136 Pt A:809-20.

VanderWaal RP, Spitz DR, Griffith CL, Higashikubo R, Roti Roti JL. Evidence that protein disulfide isomerase (PDI) is involved in DNA-nuclear matrix anchoring. J Cell Biochem. 2002;85(4):689-702.

Voss T, Ahorn H, Haberl P, Dohner H, Wilgenbus K. Correlation of clinical data with proteomics profiles in 24 patients with B-cell chronic lymphocytic leukemia. Int J Cancer. 2001 Jan 15;91(2):180-6.

Vuori K, Pihlajaniemi T, Myllyla R, Kivirikko KI. Site-directed mutagenesis of human protein disulphide isomerase: effect on the assembly, activity and endoplasmic reticulum retention of human prolyl 4-hydroxylase in *Spodoptera frugiperda* insect cells. EMBO J. 1992 Nov;11(11):4213-7.

Wagner E, Luche S, Penna L, Chevallet M, Van Dorsselaer A, Leize-Wagner E, Rabilloud T. A method for detection of overoxidation of cysteines: peroxiredoxins are oxidized *in vivo* at the active-site cysteine during oxidative stress. Biochem J. 2002 Sep 15;366(Pt 3):777-85.

Walker KW, Lyles MM, Gilbert HF. Catalysis of oxidative protein folding by mutants of protein disulfide isomerase with a single active-site cysteine. Biochemistry. 1996 Feb 13;35(6):1972-80.

Walker KW, Gilbert HF. Scanning and escape during protein-disulfide isomerase-assisted protein folding. J Biol Chem. 1997 Apr 4;272(14):8845-8.

Wang CC. Protein disulfide isomerase as an enzyme and a chaperone in protein folding. Methods Enzymol. 2002;348:66-75.

Wang CC, Tsou CL. Enzymes as chaperones and chaperones as enzymes. FEBS Lett. 1998 Apr 3;425(3):382-4.

Wells WW, Xu DP, Yang YF, Rocque PA. Mammalian thioltransferase (glutaredoxin) and protein disulfide isomerase have dehydroascorbate reductase activity. J Biol Chem. 1990 Sep 15;265(26):15361-4.

Wetterau JR, Combs KA, Spinner SN, Joiner BJ. Protein disulfide isomerase is a component of the microsomal triglyceride transfer protein complex. J Biol Chem. 1990 Jun 15;265(17):9801-7.

Wetterau JR, Combs KA, McLean LR, Spinner SN, Aggerbeck LP. Protein disulfide isomerase appears necessary to maintain the catalytically active structure of the microsomal triglyceride transfer protein. Biochemistry. 1991 Oct 8;30(40):9728-35.

Williams CH Jr. Mechanism and structure of thioredoxin reductase from *Escherichia coli*. FASEB J. 1995 Oct;9(13):1267-76.

Williams CH, Arscott LD, Muller S, Lennon BW, Ludwig ML, Wang PF, Veine DM, Becker K, Schirmer RH. Thioredoxin reductase two modes of catalysis have evolved. Eur J Biochem. 2000 Oct;267(20):6110-7.

Wolters DA, Washburn MP, Yates JR 3rd. An automated multidimensional protein identification technology for shotgun proteomics. Anal Chem. 2001 Dec 1;73(23):5683-90.

Wright SK, Viola RE. Evaluation of methods for the quantitation of cysteines in proteins. Anal Biochem. 1998 Dec 1;265(1):8-14.

Wrona MZ, Dryhurst G. A putative metabolite of serotonin, tryptamine-4,5-dione, is an irreversible inhibitor of tryptophan hydroxylase: possible relevance to the serotonergic neurotoxicity of methamphetamine. Chem Res Toxicol. 2001 Sep;14(9):1184-92.

Xia TH, Bushweller JH, Sodano P, Billeter M, Bjornberg O, Holmgren A, Wuthrich K. NMR structure of oxidized *Escherichia coli* glutaredoxin: comparison with reduced *Escherichia coli* glutaredoxin and functionally related proteins. Protein Sci. 1992 Mar;1(3):310-21.

Xu L, Eu JP, Meissner G, Stamler JS. Activation of the cardiac calcium release channel (ryanodine receptor) by poly-S-nitrosylation. Science. 1998 Jan 9;279(5348):234-7.

Yang Y, Jao S, Nanduri S, Starke DW, Mieyal JJ, Qin J. Reactivity of the human thioltransferase (glutaredoxin) C7S, C25S, C78S, C82S mutant and NMR solution structure of its glutathionyl mixed disulfide intermediate reflect catalytic specificity. Biochemistry. 1998 Dec 8;37(49):17145-56.

Yang YF, Wells WW. Identification and characterization of the functional amino acids at the active center of pig liver thioltransferase by site-directed mutagenesis. J Biol Chem. 1991 Jul 5;266(19):12759-65.

Yao Y, Zhou Y, Wang C. Both the isomerase and chaperone activities of protein disulfide isomerase are required for the reactivation of reduced and denatured acidic phospholipase A2. EMBO J. 1997 Feb 3;16(3):651-8.

Yodoi J, Tursz T. ADF, a growth-promoting factor derived from adult T cell leukemia and homologous to thioredoxin: involvement in lymphocyte immortalization by HTLV-I and EBV. Adv Cancer Res. 1991;57:381-411.

Yoshimori T, Semba T, Takemoto H, Akagi S, Yamamoto A, Tashiro Y. Protein disulfide-isomerase in rat exocrine pancreatic cells is exported from the endoplasmic reticulum despite possessing the retention signal. J Biol Chem. 1990 Sep 15;265(26):15984-90.

Zapun A, Creighton TE, Rowling PJ, Freedman RB. Folding *in vitro* of bovine pancreatic trypsin inhibitor in the presence of proteins of the endoplasmic reticulum. Proteins. 1992 Sep;14(1):10-5.

Zapun A, Missiakas D, Raina S, Creighton TE Structural and functional characterization of DsbC, a protein involved in disulfide bond formation in *Escherichia* coli. Biochemistry. 1995 18;34(15):5075-89.

Zapun A, Darby NJ, Tessier DC, Michalak M, Bergeron JJ, Thomas DY. Enhanced catalysis of ribonuclease B folding by the interaction of calnexin or calreticulin with ERp57. J Biol Chem. 1998 Mar 13;273(11):6009-12.

Zhang P, Liu B, Kang SW, Seo MS, Rhee SG, Obeid LM. Thioredoxin peroxidase is a novel inhibitor of apoptosis with a mechanism distinct from that of Bcl-2. J Biol Chem. 1997 Dec 5;272(49):30615-8.

Zhong L, Arner ES, Ljung J, Aslund F, Holmgren A. Rat and calf thioredoxin reductase are homologous to glutathione reductase with a carboxyl-terminal elongation containing a conserved catalytically active penultimate selenocysteine residue. J Biol Chem. 1998 Apr 10;273(15):8581-91.

Zhong L, Arner ES, Holmgren A. Structure and mechanism of mammalian thioredoxin reductase: the active site is a redox-active selenolthiol/selenenylsulfide formed from the conserved cysteine-selenocysteine sequence. Proc Natl Acad Sci U S A. 2000 May 23;97(11):5854-9.

Zhou L, McKenzie BA, Eccleston ED, Srivastava SP, Chen M, Ericson R, Holtzman JL. The covalent binding of [14C]-acetaminophen to mouse hepatic microsomal proteins: the specific binding to calreticulin and the two forms of the thiol:protein disulfide oxidoreductases. Chem Res Toxicol. 1996 9:1176-82.

Zhou L, Dehal SS, Kupfer D, Morrell S, McKenzie BA, Eccleston ED, Holtzman JL. Cytochrome P450 catalyzed covalent binding of methoxychlor to rat hepatic microsomal iodothyronine 5'monodeiodinase, type I: does exposure to methoxychlor disrupt thyroid hormone metabolism? Arch Biochem Biophys. 1995 322:390-94.